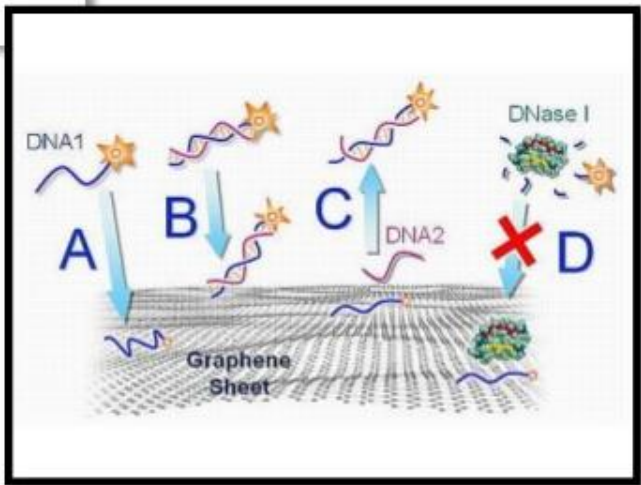
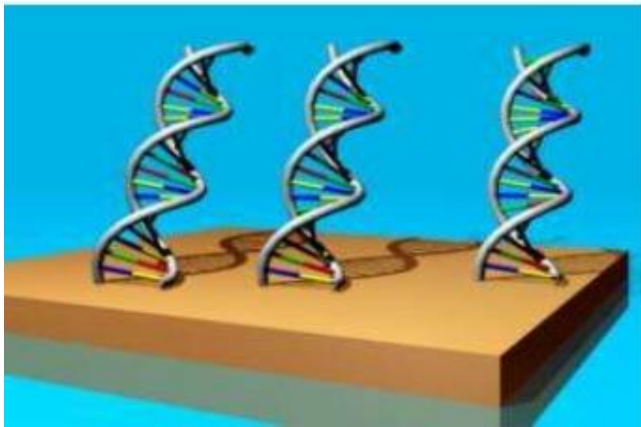
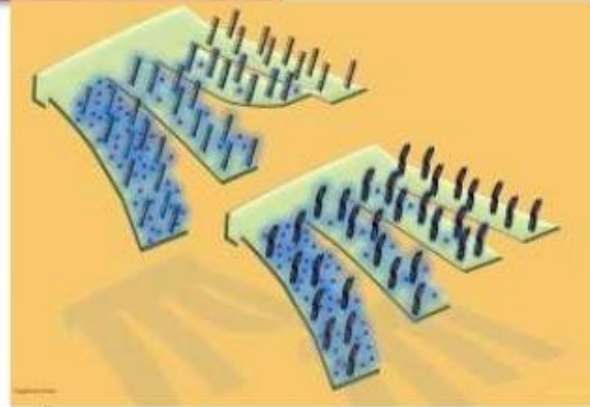
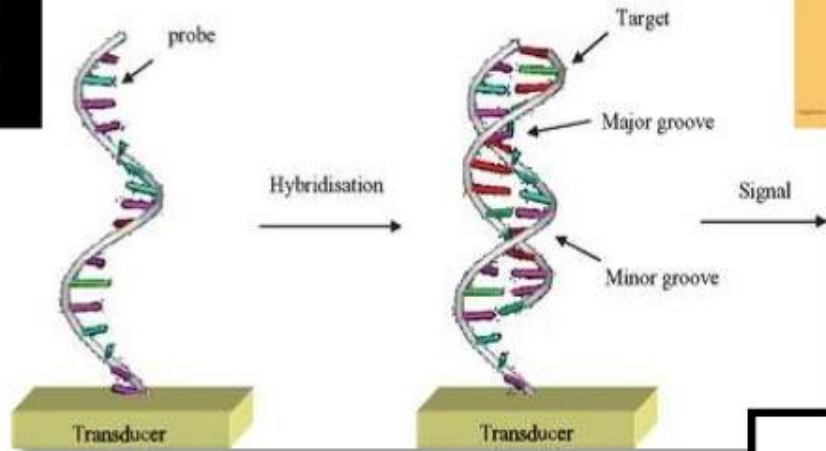
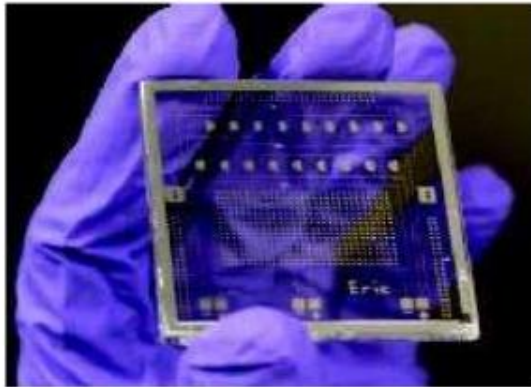


DNA biosensors

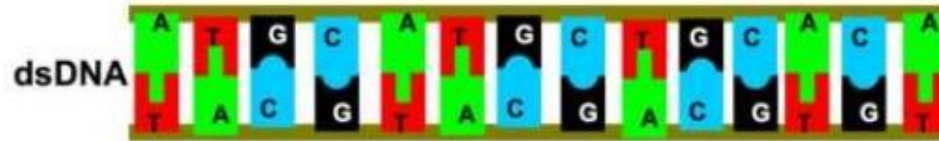


Principles of DNA biosensors

❖ Nucleic acid hybridization

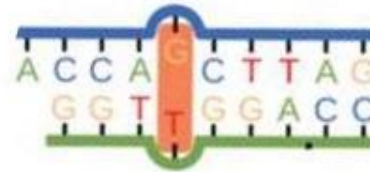
➤ Perfect match

stable dsDNA, strong hybridization



➤ One or more base mismatches

weak hybridization



❖ **Forms of DNA Biosensors**

- Electrodes
- Chips
- Crystals

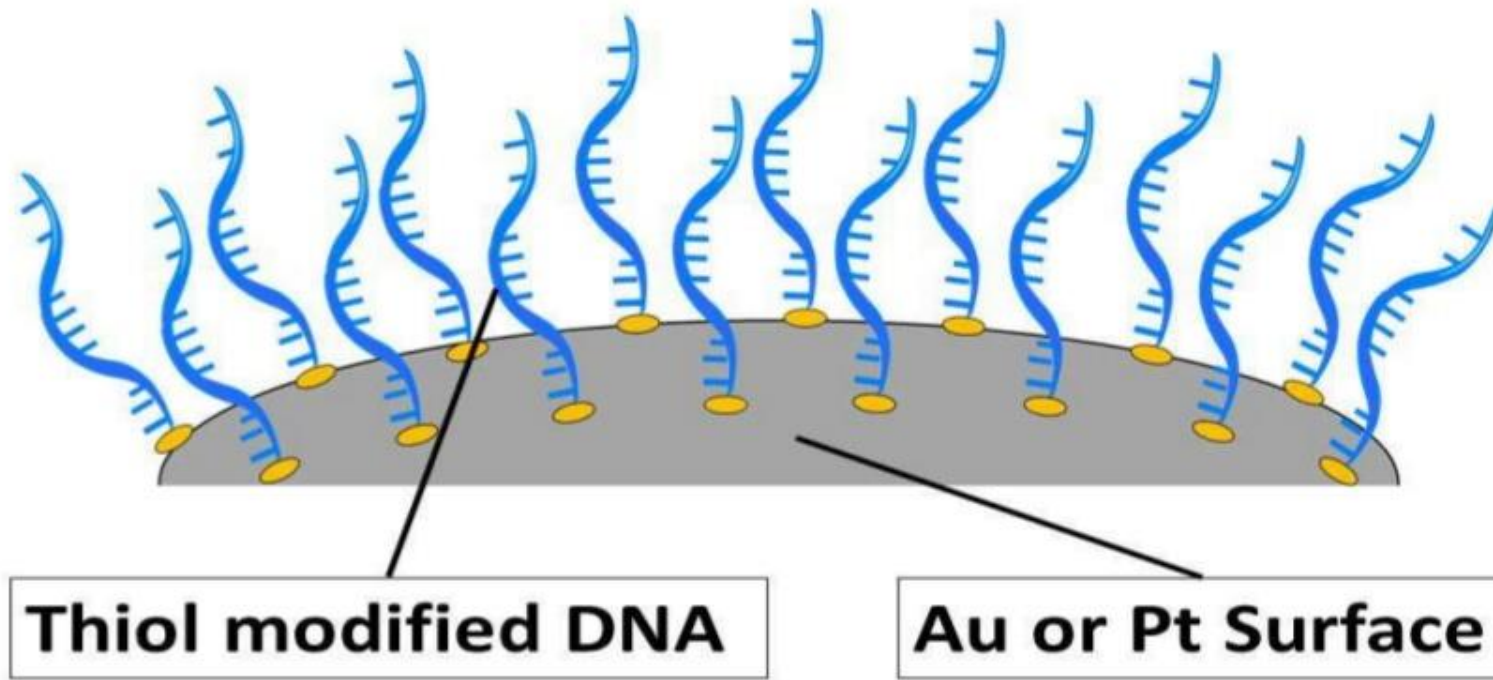
❖ **Types of DNA Based Biosensors**

- Optical
- Electrochemical
- Piezoelectric

Immobilization of DNA Probe onto Transducer Surface

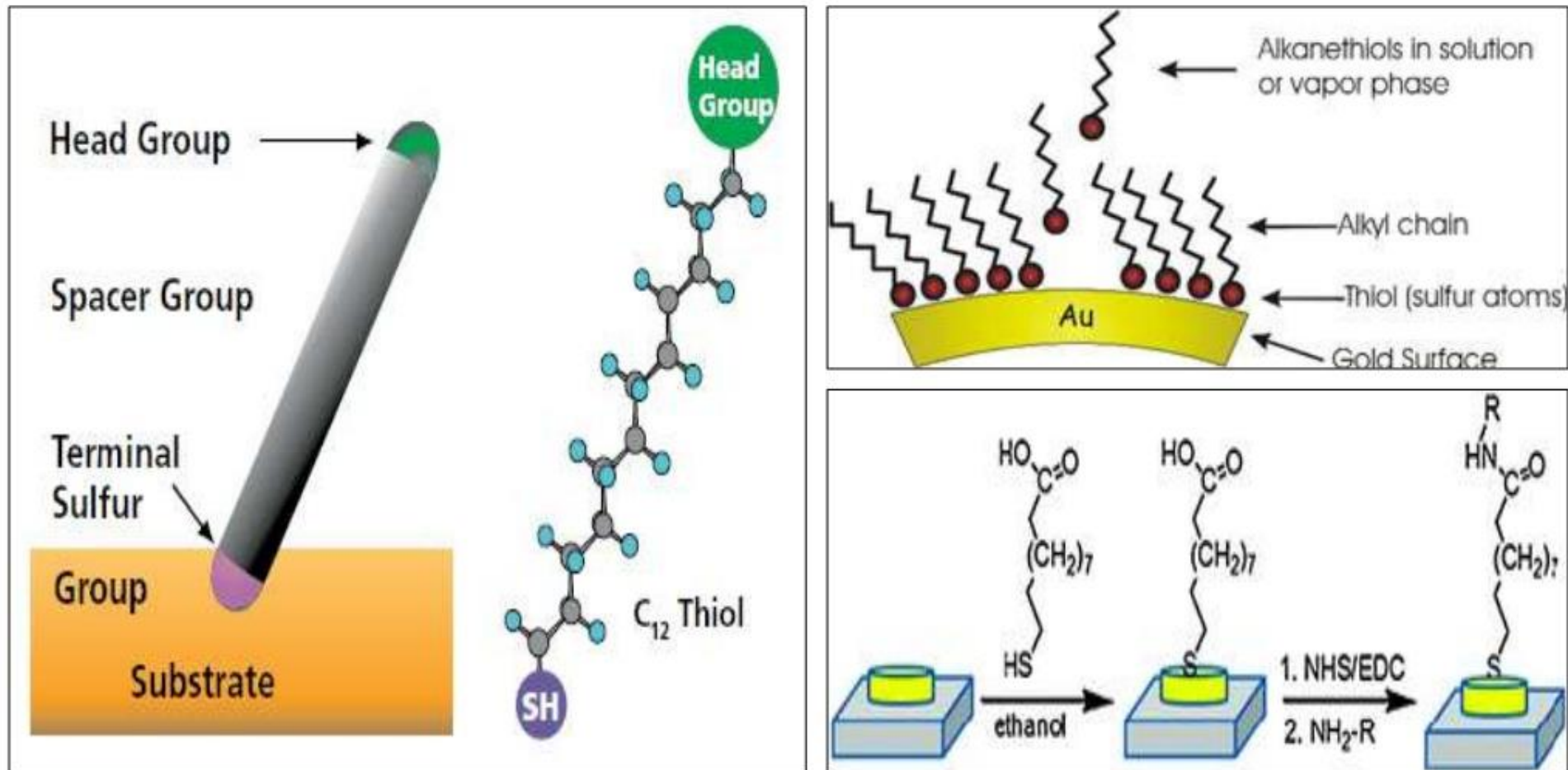
- Thiolated DNA for self assembly onto gold (or platinum) transducers

SAM conjugation



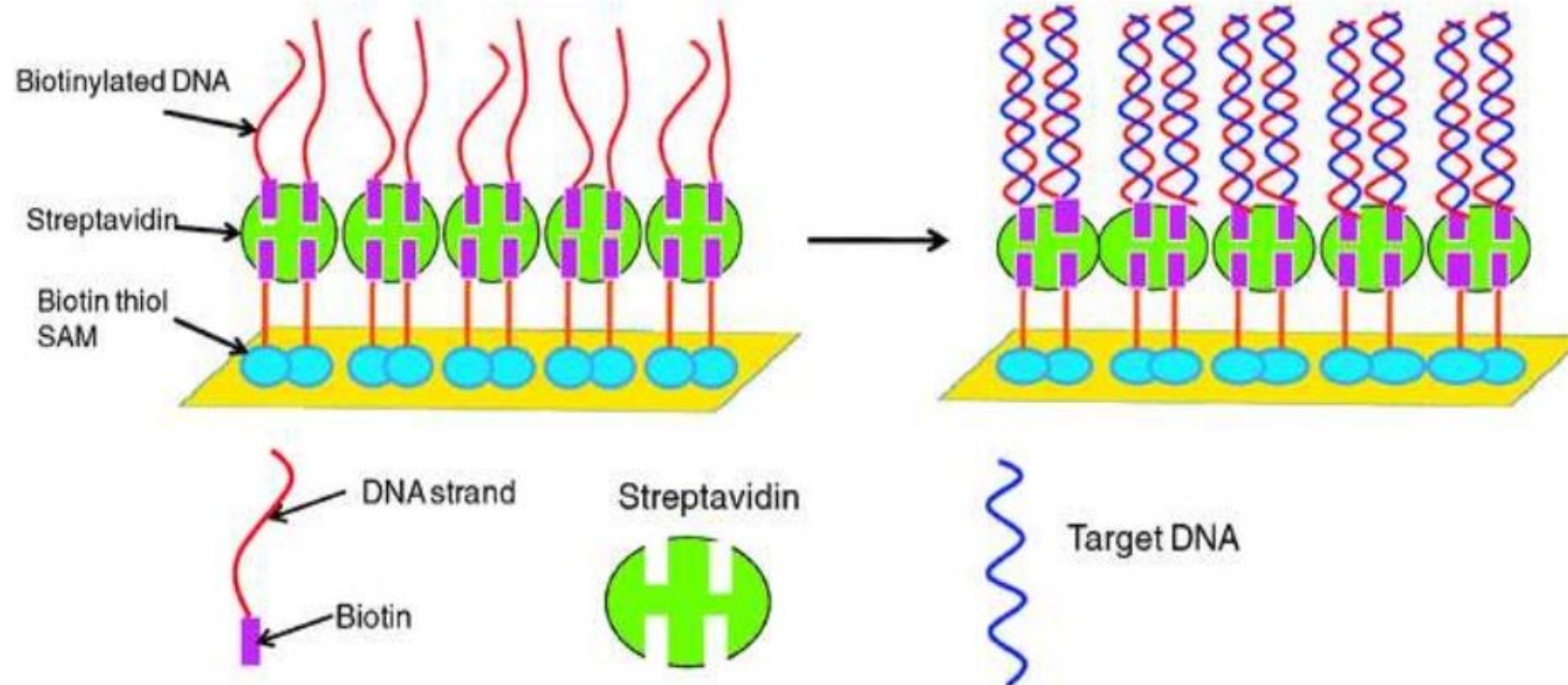
Immobilization of DNA Probe onto Transducer Surface

- Covalent linkage to the gold surface via functional **alkanethiol-based** monolayers



Immobilization of DNA Probe onto Transducer Surface

- Use of biotinylated DNA for complex formation with a surface-confined avidin or streptavidin





UNIVERSITÀ
degli STUDI
di CATANIA

DIPARTIMENTO DI SCIENZE CHIMICHE
Viale Andrea Doria, 6 – I-95125 Catania

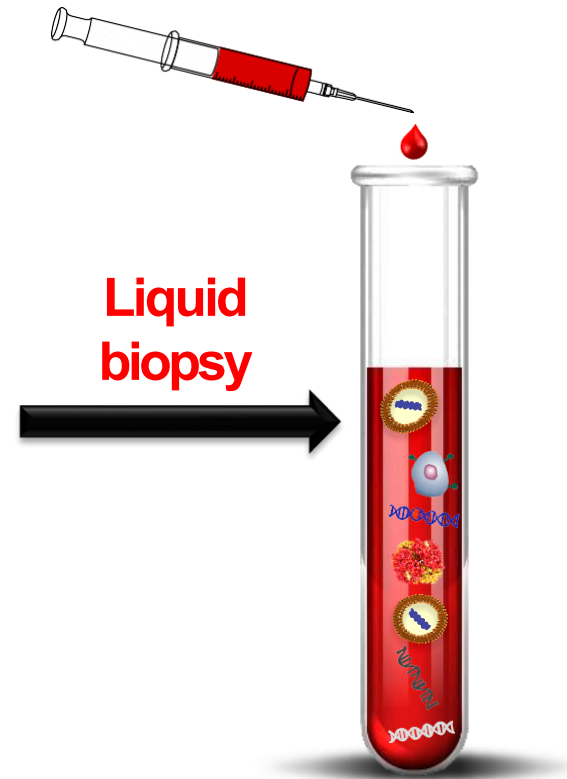
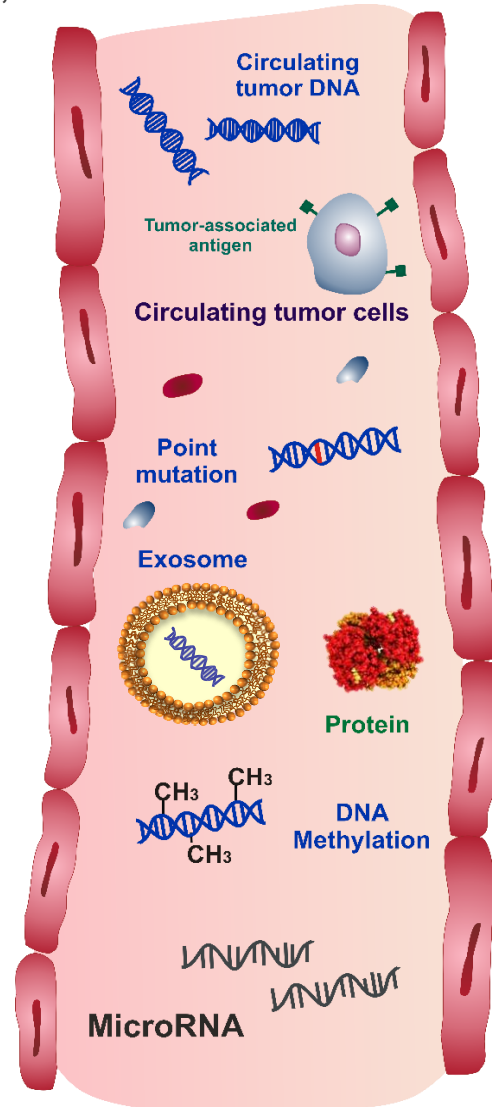
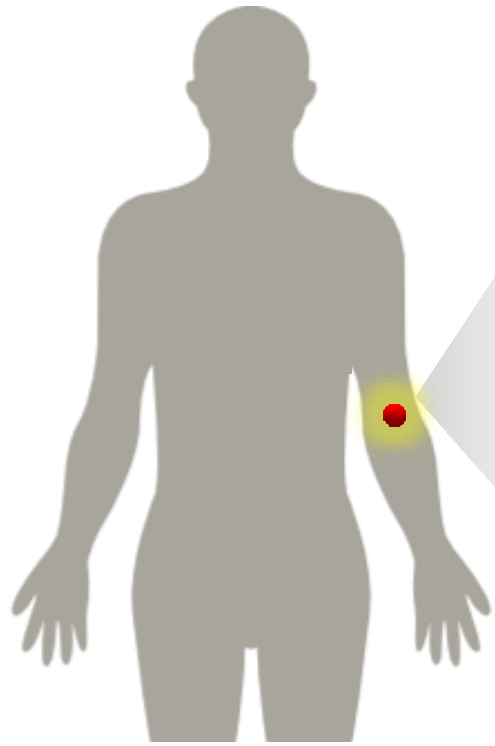
Tecniche innovative ed ultrasensibili PCR-free per la diagnosi precoce di acidi nucleici in biopsia liquida

Noemi Bellassai

Webinar, 28 Aprile 2021

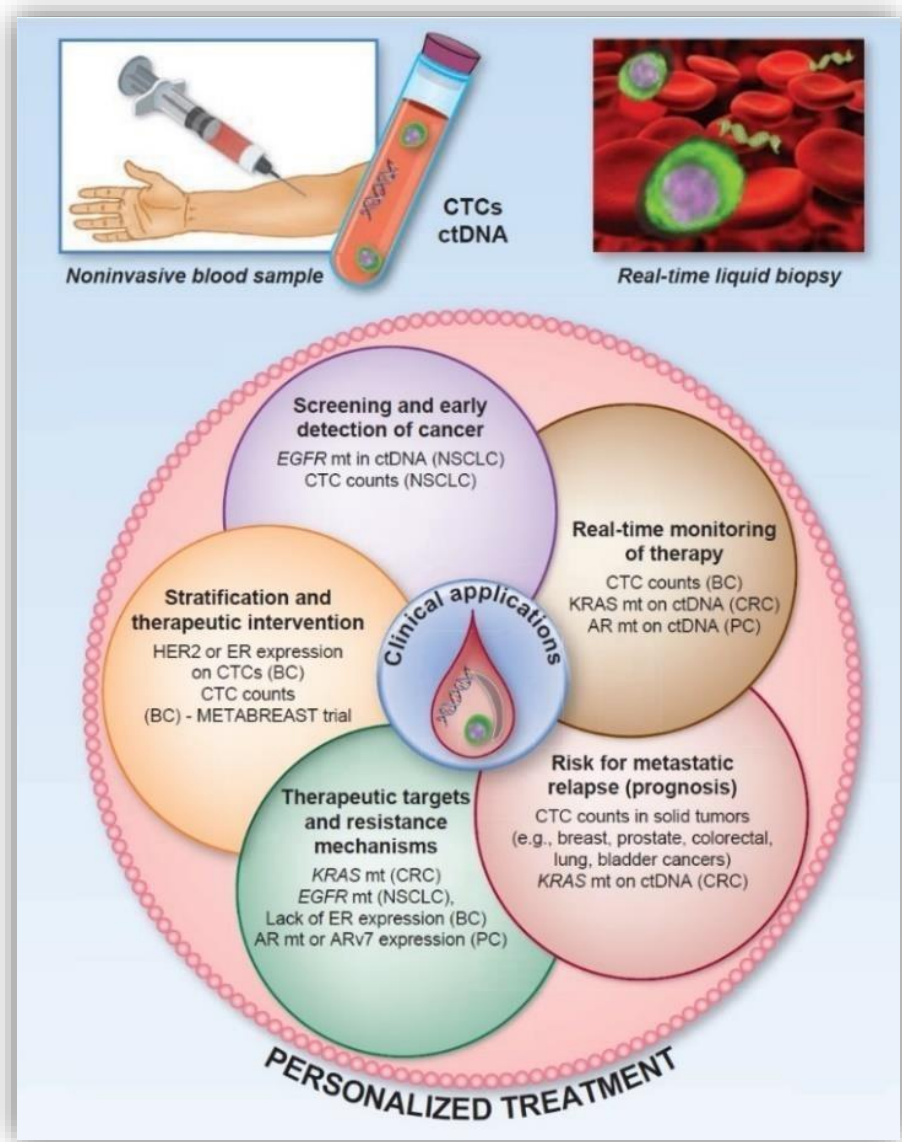
Liquid biopsy

Non-invasive test based on the detection of biomarkers related to specific disease circulating in body fluids (blood, plasma, serum, urine, saliva, synovial fluid etc.).



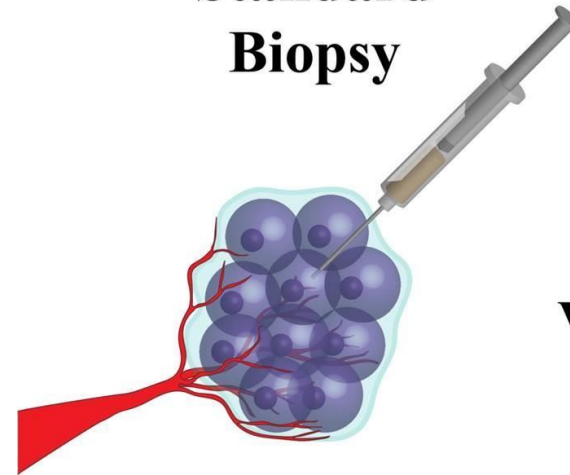
- ctDNA
- miRNA
- Protein
- CTCs

Liquid biopsy



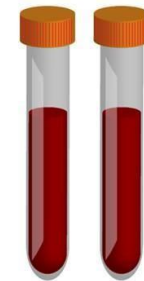
Alix-Panabières et al., Cancer Discov. 2016; 6(5), 479

Standard Biopsy



Time-Intensive Procedure
 Localized Sampling of Tissue
 Not Easily Obtained
 Some Pain/Risk
 Invasive

Liquid Biopsy



Quick
 Comprehensive Tissue Profile
 Easily Obtained
 Minimal Pain/Risk
 Minimally Invasive

VS.

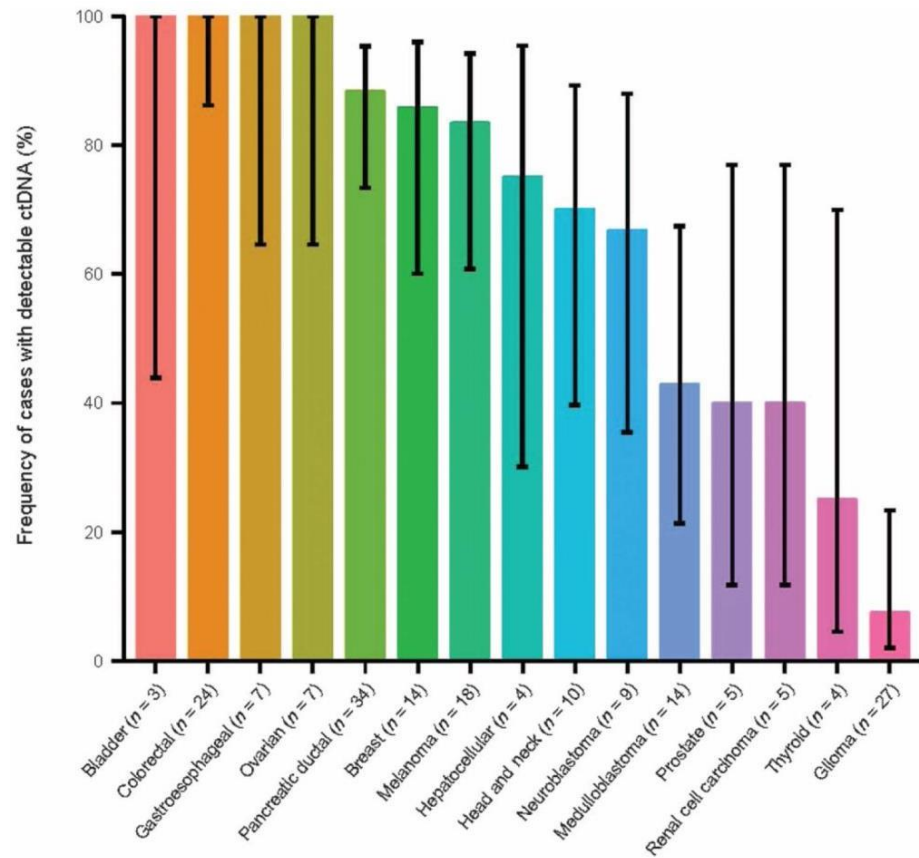
Lovly et al. 2016. Circulating Tumor DNA. My Cancer Genome (Updated February 8).

Sosa et al., Nat. Rev. Cancer. 2014; 14:611-622

Liquid biopsy for early diagnosis disease

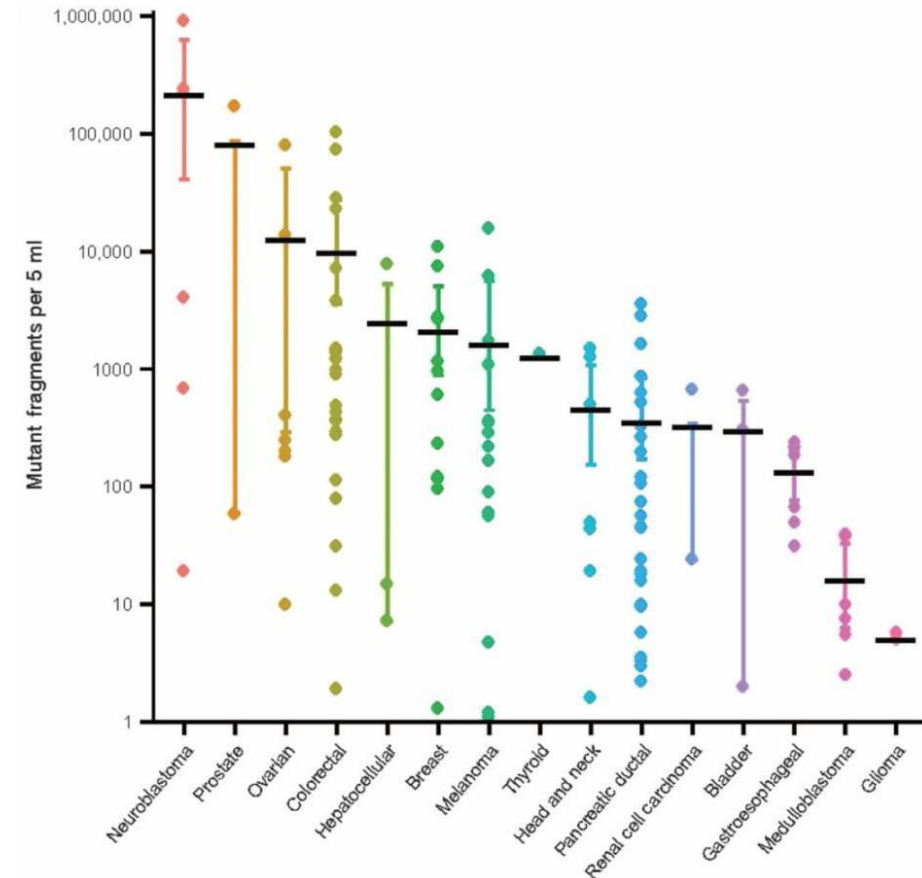
The opportunity

Circulating tumour DNA (ctDNA) is easy accessible and can be detected in most metastatic cancers

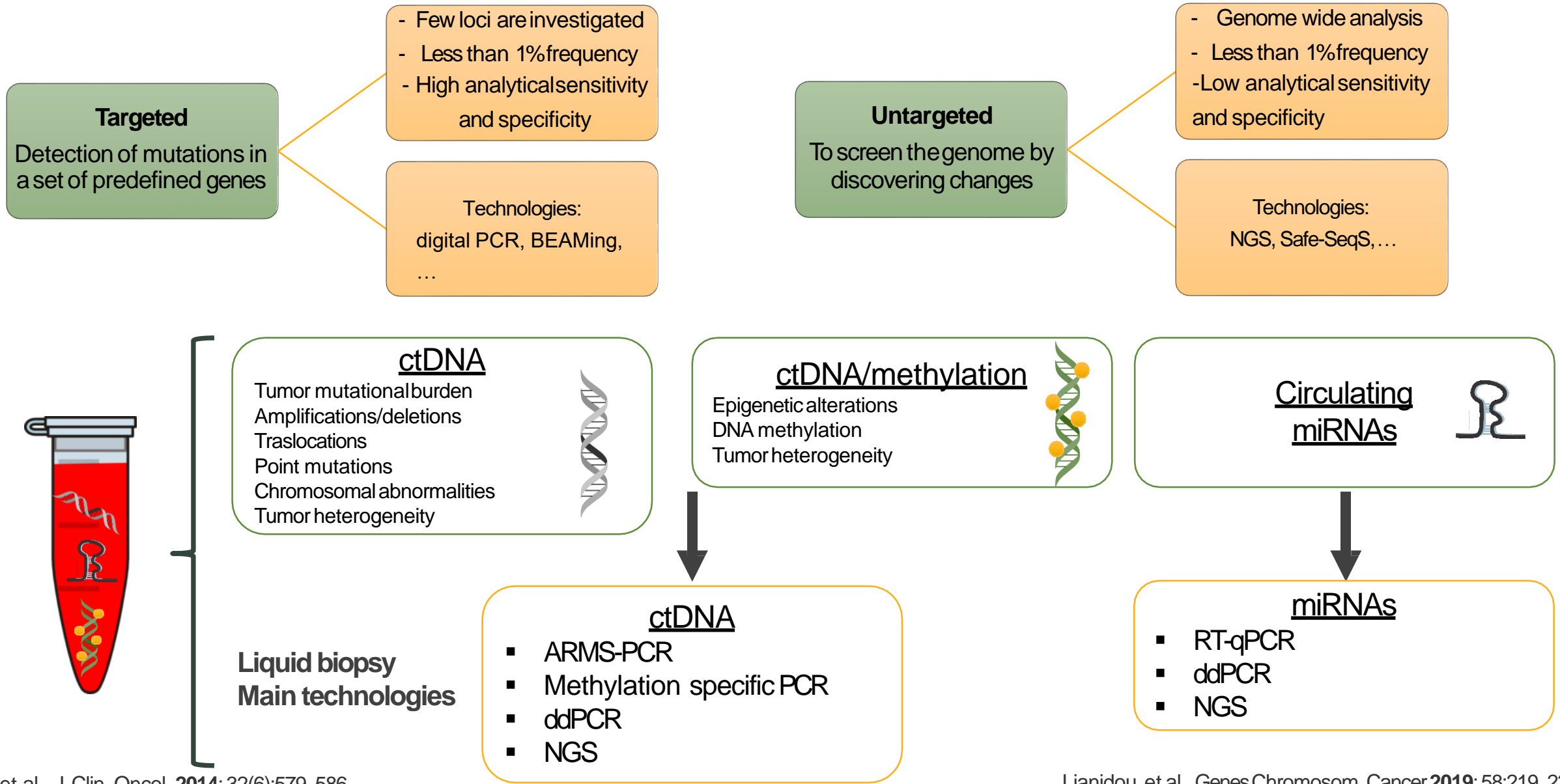


The challenge

ctDNA is often only present at low levels



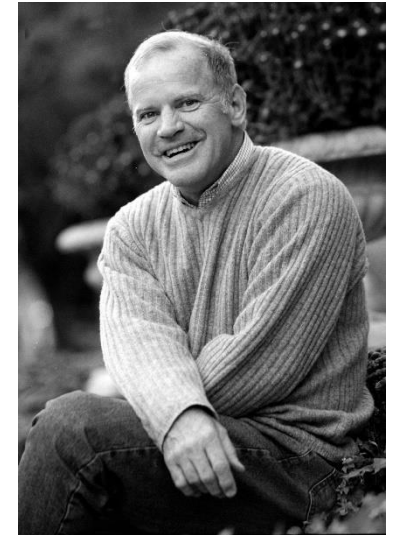
Detection of nucleic acid biomarkers



Target Amplification Methods

- **Polymerase chain reaction (PCR)**
 - **PCR using specific probes**
 - **RT PCR**
 - **Nested PCR-increases sensitivity, uses two sets of amplification primers, one internal to the other**
 - **Multiplex PCR-two or more sets of primers specific for different targets**
 - **Arbitrarily Primed PCR/Random Primer PCR**
- **Isothermal methods**

**Polymerase chain reaction
(PCR) Inventor**



**Kary Banks Mullis
(1944-2019)**

**Nobel Prize in Chemistry
1993**

Beyond PCR ... Isothermal amplification

Nucleic acids amplification operated at a constant temperature

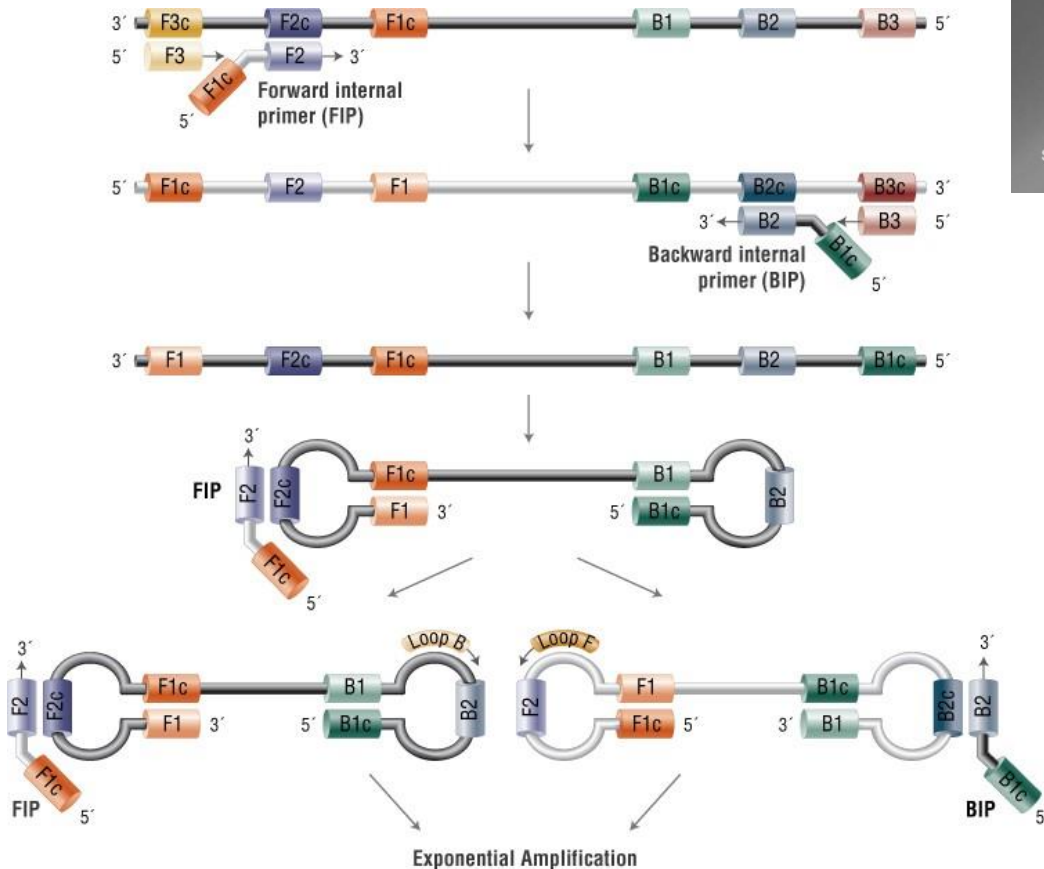
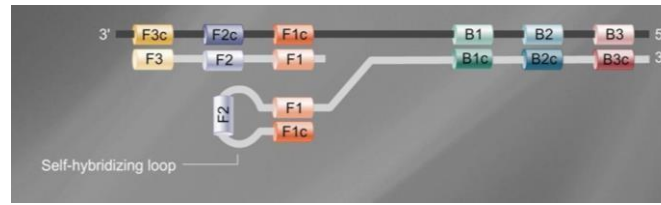
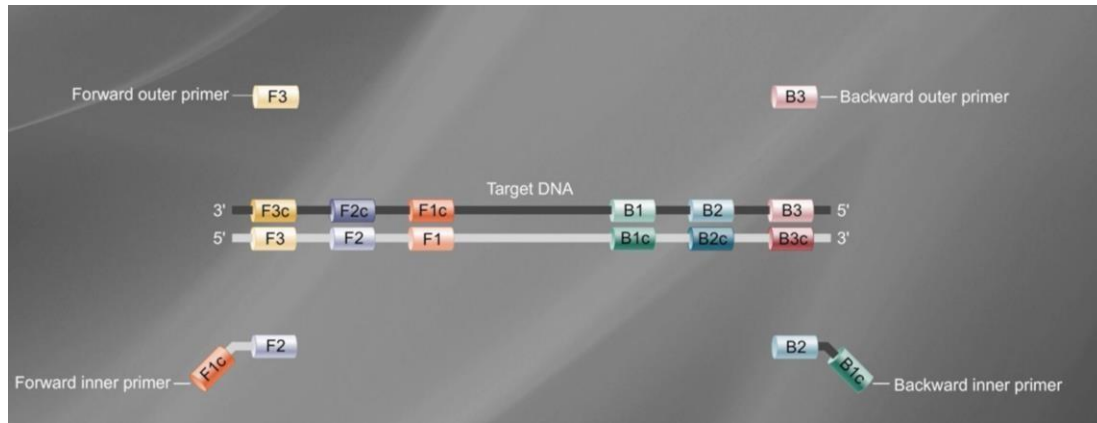
- Implementation in point-of-care devices is simplified
- Can be performed under simple conditions (e.g., water bath)
- Many isothermal amplification methods are available providing exponential or linear amplification
- Enzymatic and enzyme-free isothermal amplification methods are available

Method	Temp (°C)	Reaction time (min)	Amplification	Target	Primers	Main applications
LAMP	60-65	30-60	10^9	dsDNA hundred base- pair long	4-6	Bacteria, Viruses
RPA	25-42	5-20	10^9 - 10^{11}	dsDNA A ssDNA RNA	2	Pathogens, Viruses
NASBA	~41	90-120	10^9	RNA	2	Bacteria, Pathogens
RCA	30-65	60-120	10^3 linear 10^9 expon.	ssDNA	1	Plasmid, Viruses
NEEA	54-58	15-30	10^9	dsDNA RNA	2	Viruses, RNA DNA
HDA	37-60	60-120	10^6	dsDNA	2	Biomarkers, Viruses

Loop mediated isothermal amplification (LAMP)

- Amplification takes place at a single temperature (65°C)
(No need of thermal cycler)
- Uses polymerase with high strand displacement activity
(*Bacillus stearothermophilus* Bst DNA Polymerase instead of *Taq*Poly)
- Amplification efficiency is high (up to 10^9)
- Can be also used for RNA templates by addition of reverse transcriptase

Loop mediated isothermal amplification (LAMP)



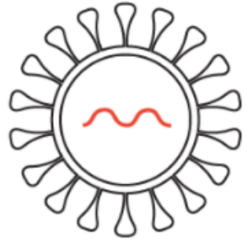
Loop-mediated isothermal amplification (LAMP) uses 4-6 primers recognizing 6-8 distinct regions of target DNA.

A strand-displacing DNA polymerase initiates synthesis and 2 of the primers form loop structures to facilitate subsequent rounds of amplification.

<https://www.youtube.com/watch?v=L5zi2P4lggw>

LAMP-Based SARS-CoV-2 Testing Methods

SARS-CoV-2 Rapid Colorimetric LAMP Assay Kit



SARS-CoV-2

ORF1ab E N

B3 LB BIP LF FIP F3

SARS-CoV-2 (+) ssRNA
(30 kb)

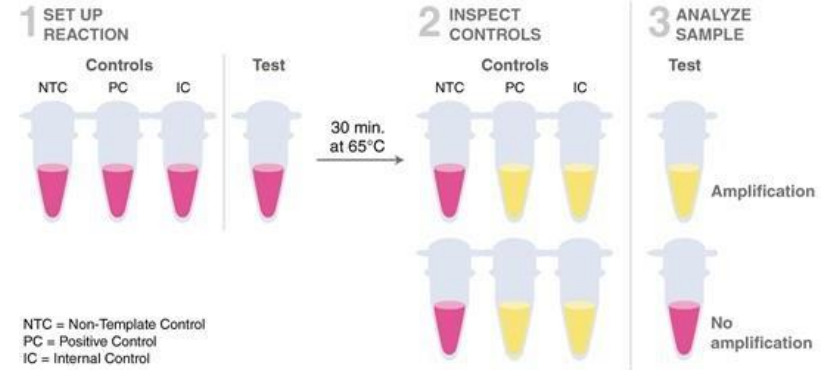
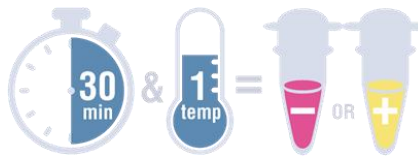
target region

RT - 1st strand

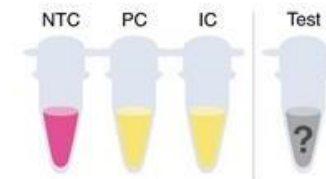
cDNA - 2nd strand

dumbbell DNA structure

high molecular weight
amplicons

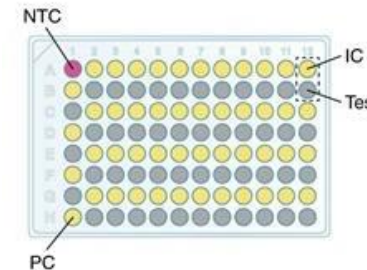


ON-DEMAND TESTING



Reactions/sample	4
Reactions/kit	96
Samples/kit	24

HIGH-THROUGHPUT TESTING



Reactions/sample	2	+1 NTC per plate +1 PC per plate
Reactions/kit	96	
Samples/kit	47	

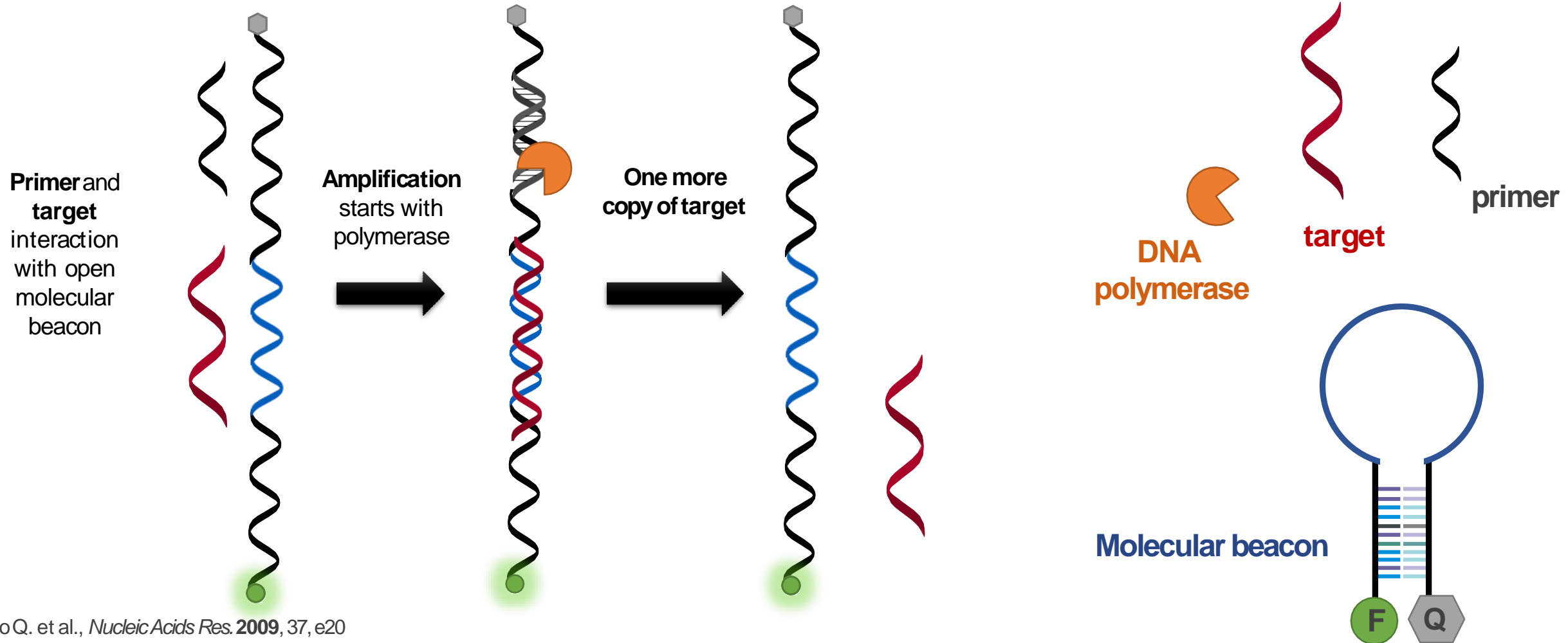
NTC = Non-Template Control PC = Positive Control IC = Internal Control

Molecular beacon-assisted isothermal circular strand displacement polymerization (ICSDP)

Isothermal amplification

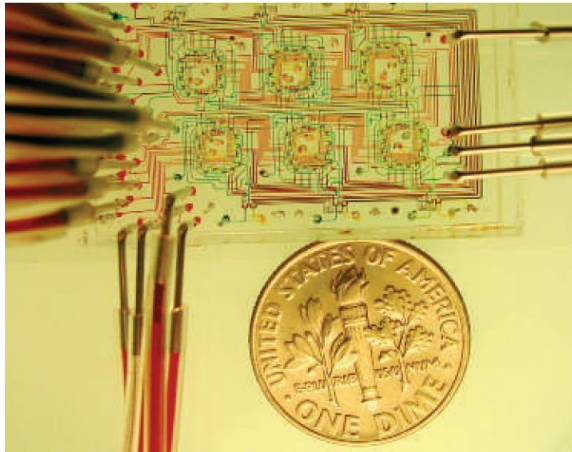
Isothermal circular strand displacement polymerization. Displaced target available for a new cycle.

Linear amplification



MICROFLUIDICS

It is the science and technology of systems that process or manipulate small (10^{-9} to 10^{-18} litres) amounts of fluids, using channels with dimensions of tens to hundreds of micrometres.



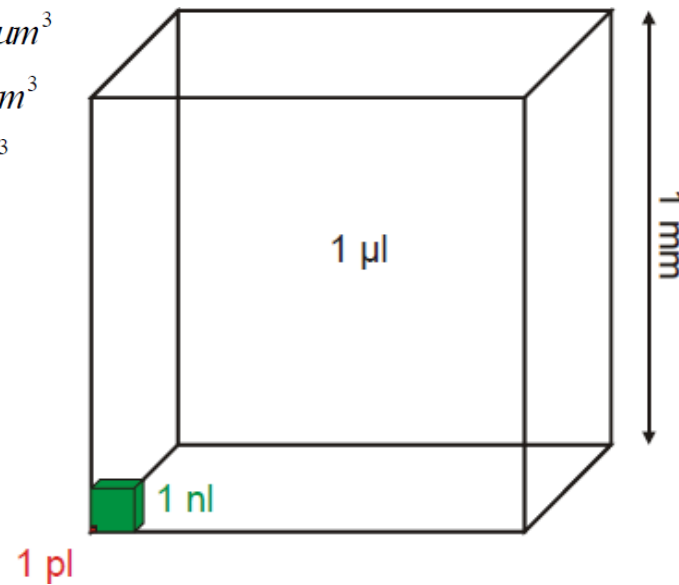
$$1l = 1dm^3$$

$$1\mu l = 1mm^3$$

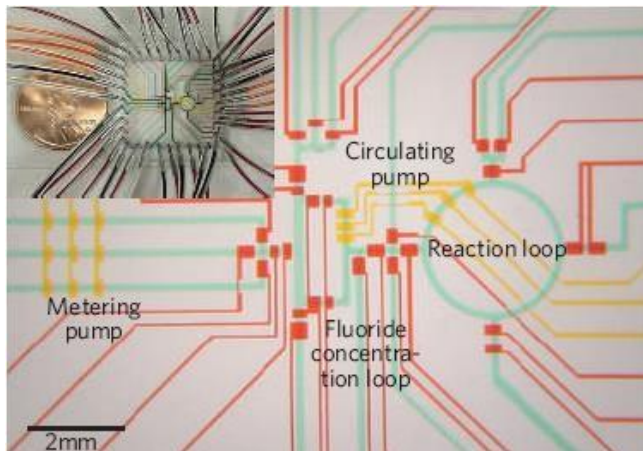
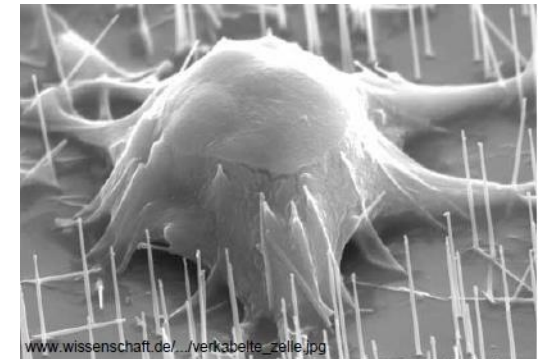
$$1nl = 100\mu m^3$$

$$1pl = 10\mu m^3$$

$$1fl = 1\mu m^3$$



Typical size of a cell $1-30\mu m$

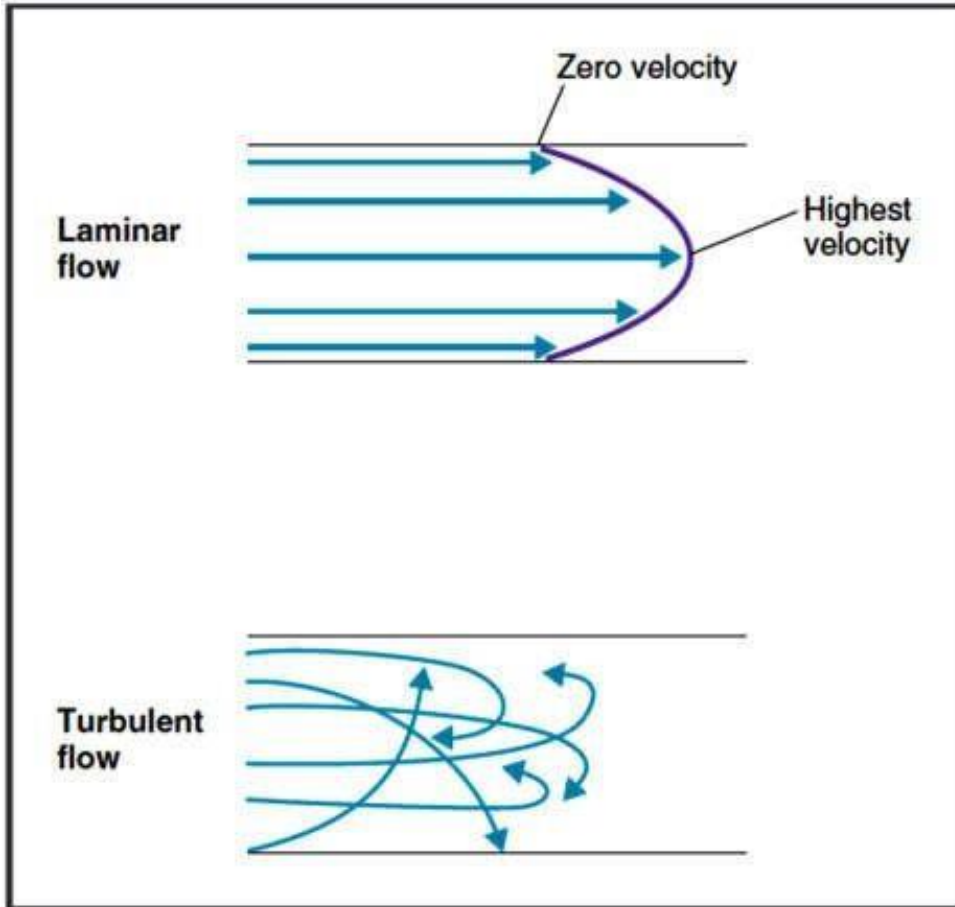


Drug inhaler, Droplet diameter $\sim 5\mu m$



MICROFLUIDICS

Newtonian fluid → laminar flow



Model for the description of the motion of fluids

- Non-dimensional Navier-Stokes equation

$$\frac{\rho UL}{\mu} \left(\frac{\partial \mathbf{u}'}{\partial t'} + \mathbf{u}' \nabla \mathbf{u}' \right) = -\nabla p' + \eta \nabla^2 \mathbf{u}' + \mathbf{f}'$$

Reynolds number

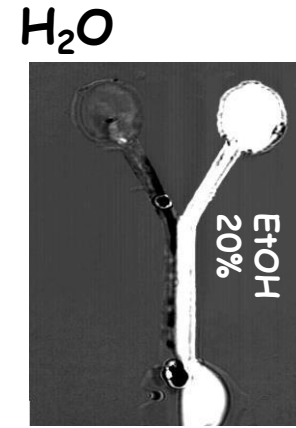
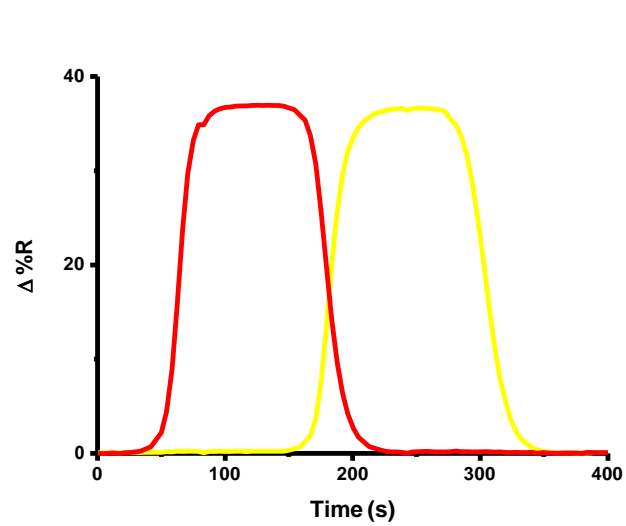
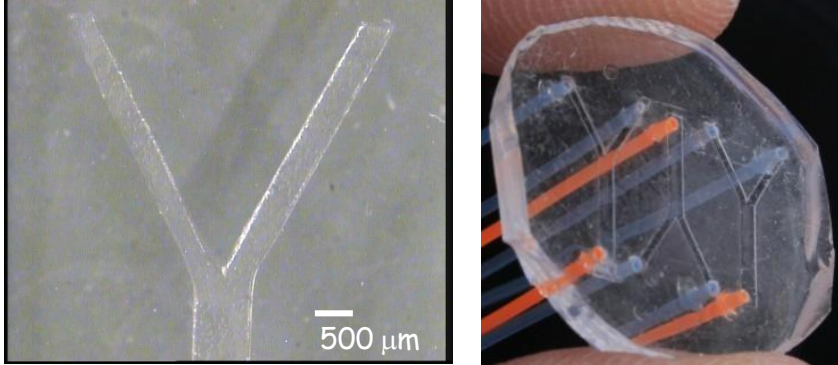
$$Re = \frac{\rho UL}{\mu} \approx \frac{\text{Inertial forces}}{\text{Viscous forces}}$$

Re > 2000
Turbulent

Re < 2000
Laminar

MICROFLUIDICS: devices fabrication

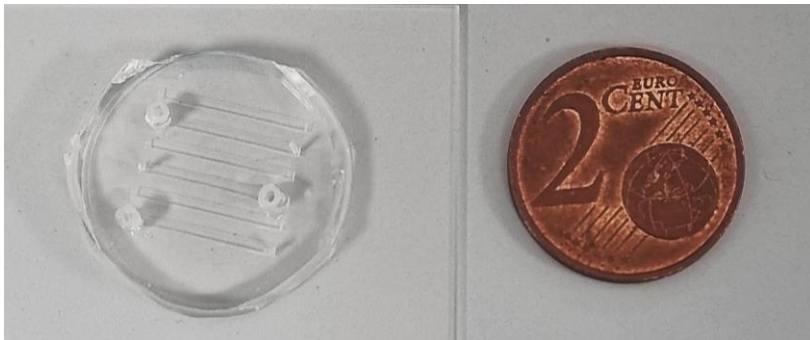
Fabrication of microfluidic device by PDMS replica molding



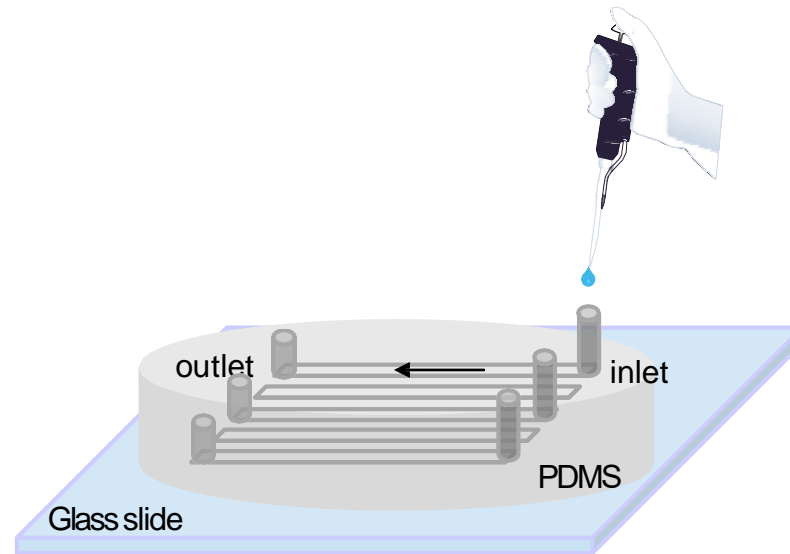
$Re \approx 100$

Laminar flow

Immiscible liquids



microfluidic channels (14×0.4×0.8mm)

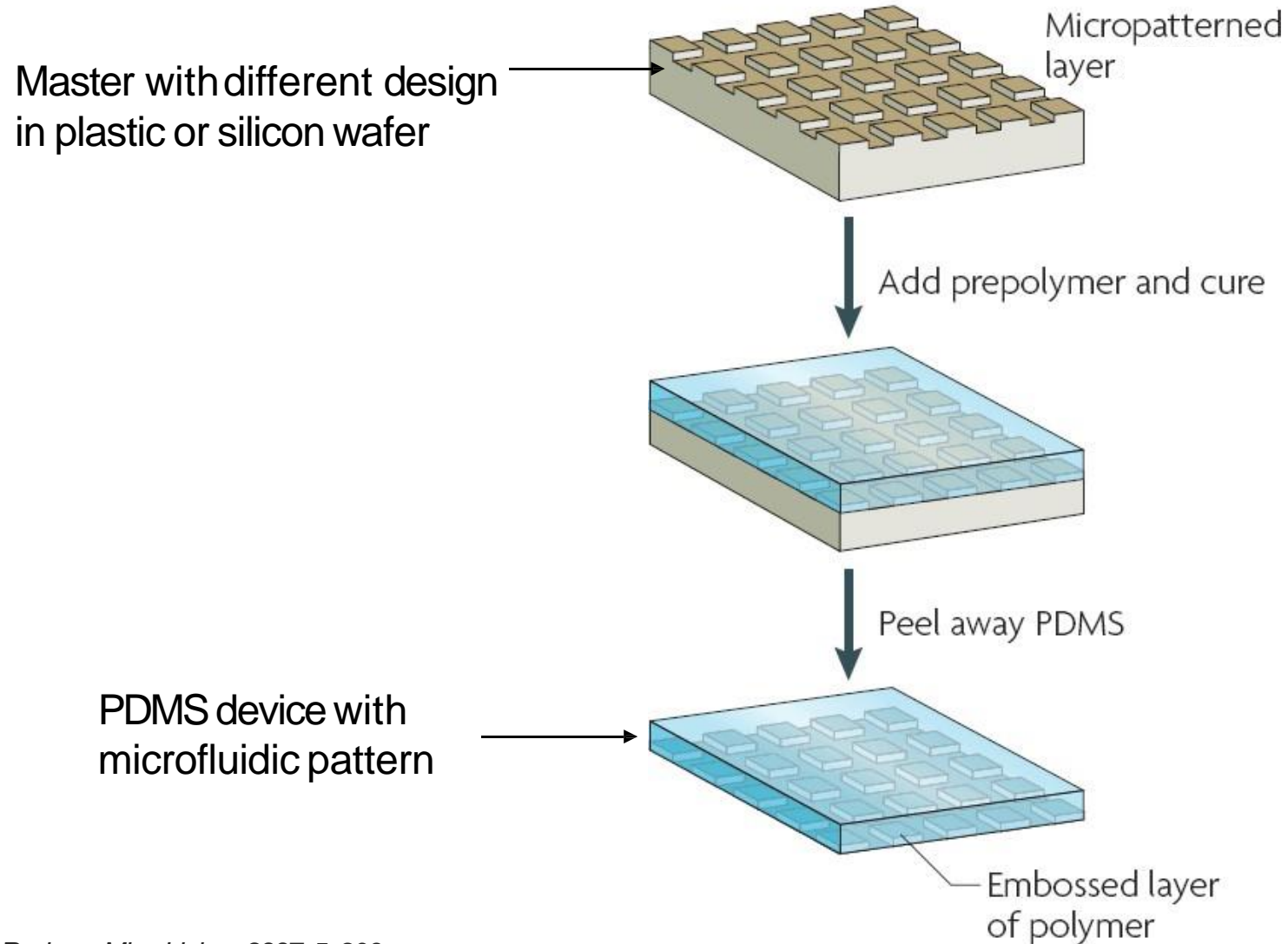


< 1 μ L of sample volume

Parallel microchannels for multiple detection

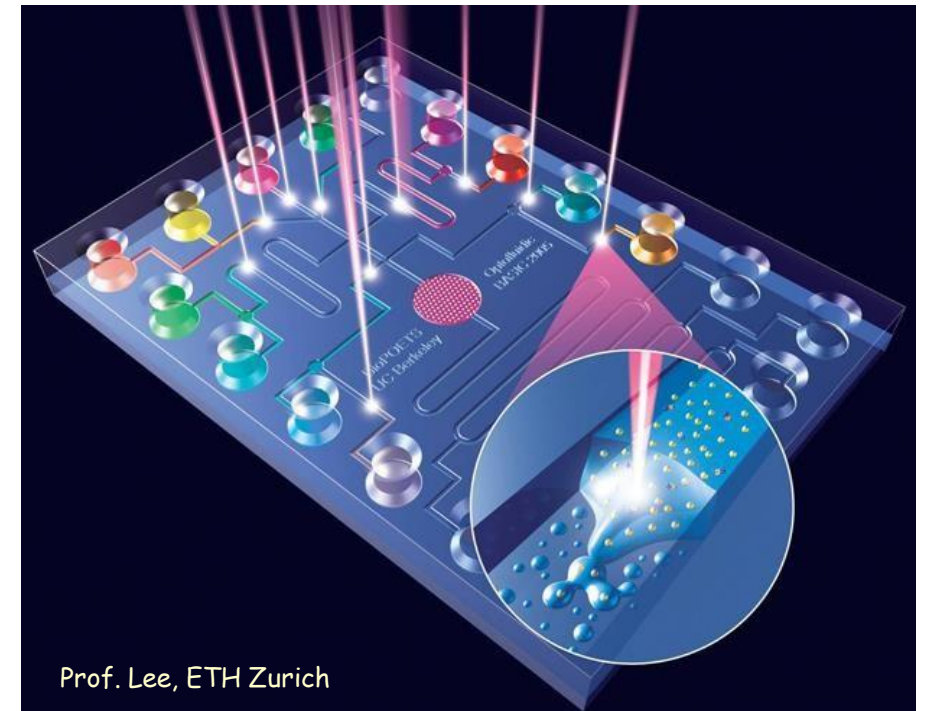
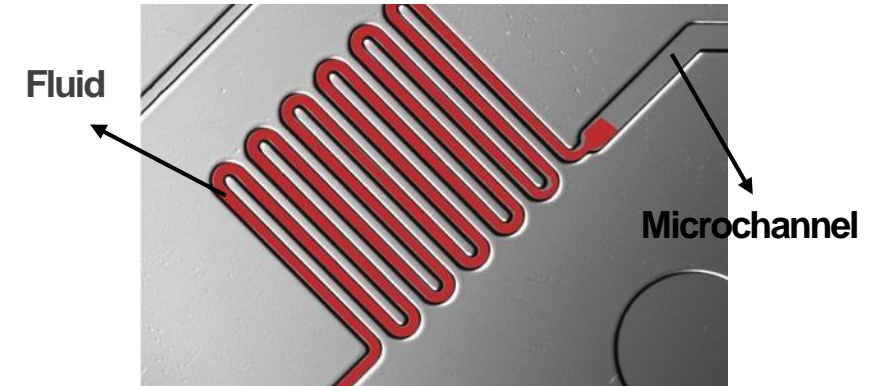
MICROFLUIDICS: devices fabrication

Fabrication of microfluidic device by PDMS
(polydimethylsiloxane) replica molding



MICROFLUIDICS: Why?

- **Small sample volume**
- **Miniaturization**
- **Reduction of analysis time**
- **Parallel devices and faster processes**
- **High-throughput**
- **Integration and portable devices**
(lab-on-a-chip, micro Total Analysis Systems μ TAS)



microRNA (miRNA)

- **Single-stranded, non-coding RNA molecules**
- **Key-role in protein expression**
- **mRNA silencing**
- **Remarkable stability when released into biofluids**



Challenges for miRNA detection

- Analytes are present at low concentrations

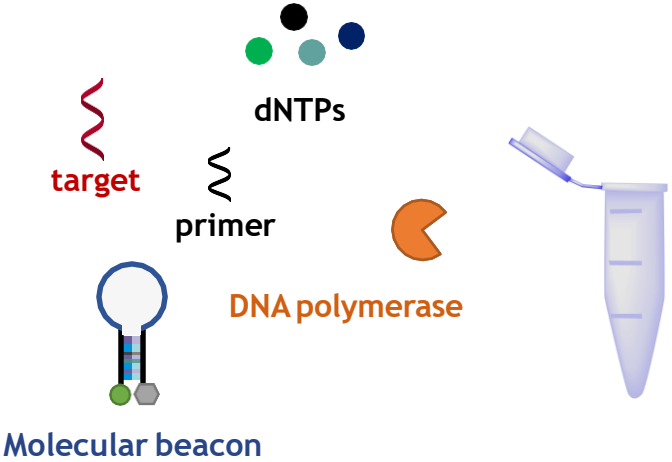
Biomarker levels: fg mL⁻¹ - ngmL⁻¹

- Short length sequence

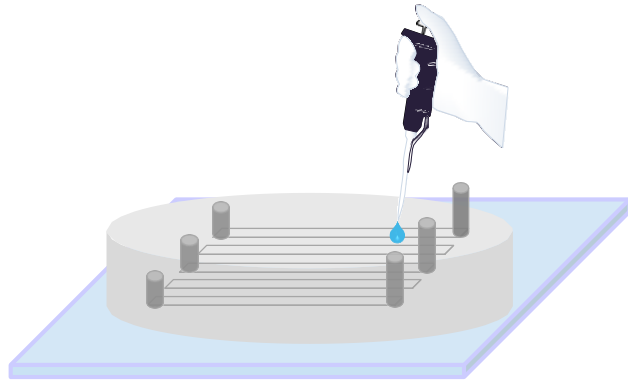
Length: 19-23 nt

- High sequence homology

Microfluidic lab-on-a-chip platform for liquid biopsy: microRNA

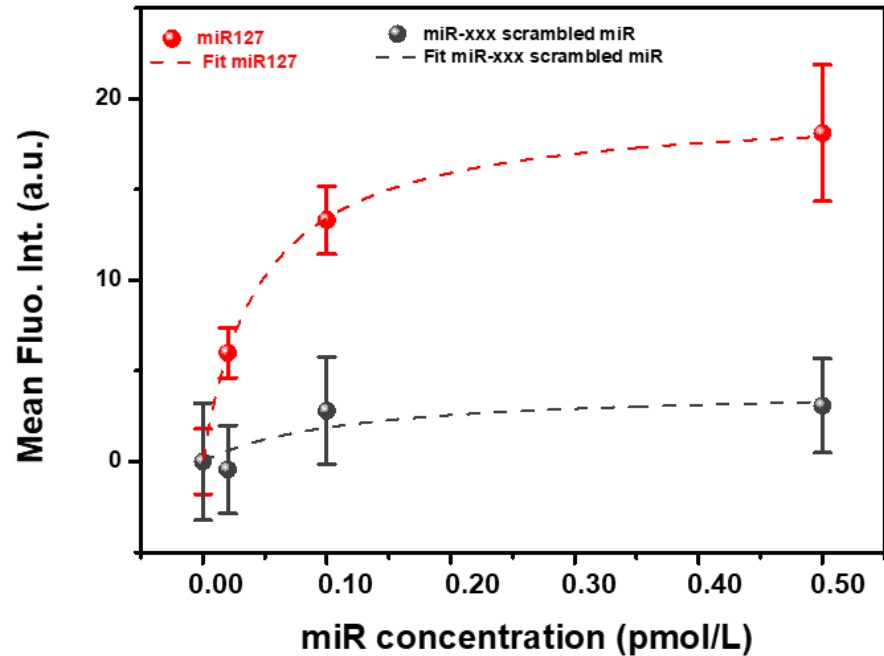


ICSDP
amplification
30 °C 2 hr
constant
temperature



Fluorescence
detection

microRNA-127
biomarker for chronic joint disease

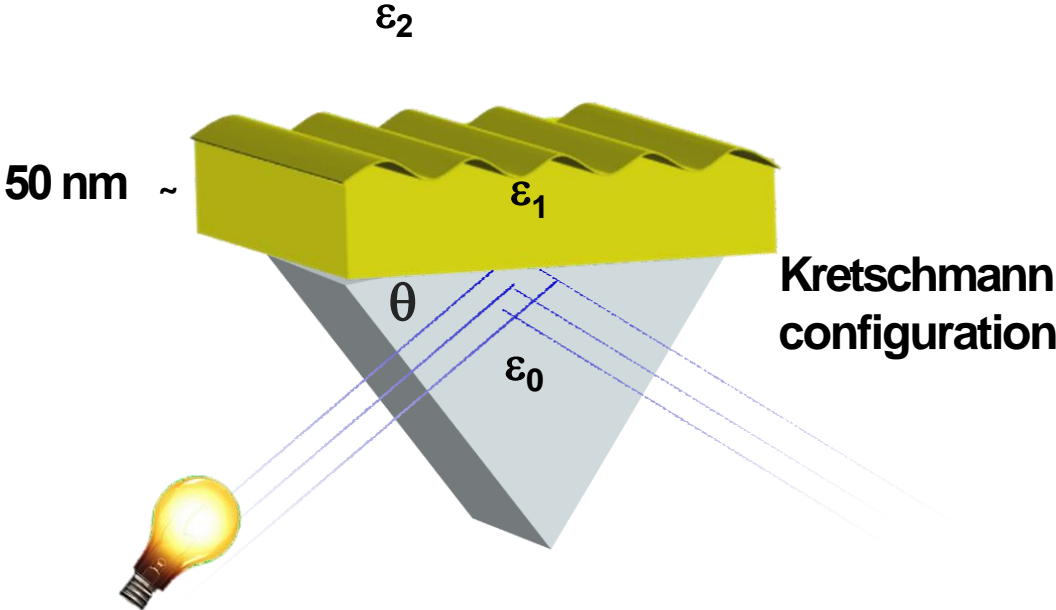


- Low sample volume
- No time consuming
- High selectivity in buffer
- Discrimination in synovial fluid
- Low detection

Optical biosensors: Surface Plasmon Resonance

Electromagnetic radiation in resonance with surface plasmon oscillation.

Surface plasmon polaritons : quasi-particles resulting from the coupling of surface plasmons and photons



Plasmon wave vector = radiation wave vector

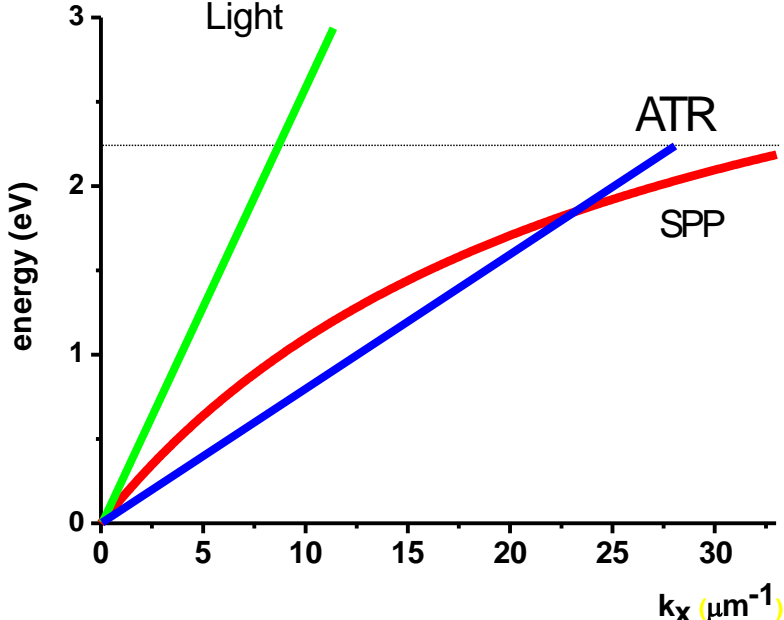
$$K_{SPP} = \frac{\omega}{c} \sqrt{\frac{\epsilon_1' \epsilon_2}{\epsilon_1' + \epsilon_2}} = \frac{\omega}{c} \sqrt{\epsilon_0} \sin \theta = K_{Light}$$

Radiation wave vector

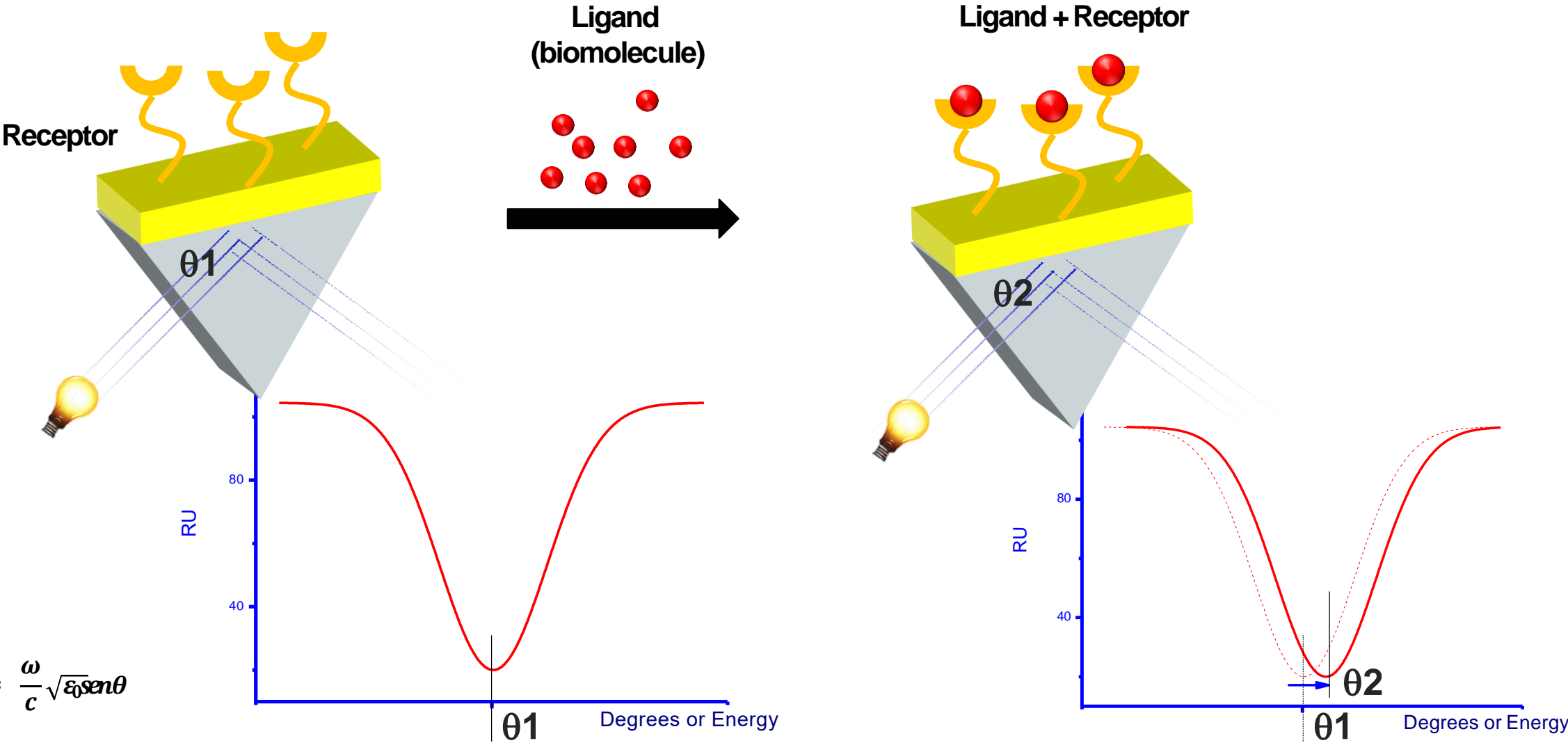
$$k_{light} = \frac{\omega}{c} \sqrt{\epsilon_0} \sin \theta$$

Snell's Law

$$\sin \theta = \frac{\epsilon_1}{\epsilon_0}$$



Optical biosensors: Surface Plasmon Resonance

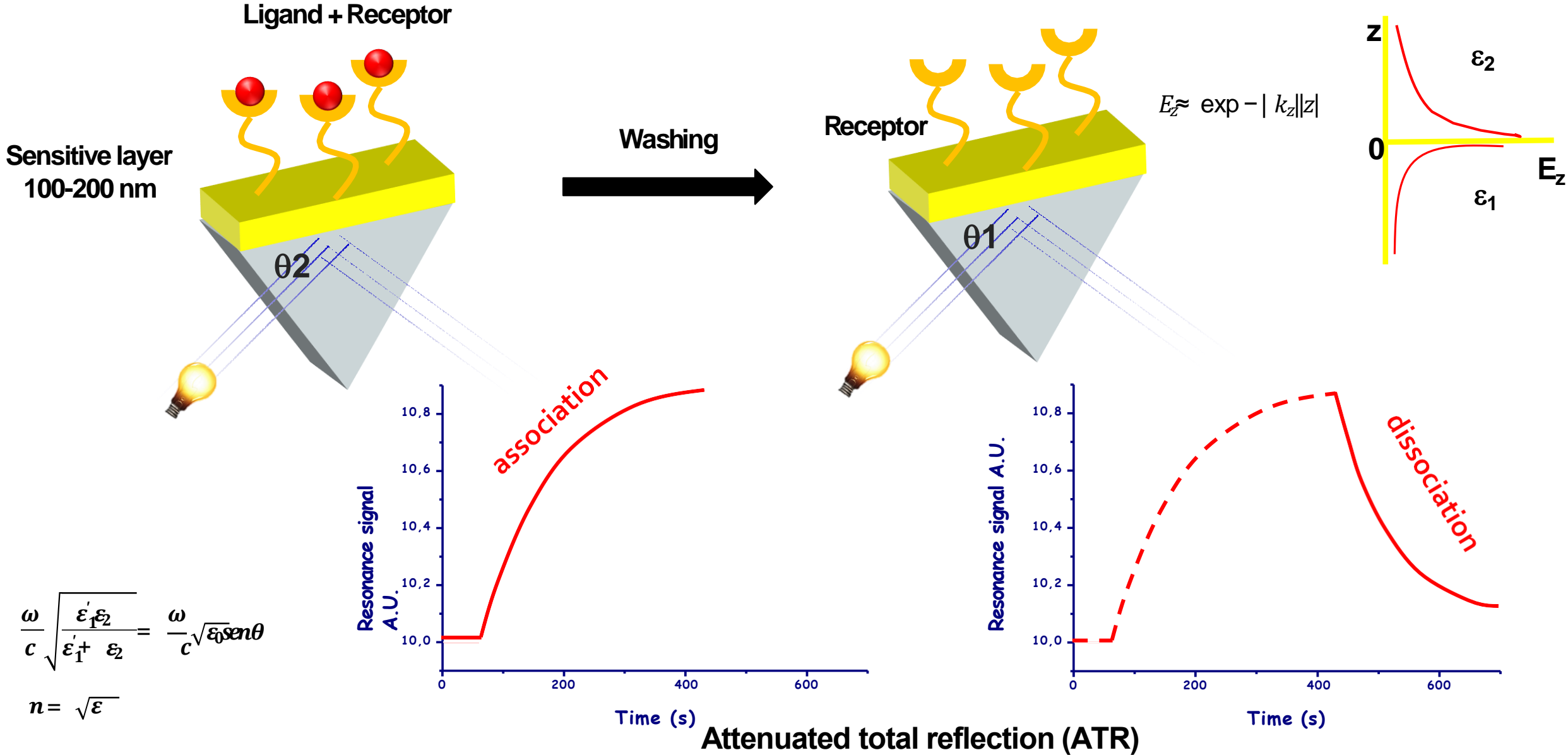


$$\frac{\omega}{c} \sqrt{\frac{\epsilon'_1 \epsilon_2}{\epsilon'_1 + \epsilon_2}} = \frac{\omega}{c} \sqrt{\epsilon_0} \sin \theta$$

$$n = \sqrt{\epsilon}$$

Attenuated total reflection (ATR)

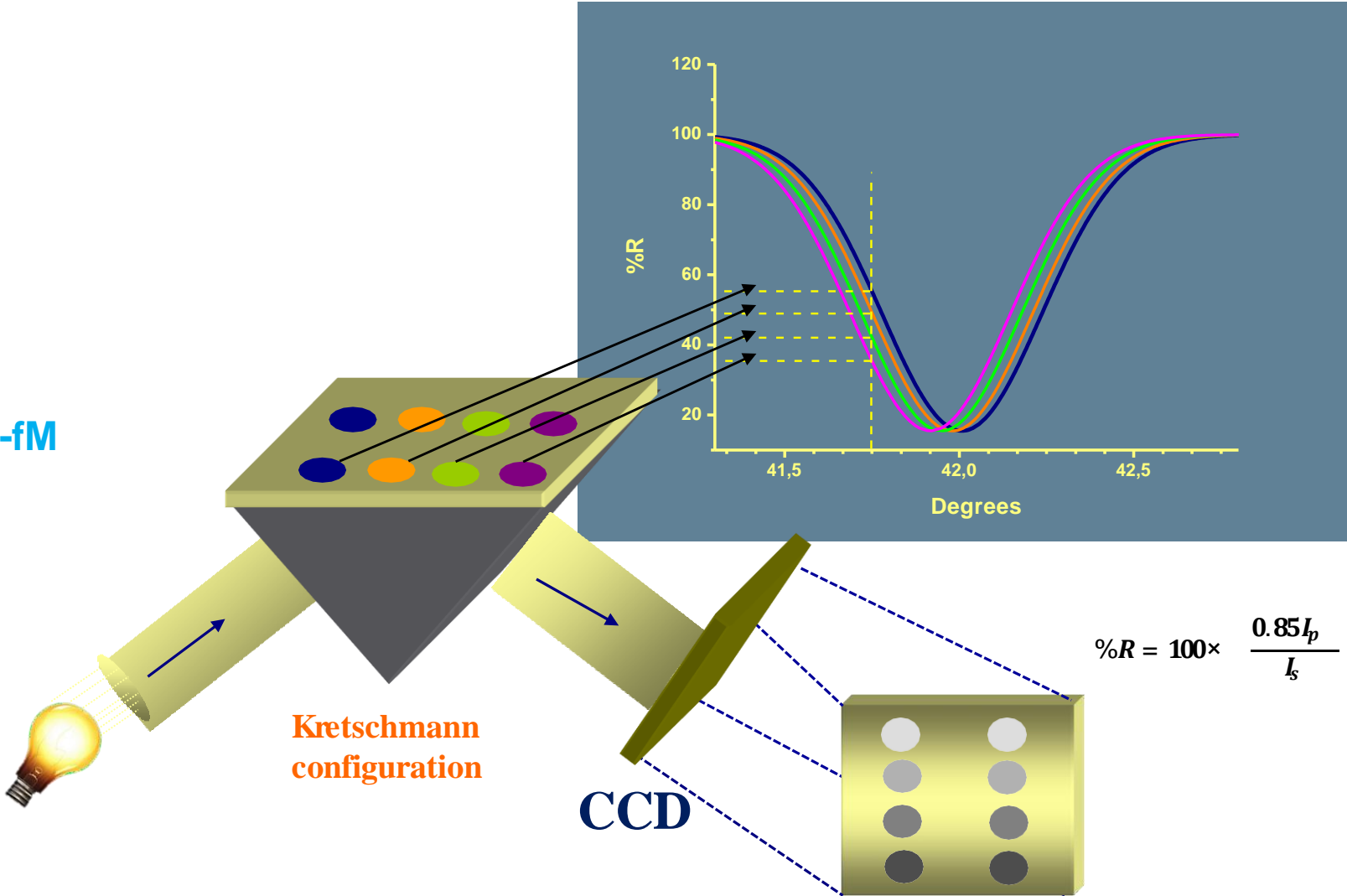
Optical biosensors: Surface Plasmon Resonance



Surface Plasmon Resonance Imaging (SPRI)

- Real-time analysis
- Label-free
- High sensitivity
- Multi-analyte monitoring

Sensitivity can be improved up to nM-fM
PCR-free method!



Rothenhäusler et al. Surface-plasmon microscopy. **1988**, Nature 332, 615–617
D'Agata et al. Anal Bioanal Chem. **2013**; 405(2-3):573-84.

Surface Plasmon Resonance Imaging (SPRI)

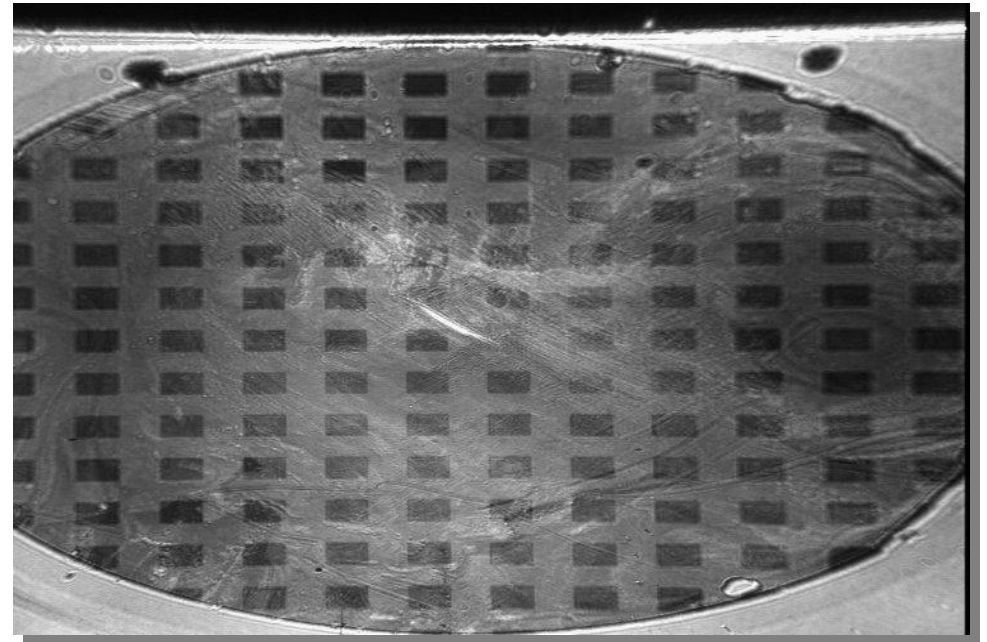
The lateral resolution of a SPR image is limited by the surface plasmon decay distance L_x that is the distance on the surface by which the intensity of the field associated to plasmons decreases by a $1/e$ factor.

$$L_x = \frac{1}{2k''_x}$$

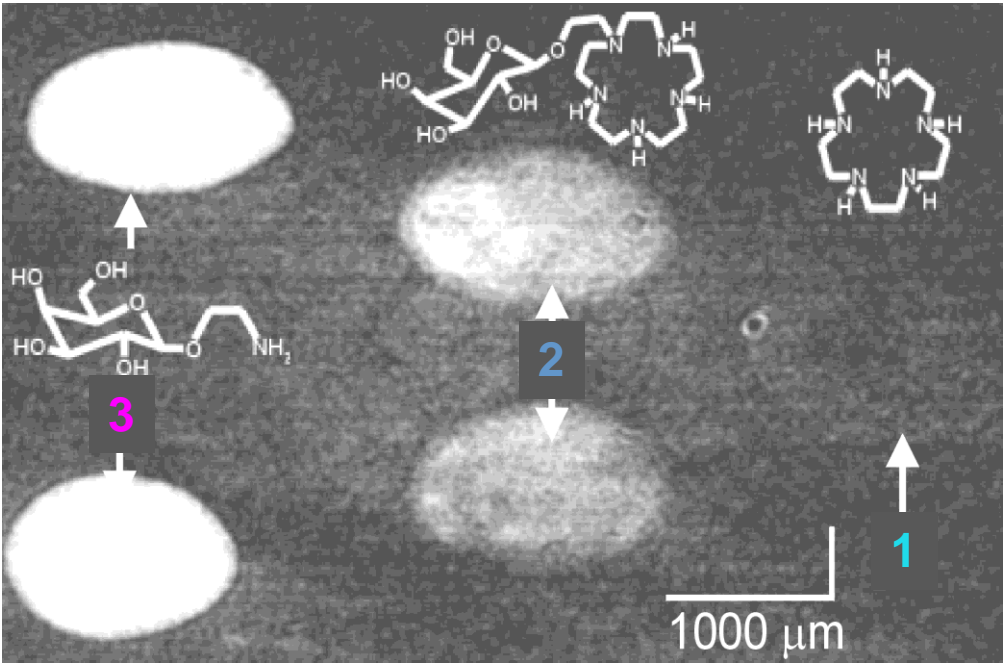
k''_x is the imaginary part of the x component of the wave-vector

For gold:

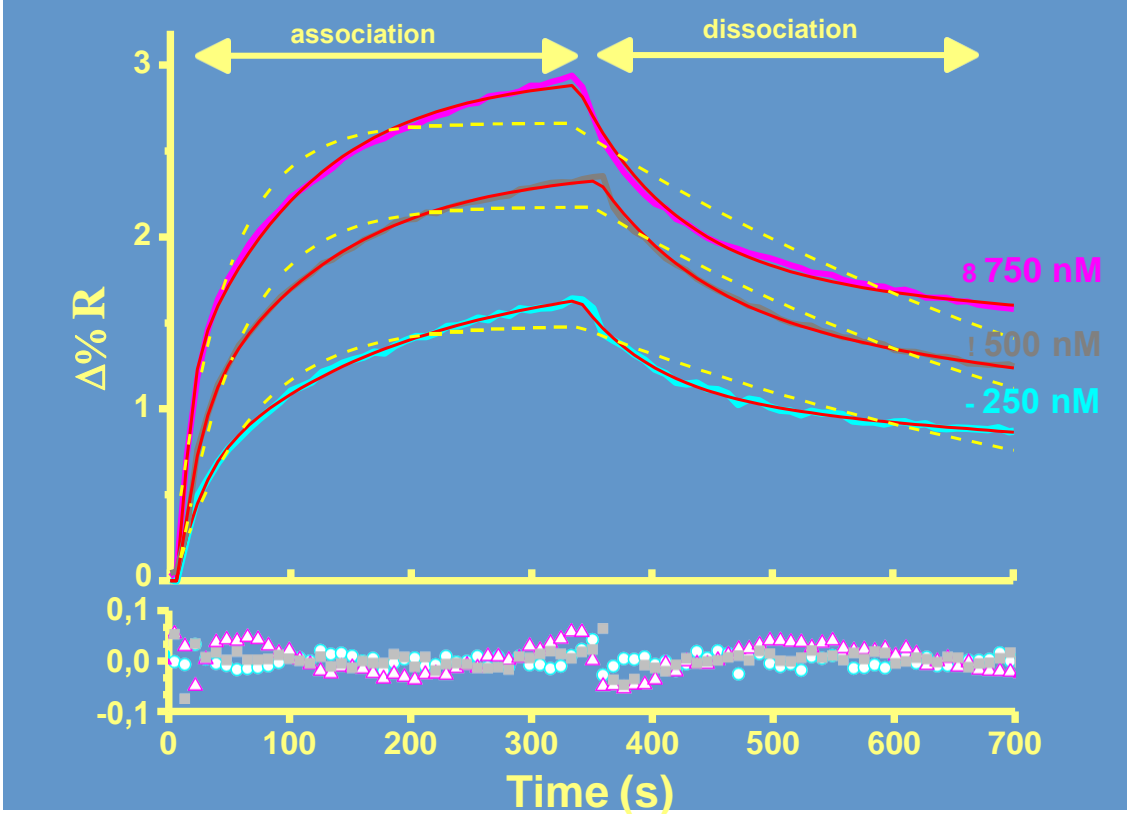
$L_x = 0.1 \mu\text{m}$ at $\lambda = 488 \text{ nm}$, $L_x = 10 \mu\text{m}$ at $\lambda = 647 \text{ nm}$



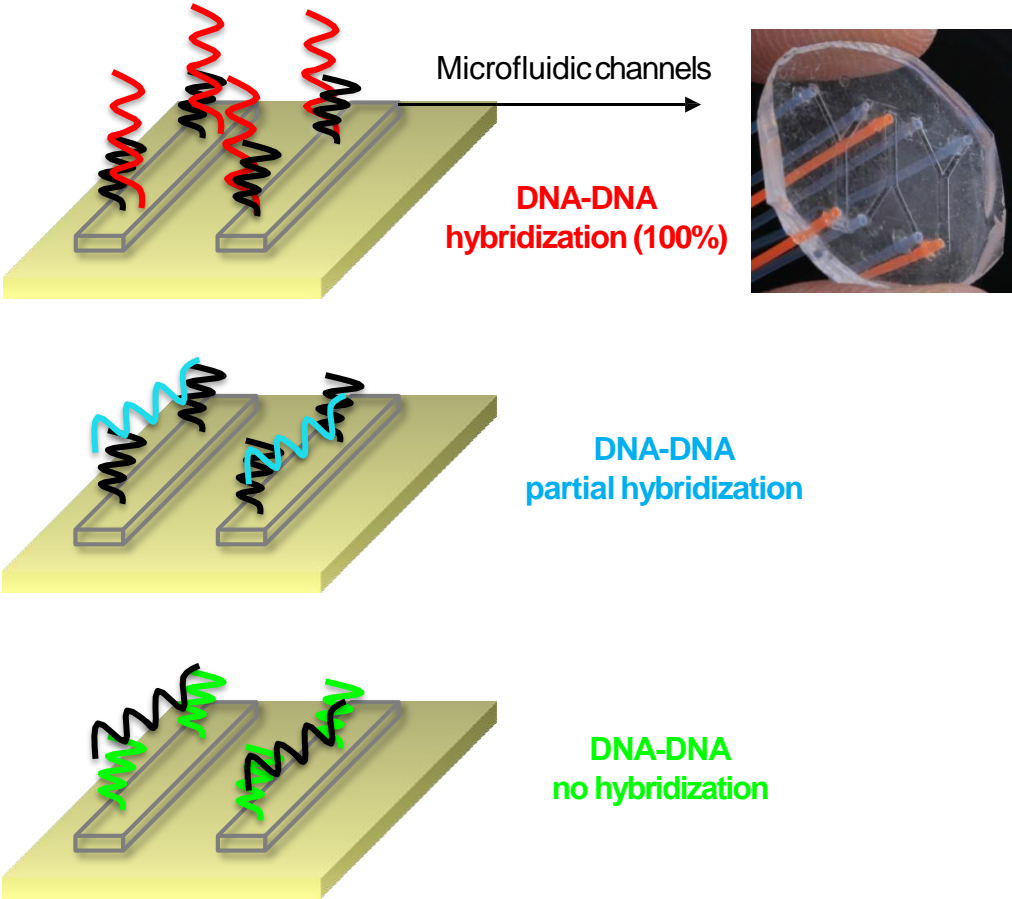
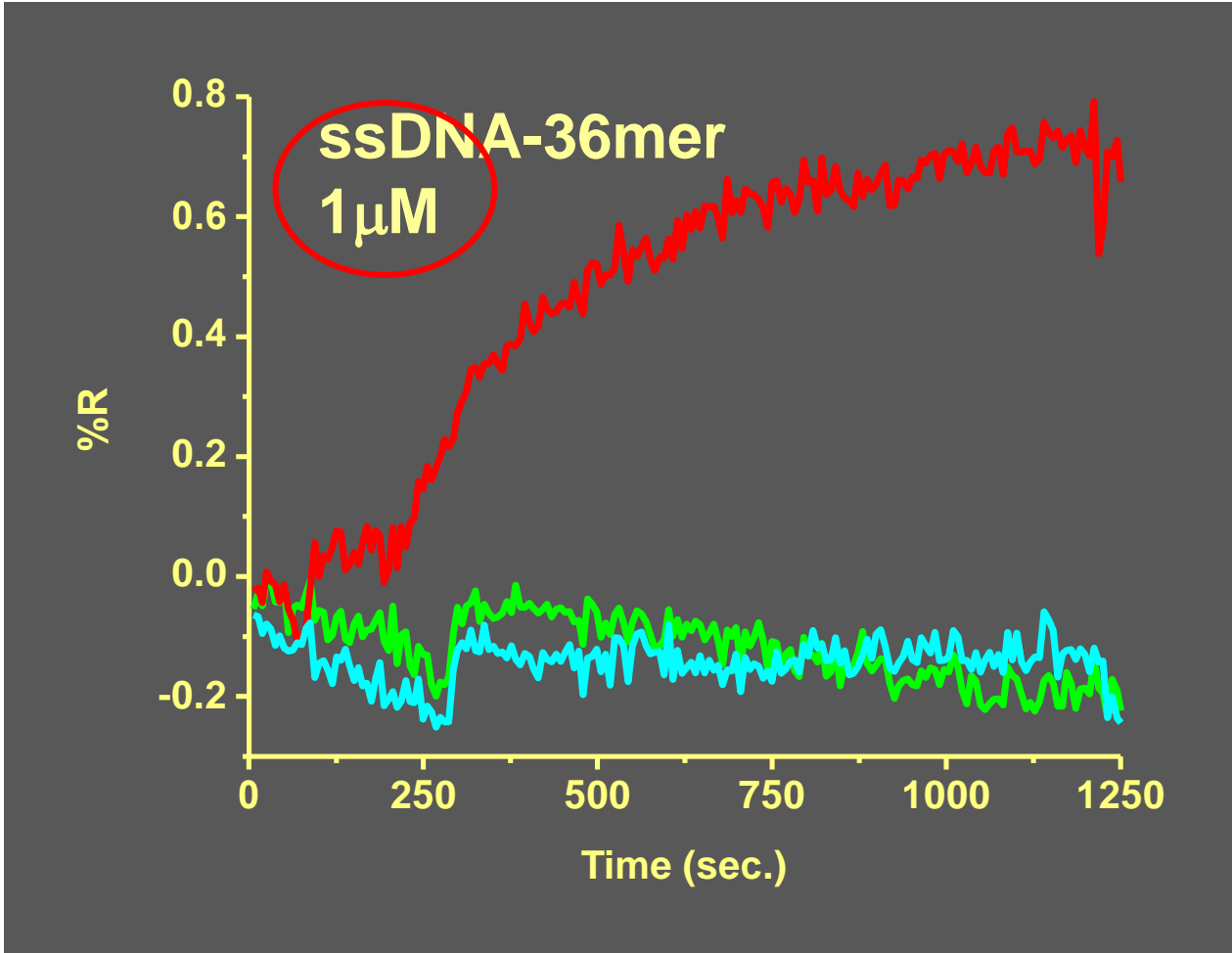
Surface Plasmon Resonance Imaging (SPRI)



Example of SPRI image



Microfluidic lab-on-a-chip plasmonic platform: detection of DNA

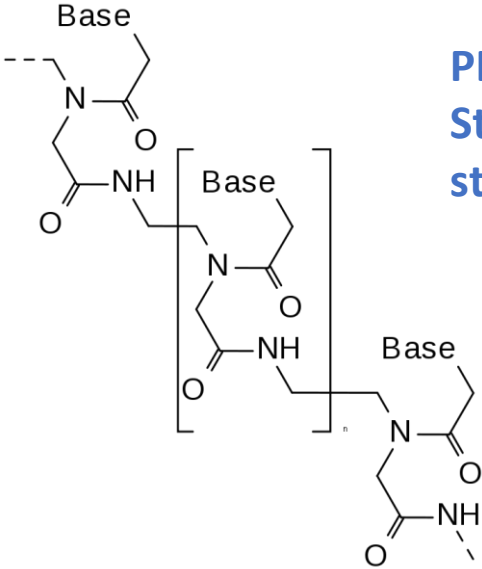
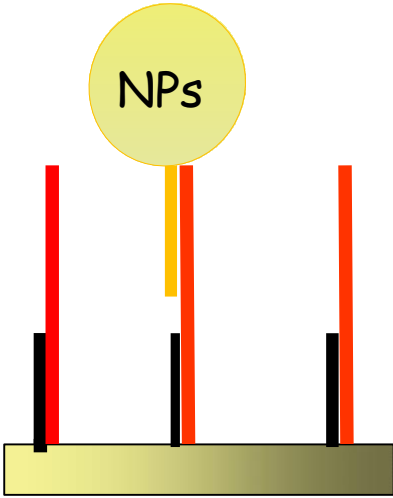


5'-LL-AAACCCTTAATCCCA-3' PROBE

3'-TTTGGGAATTAGGGTTTTTTTTTTTCGTCGAATAGCA-5'
ssDNA-36mer-match

Nanoparticle amplification-SPRI

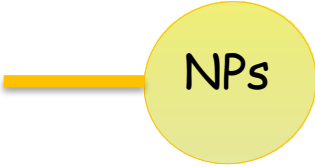
Surface Plasmon resonance
 Gold nanoparticles (NPs) + gold surface



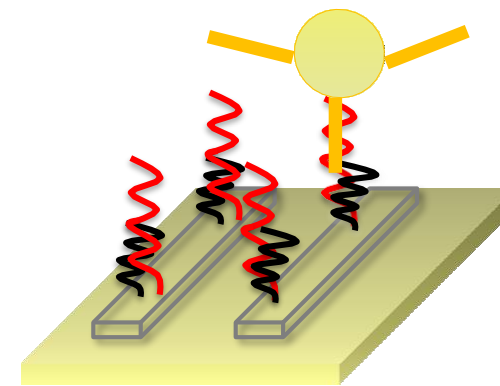
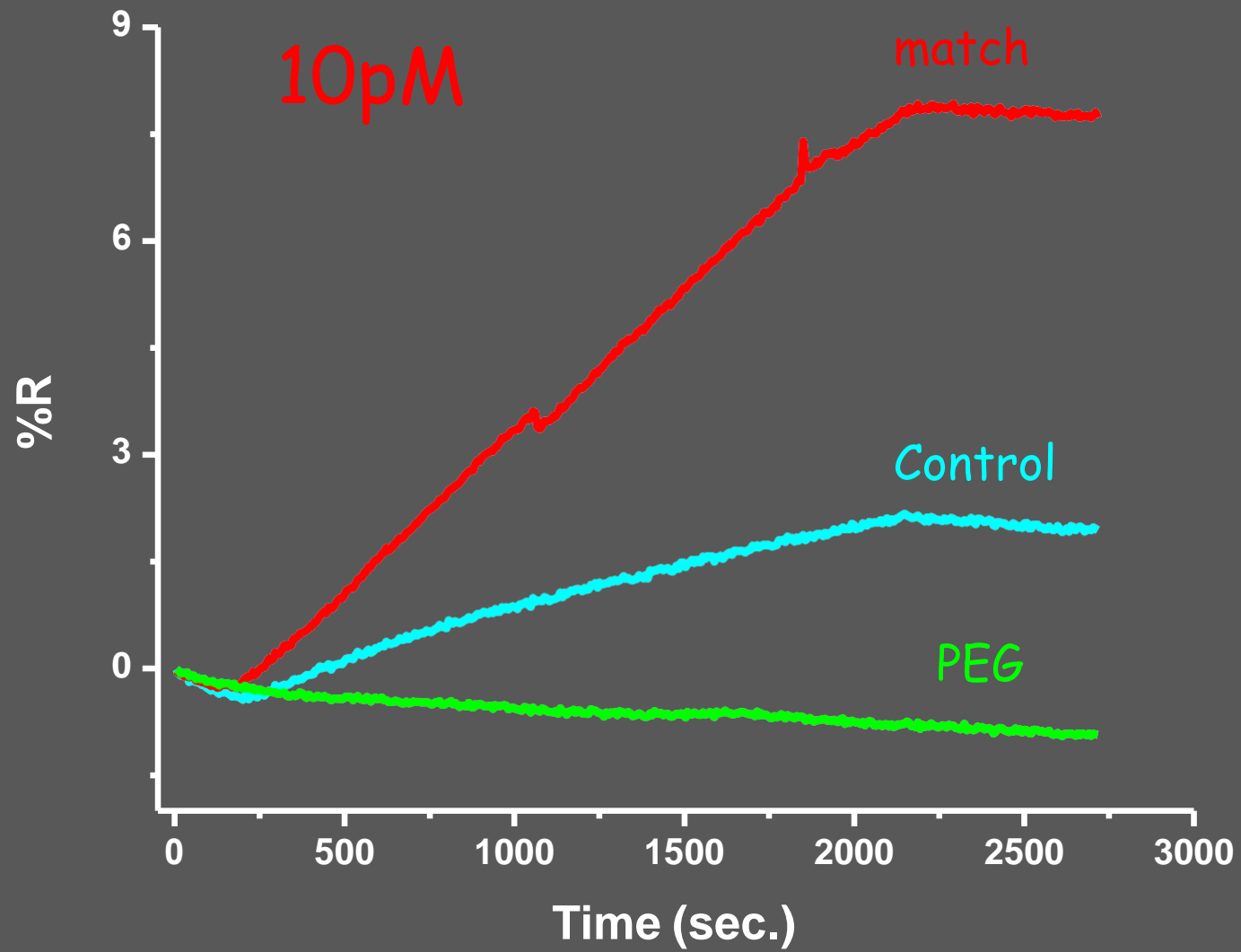
PEPTIDE NUCLEIC ACID –PNA
 Stronger affinity for complementary
 strands of DNA

By Mixtures - Own work, CC BY-SA
 3.0,
<https://commons.wikimedia.org/w/index.php?curid=1737834>

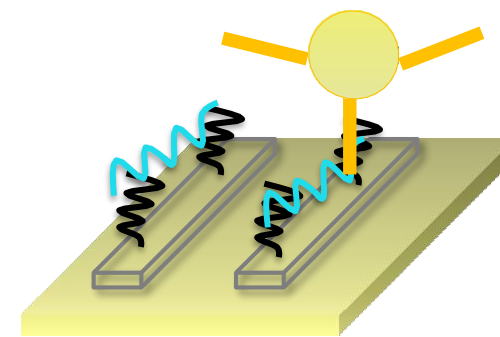
5'-GCAGCTTATCGT-3'-Biotin
 ssDNA-12merC₆Biotin



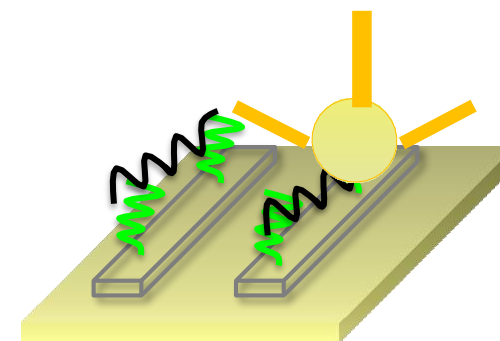
— 5'-LL-AAACCCTTAATCCCA-3' **PNA**-15mer
 — 3'-TTTGGGAATTAGGGTTTTTTTTTTTCGTCGAATAGCA-5'
 ssDNA-36mer-match



DNA-DNA
hybridization (100%)

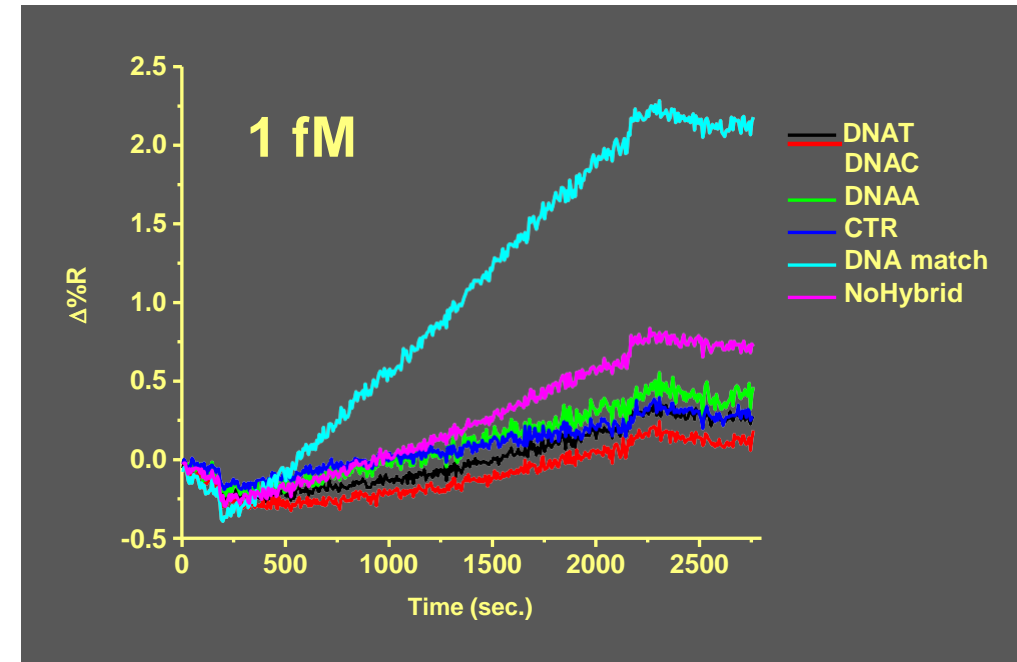
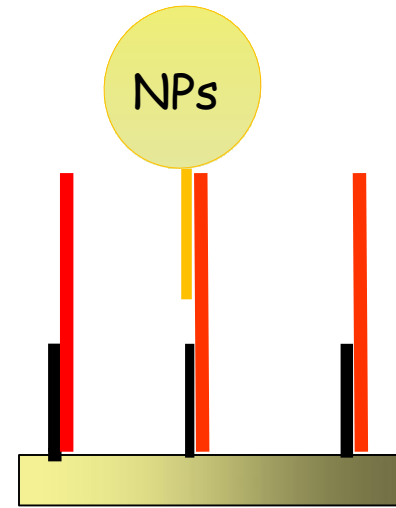
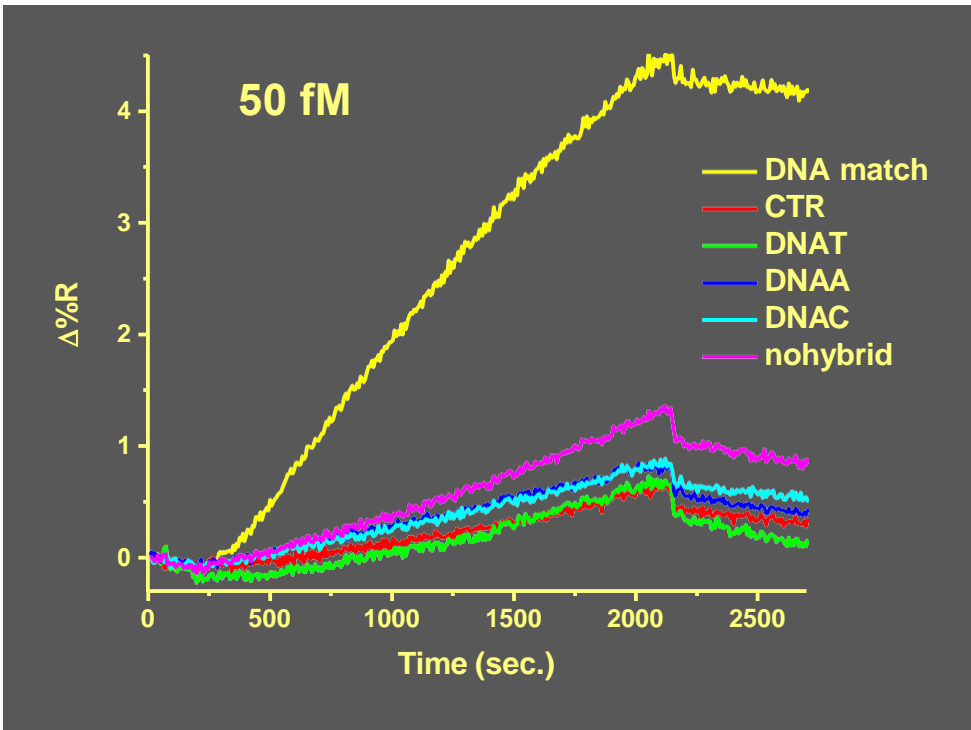


DNA-DNA
partial hybridization



DNA-DNA
no hybridization

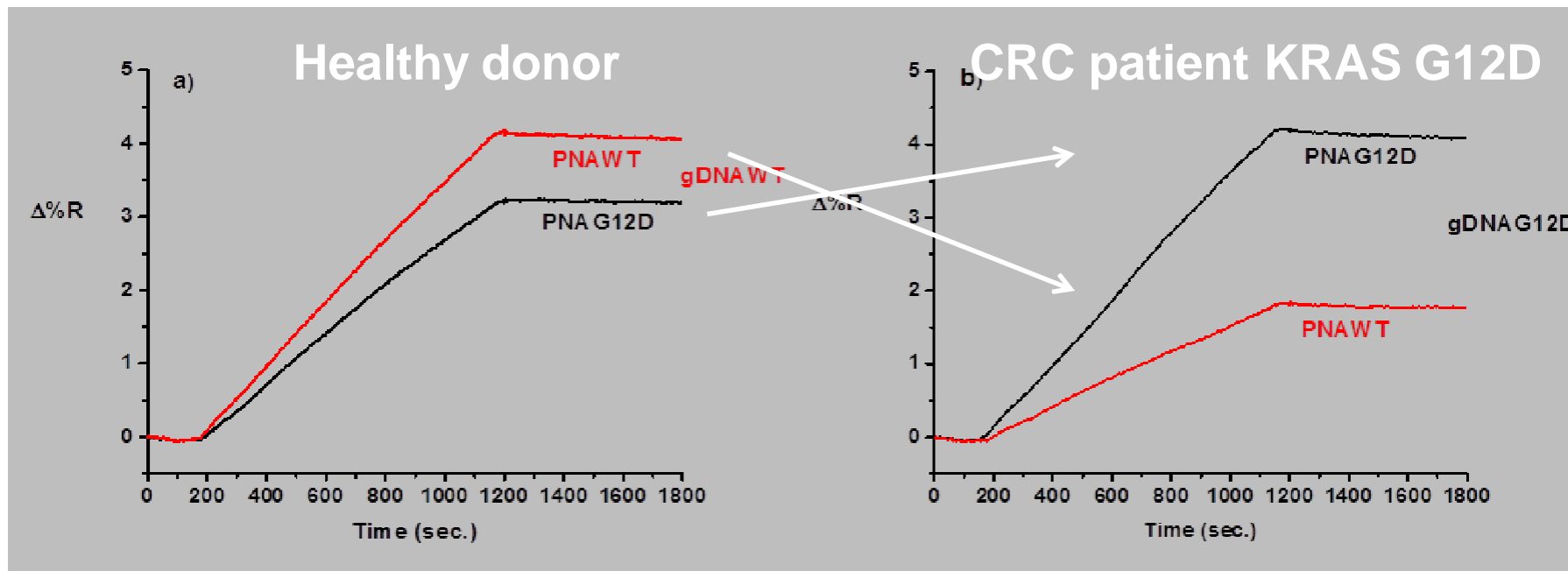
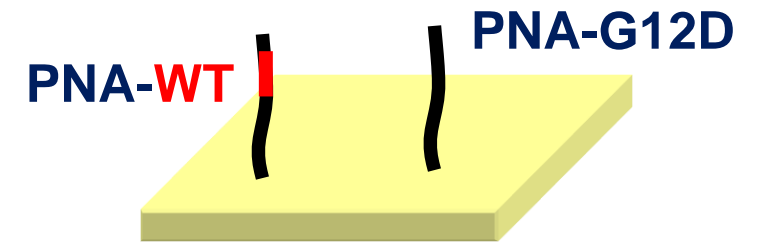
Nanoparticle amplification-SPRI: SNPs detection

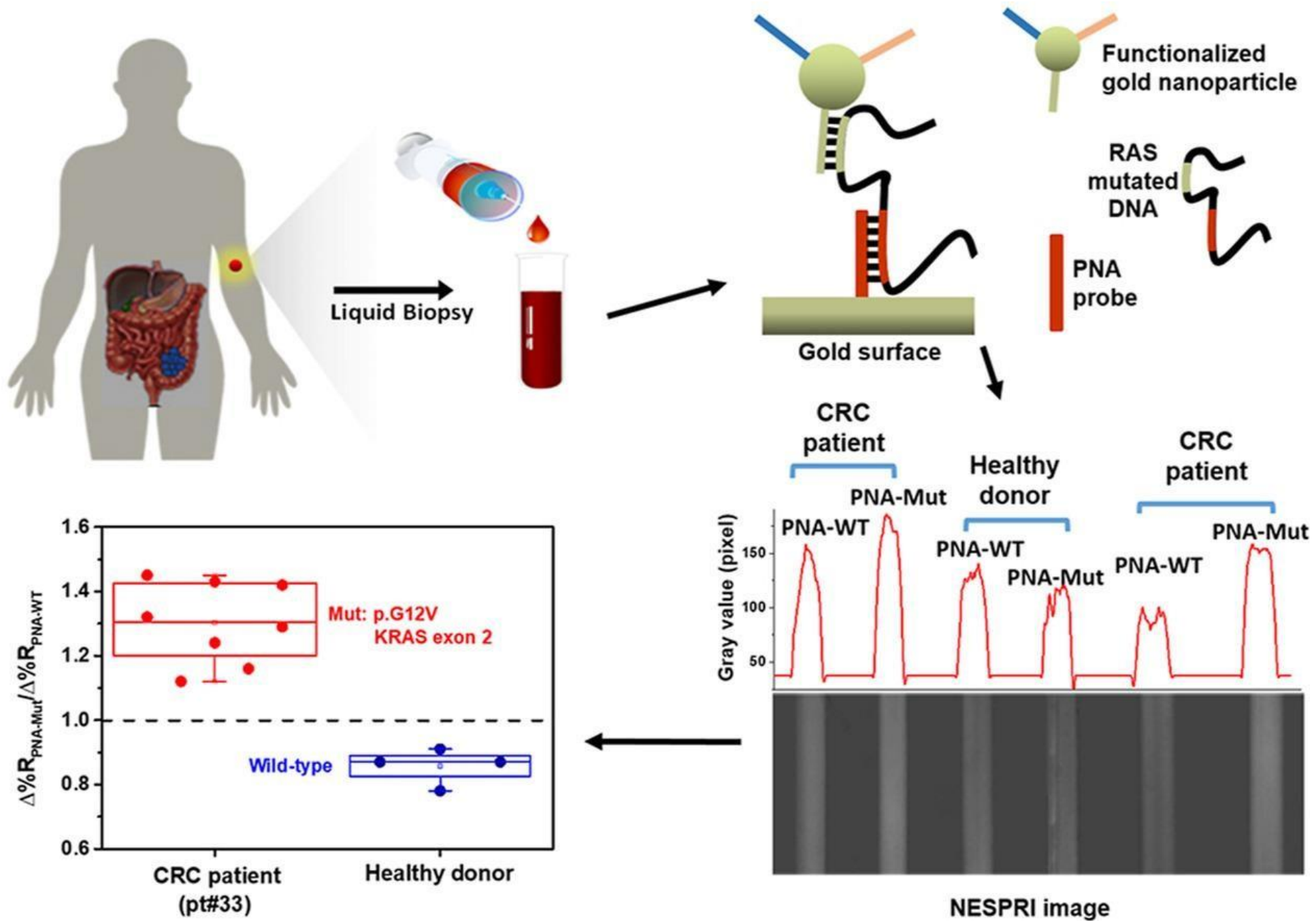




PCR-free detection of KRAS mutations (Plasma from colorectal cancer patients)

YouTube <https://youtu.be/88n3IRsWTm8>





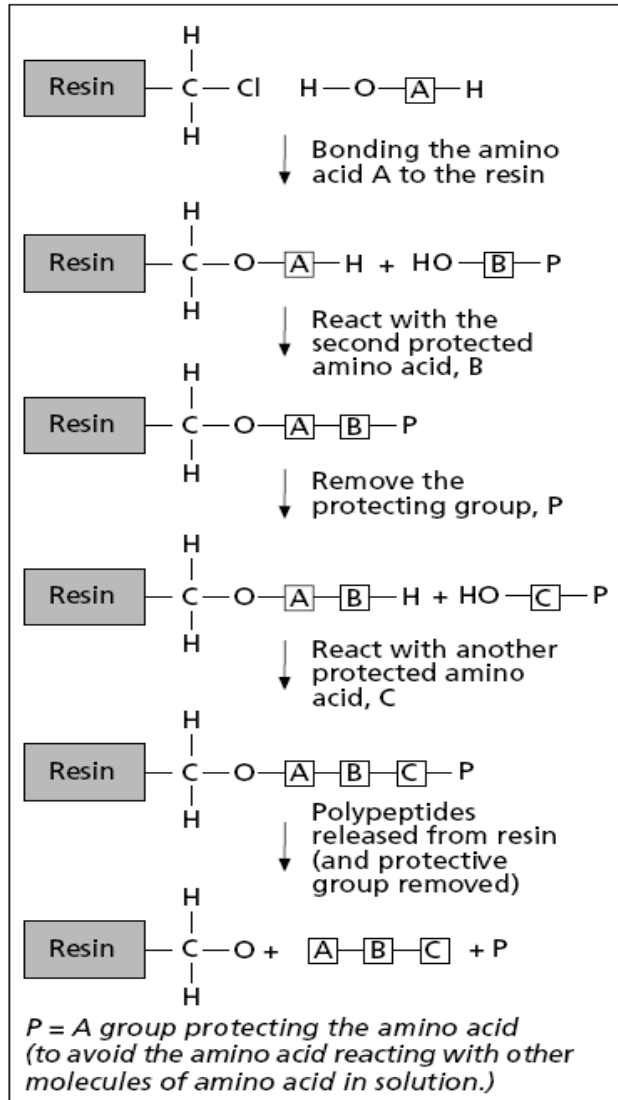
Biomimetic receptors

Used for biosensors or for sample preparation/purification

Obtained via combinatorial chemistry and/or molecular modelling

- Peptides
- Aptamers
- MIP (Molecularly Imprinted Polymers)

Combinatorial chemistry approach: Synthesis of amino acids via split and mix



Split synthesis

Stage	Reaction vessel 1 (A)	Reaction vessel 1 (B)	Reaction vessel 1 (C)	
1	Resin + A	Resin + B	Resin + C	3 compounds
	MIX			
2	Resin-A+A Resin-B+A Resin-C+A	Resin-A+B Resin-B+B Resin-C+B	?	9 compounds
	MIX			
3	Resin-A-A+A Resin-B-A+A Resin-C-A+A Resin-A-B+A Resin-B-B+A Resin-C-B+A Resin-A-C+A Resin-B-C+A Resin-C-C+A	Resin-A-A+B Resin-B-A+B Resin-C-A+B Resin-A-B+B Resin-B-B+B Resin-C-B+B Resin-A-C+B Resin-B-C+B Resin-C-C+B	Resin-A-A+C Resin-B-A+C Resin-C-A+C Resin-A-B+C Resin-B-B+C Resin-C-B+C Resin-A-C+C Resin-B-C+C Resin-C-C+C	27 compounds
	MIX			

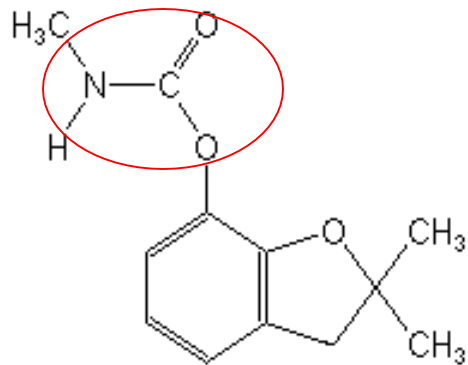
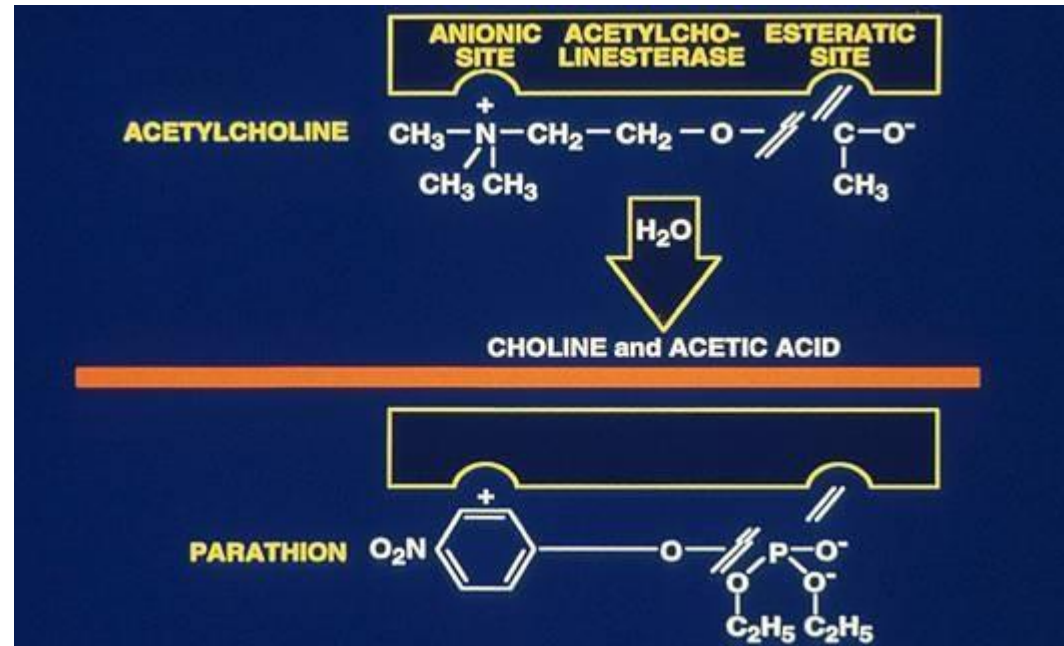
Biomimetic Approach

- Starting from the biological structure it is possible to reproduce with natural amino acids the proper shape of binding dock
- The biomimetic approach relies on the design and development of artificial oligopeptides as a mimic of the biological binding site by using molecular modeling

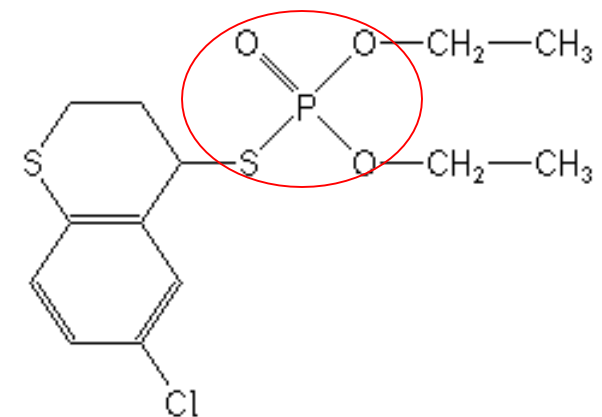
✓ Why oligopeptides?

- Nature exploited aminoacids structures to obtain the most of receptors
- Oligopeptides have the advantage of informatics help from the point of the crystallographic informations from native proteins
- Great number of combinations using 20 aminoacids which can do any binding traps

BIOMIMETIC RECEPTORS FOR PESTICIDES



Carbamate



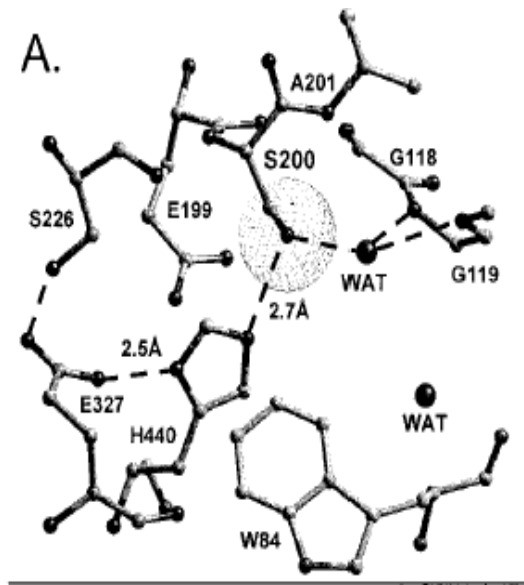
organophosphate

✓ Mechanism of AChE inhibition

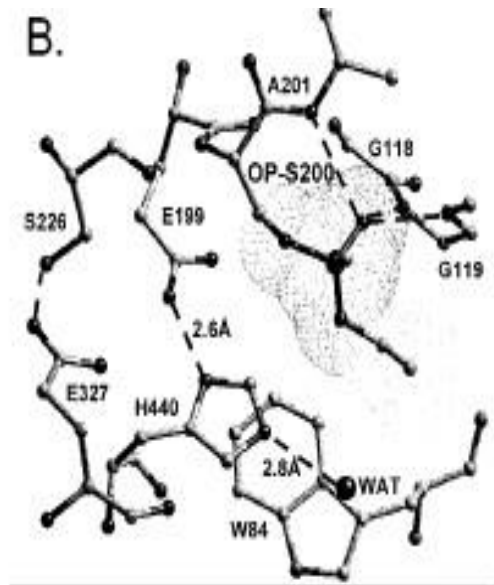
AChE, the target enzyme of pesticides, **is an efficient serine hydrolase** that catalyzes the breakdown of acetylcholine (ACh)



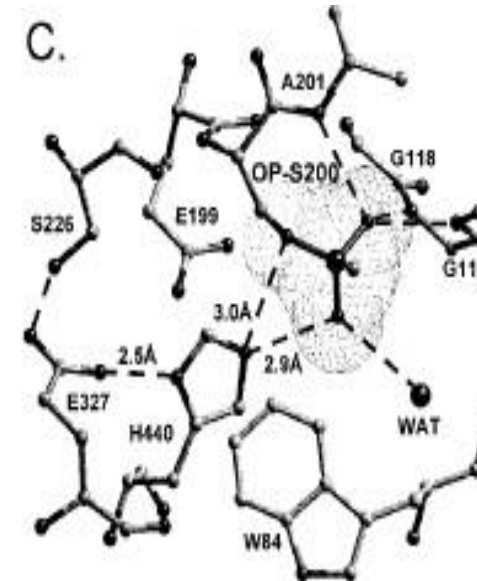
How pesticides work



Native structure: the active site, including the catalytic triad (S200-H440-E327) and the oxanyon hole (-NH of G118, G119, and A201)



Pro-aged structure: Phosphonylation triggers a conformational change for H440 that disrupts the H-bond to E327

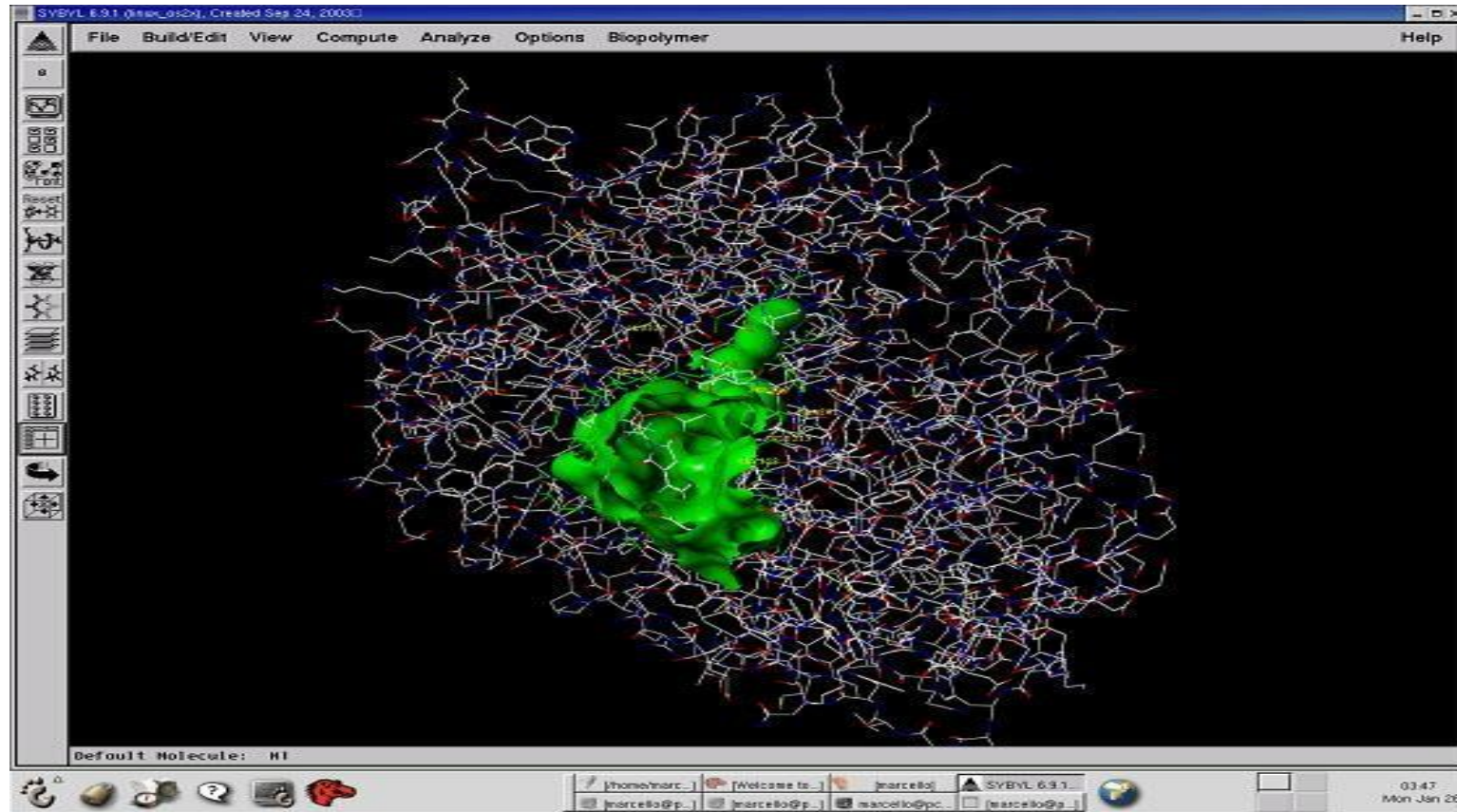


Aged structure: For reaction of AChE with VX and most phosphonates, aging predominates, and dealkylation results in movement of H440 to the negatively charged pocket formed by E327 Ox, S200 Ox, and one anionic oxygen of the dealkylated OP

❖ Computational screening

✓ AChE-OP crystallographic structure (PDB ID: 1VXO)

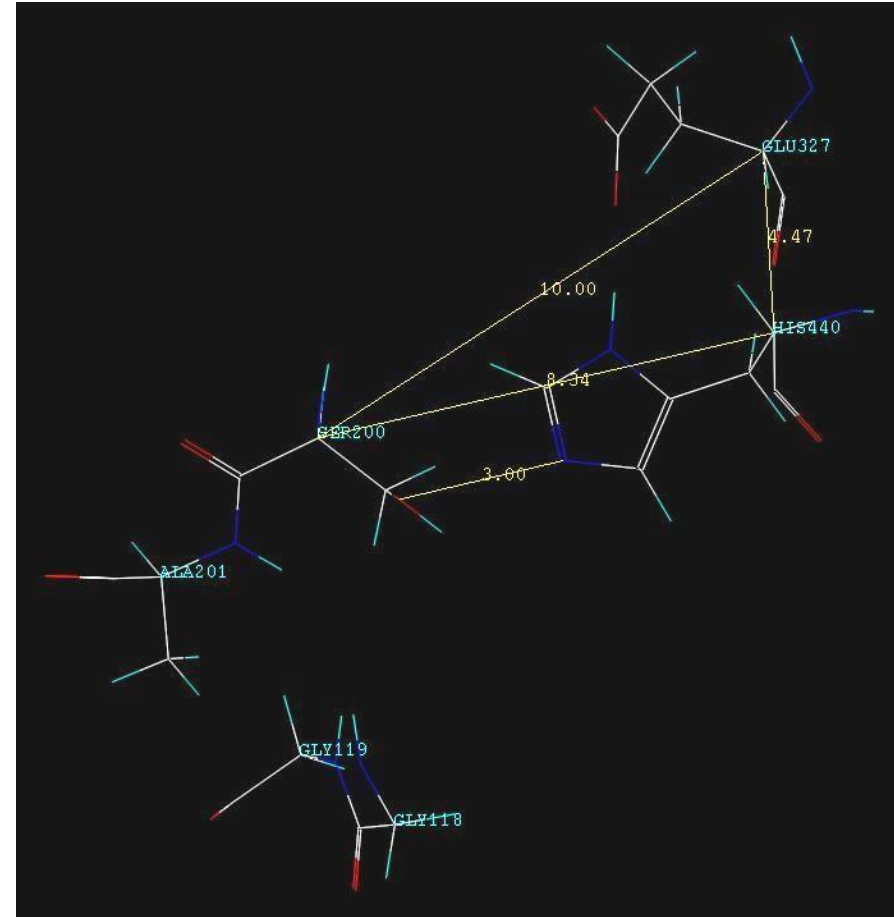
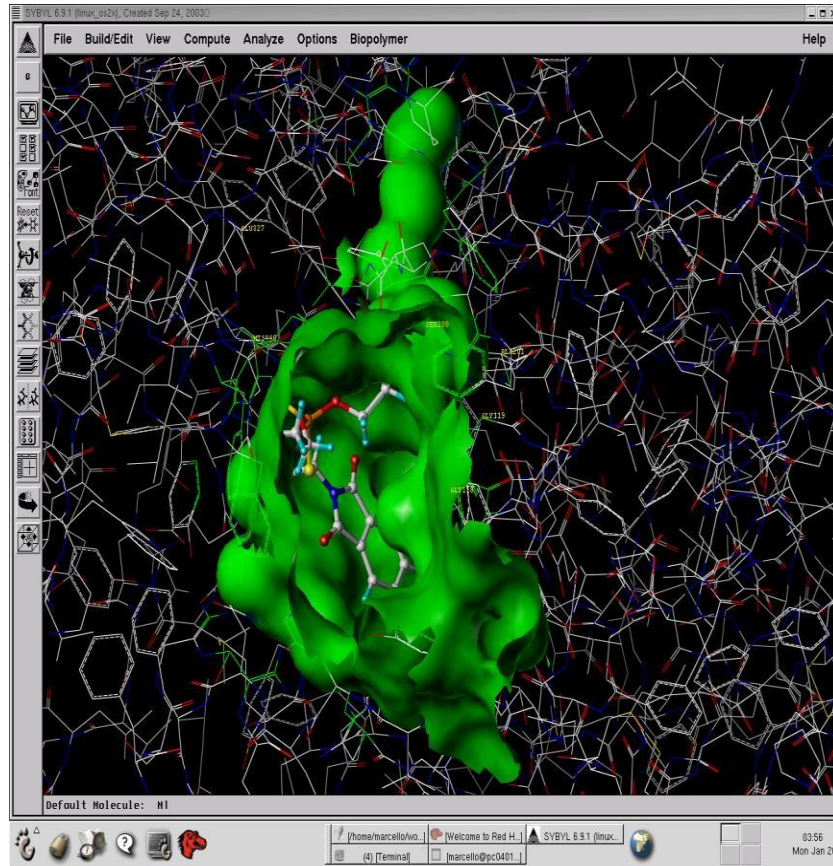
Methylphosphonylated Acetylcholinesterase (Aged) Obtained By Reaction With O-Ethyl-S-[2-[Bis(1-Methylethyl) Amino]Ethyl] Methylphosphonothioate (Vx) conventional X-ray crystallography resolution [Å]: 2.40



In green the molecular electrostatic potential distribution on the surface of the enzyme binding pocket

✓ Design of the oligopeptides library as possible receptors

The geometry of the binding pocket was investigated to create oligopeptides library



Three dimensional coordinates of the asymmetric carbon ($C\alpha$) of each aminoacid involved in the binding pocket were calculated in order to reproduce the geometry observed

✓ Tetrapeptides library

- easy to synthesise
- more possibility to preserve in solution the secondary structure predicted

•A series of tetrapeptides, containing the possible combinations of the catalytic triad (SER 200, HIS 440, GLU 327) and the catalytic oxyanion hole (GLY 118 GLY 119 ALA 201) was drawn

•The proper geometry of binding pocket was achieved using alternatively a GLY or a PRO residue

Library

(24 tetrapeptides)

Ser-Gly-His-Glu	Glu-Gly-Ser-Ala
Ser-Gly-Glu-His	His-Gly-Ser-Ala
His-Glu-Gly-Ser	Gly-Pro-Ser-Ala
Glu-His-Gly-Ser	Ser-Ala-Pro-Glu
Ser-Pro-His-Glu	Ser-Ala-Pro-His
Ser-Pro-Glu-His	Ser-Ala-Pro-Gly
His-Glu-Pro-Ser	Glu-Pro-Ser-Ala
Glu-His-Pro-Ser	His-Pro-Ser-Ala
Gly-Gly-Ser-Ala	Gly-Ser-Gly-Ala
Ser-Ala-Gly-Glu	Ala-Gly-Ser-Gly
Ser-Ala-Gly-His	Ser-Gly-Pro-Ala
Ser-Ala-Gly-Gly	Ala-Pro-Gly-Ser

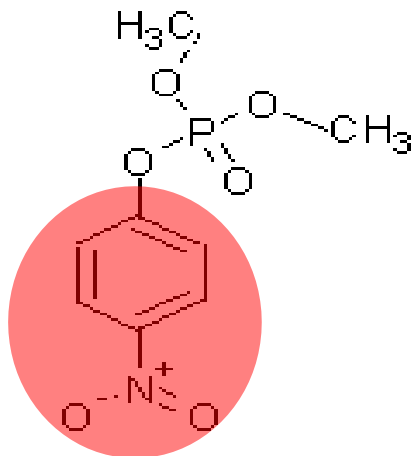
✓ Simulated binding results vs paraoxon of the tetrapeptides selected for experimental screening

	A	B	C	D
	Ser-Ala-Gly-Glu	His-Gly-Ser-Ala	Glu-Pro-Ser-Ala	His-Glu-Pro-Ser
Binding Score (KJ/mol)	38	73	21	93

Negative control (NC): Glu-His-Ser-Gly

Primary sequence of AChE catalytic triad

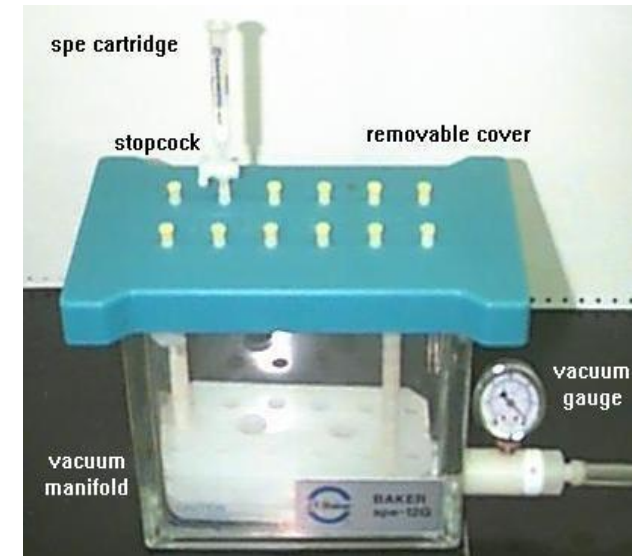
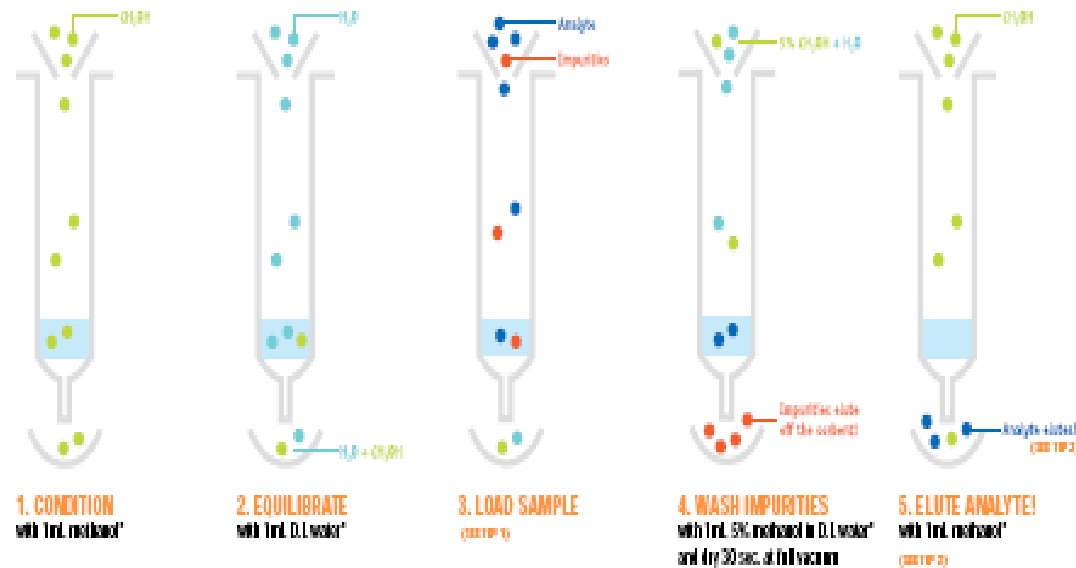
PARAOXON



→ A **Ser-Ala-Gly-Glu**
 → B **His-Gly-Ser-Ala**
 → C **Glu-Pro-Ser-Ala**
 → D **His-Glu-Pro-Ser**
 NC **Glu-His-Ser-Gly**

✓ Pre-analytical applications: selective affinity columns

(Extraction or purification)



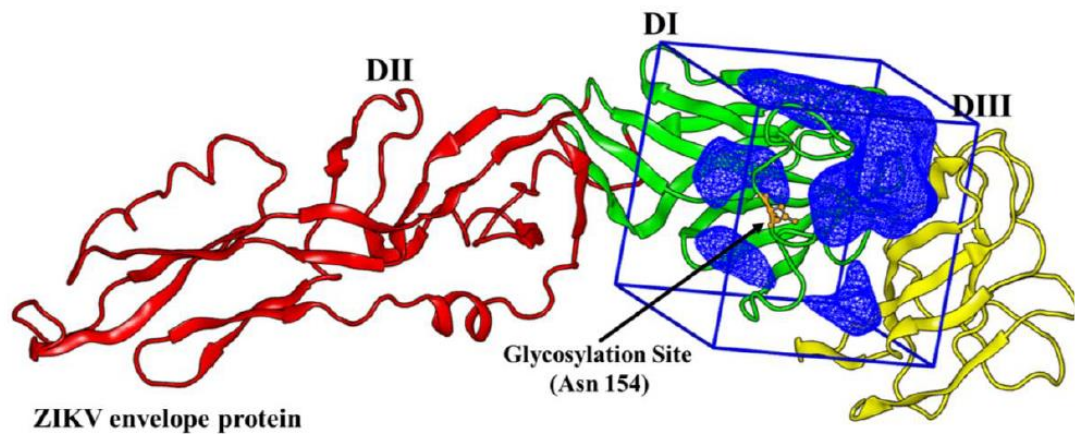
is a technique enabling purification of a biomolecule with respect to biological function or individual chemical structure. The substance to be purified is specifically and reversibly adsorbed to a ligand (binding substance), immobilized by a covalent bond to a chromatographic bed material (matrix). Samples are applied under favourable conditions for their specific binding to the ligand. Substances of interest are consequently bound to the ligand while unbound substances are washed away. Recovery of molecules of interest can be achieved by changing experimental conditions to favour desorption.

Article

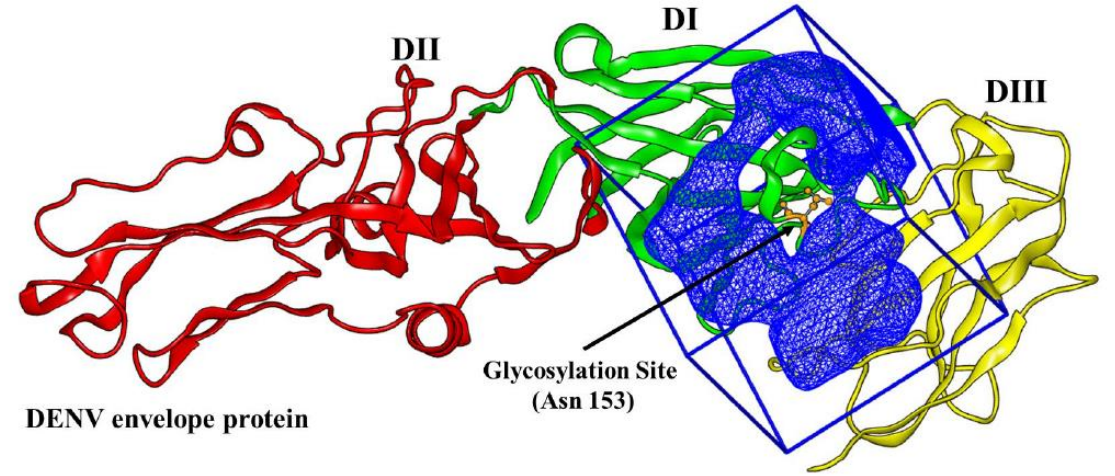
Computationally Designed Peptides for Zika Virus Detection: An Incremental Construction Approach

Marcello Mascini ^{1,2,*} , Emre Dikici ^{3,4}, Marta Robles Mañueco ³, Julio A. Perez-Erviti ⁵, Sapna K. Deo ^{3,4}, Dario Compagnone ² , Joseph Wang ⁶, José M. Pingarrón ¹ and Sylvia Daunert ^{3,4,7,*}

- Zika infection is known to cause neurological problems to pregnant women and potentially cause microcephaly and other congenital malformations and diseases to the unborn child. Zika affects, both male and females and it has been reported that the virus can be transmitted sexually through semen and vaginal fluids.
- The Zika virus is a mosquito-borne flavivirus, and due to the lack of specific antibodies/binders that can be used in immunoassays for diagnosis of the disease, these immunoassays present cross-reactivity with other flaviviruses and arboviruses. It is well established that ZIKV has many common genetic sequences and protein structures with other flaviviruses, like DENV, West Nile virus or Chikungunya. This limits the use of immunoassays for the detection of human pathogens within the flavivirus genus.
- The flavivirus envelope protein is responsible for virus entry and represents a major target for neutralizing antibodies. The Zika virus structure is similar to other known flaviviruses structures except for the ~10 amino acids that surround the Asn-154 glycosylation site found in each of the 180 envelope glycoproteins that make up the icosahedral shell

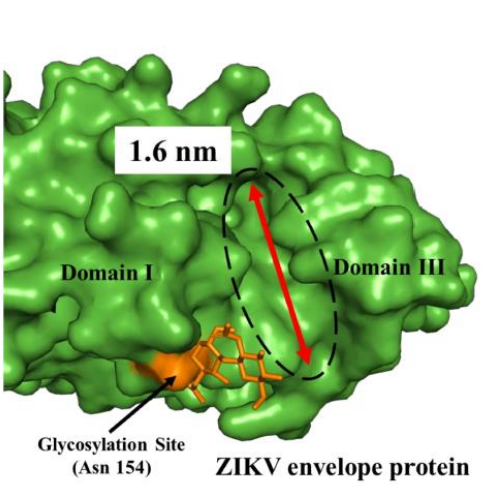


(a)

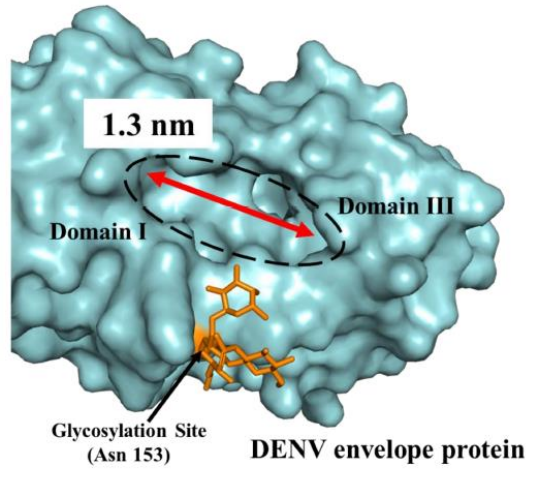


(b)

Glycosylation site

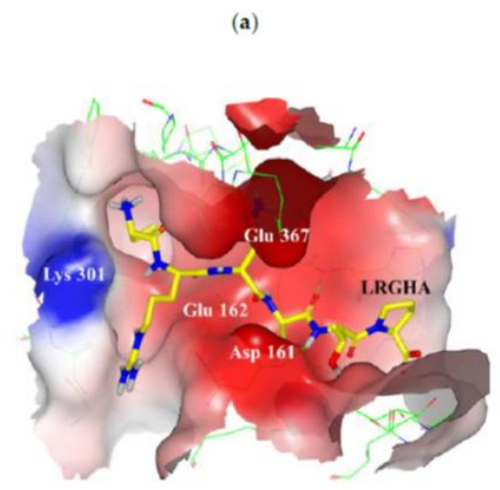


(a)

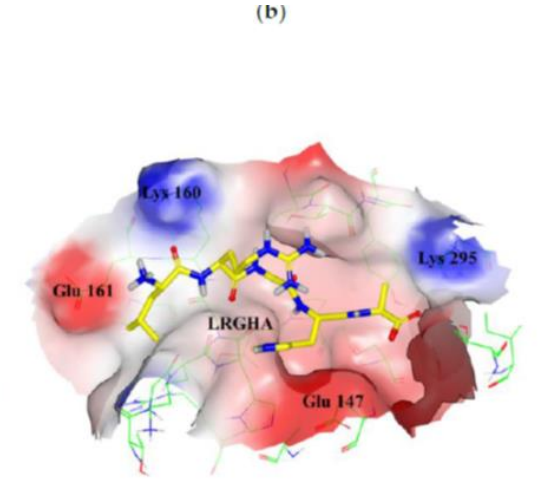


(b)

Molecular docking



(c)



(d)

Figure 4. Cont.

Figure 5. Cont.

8 different peptides selected,
 synthesized, biotinylated and tested
 with direct ELISA test using Avidin-HRP

i.e. inactivated virus onto ELISA
 microwells, reaction with peptides,
 incubation with Avidin-HRP

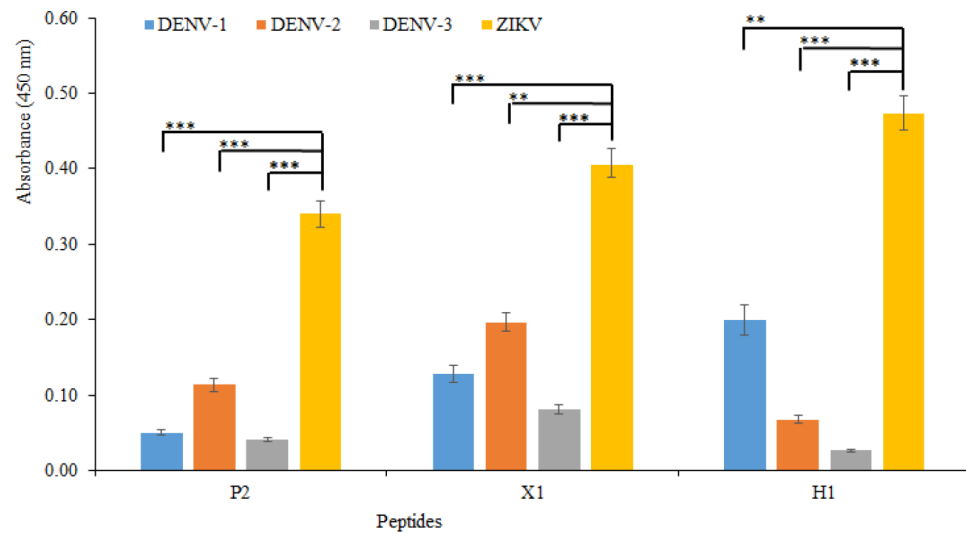


Figure 7. Cross-reactivity study. In the ELISA direct assay, the spectrophotometric absorbance signals were obtained by using the best three peptides (P2, X1, and H1) binding the ZIKV and three serotypes of DENV (DENV-1, -2, and -3) at the concentration of 10^6 copies/mL. Statistical significance between ZIKV and DENV serotypes (1–3) was calculated using two-way analysis of variance. Different p values were indicated by $** (p < 10^{-3})$ or $*** (p < 10^{-4})$.

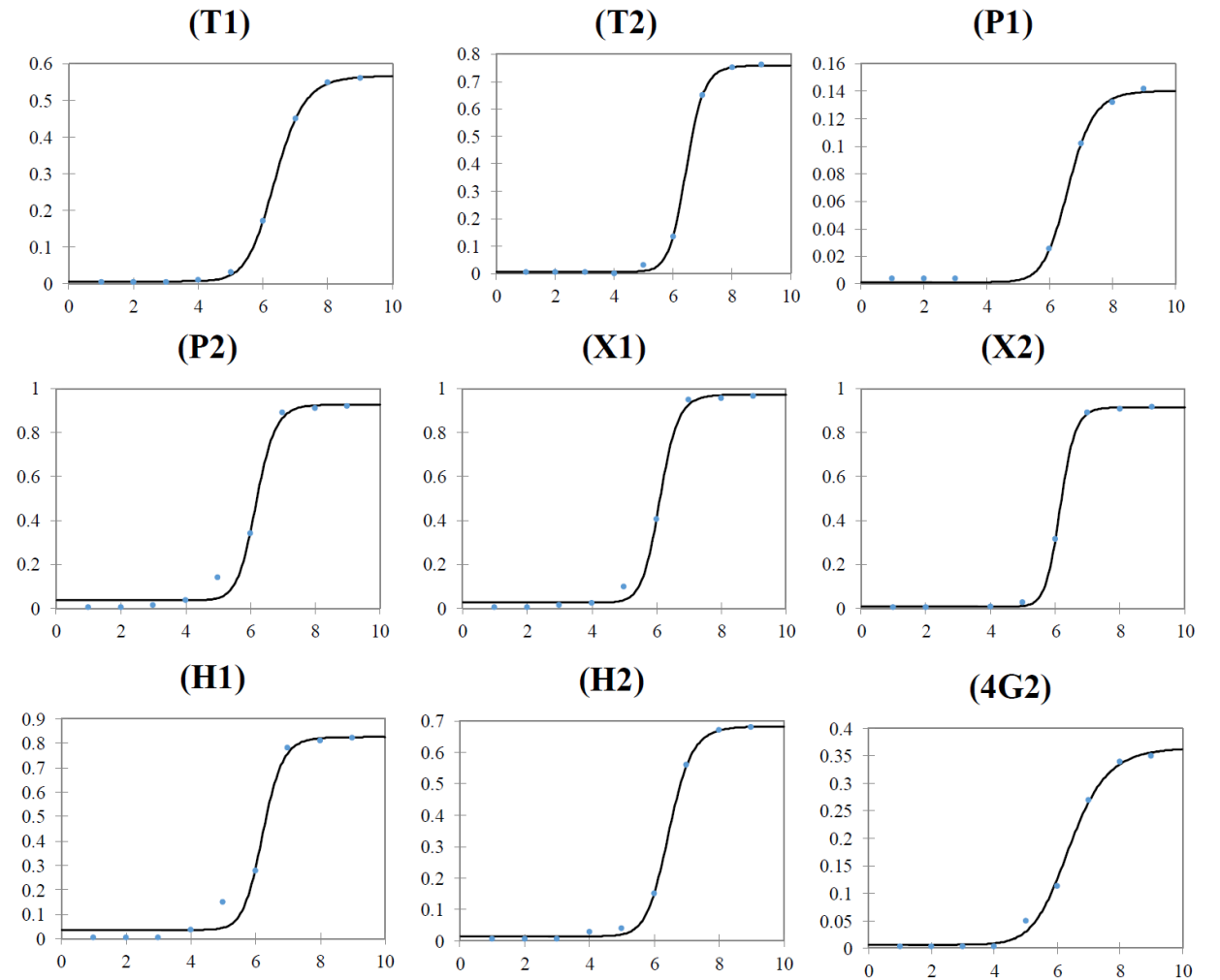


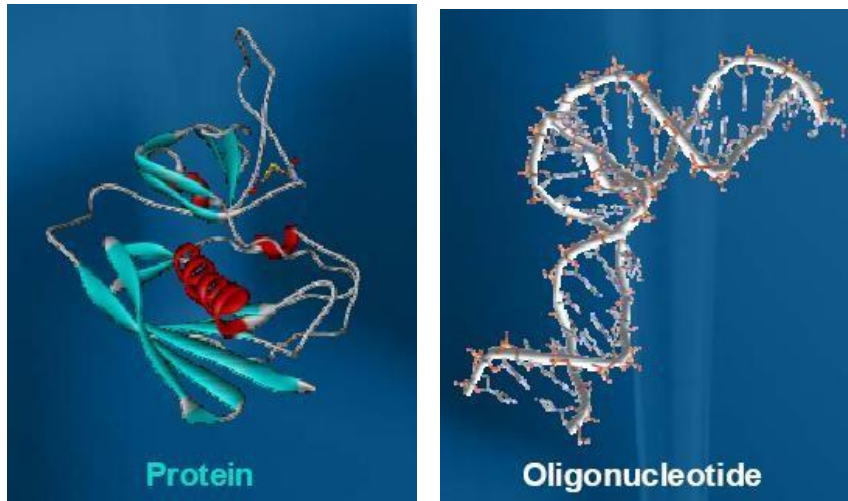
Figure 6. Sigmoidal ZIKV particles concentration response trend of the ELISA assay obtained using the eight peptides and antibody 4G2. Y-axis = absorbance (450nm); X-axis = $\log [ZIKV]$, copies/mL.

Aptamers are oligonucleotides (DNA or RNA molecules) that can bind with high affinity and specificity to a wide range of target molecules (proteins, peptides, drugs, vitamins and other organic or inorganic compounds).

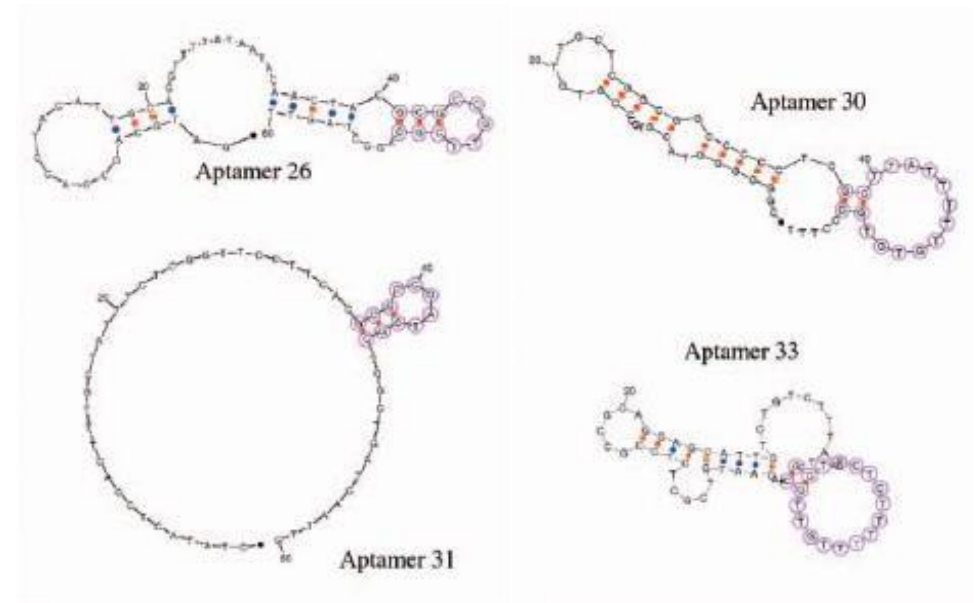
They were “discovered” in 1990 by the development of an in vitro selection and amplification technique, known as SELEX (Systematic Evolution of Ligands by Exponential enrichment).

(Ellington et al., **Nature** 346, 818; Tuerk and Gold, **Science** 249, 505)

Their name is derived from the Latin word “**aptus**” which means “to fit”.



Similar to proteins short oligonucleotides can adopt complex three-dimensional structures



Starting point: Combinatorial oligonucleotide library



A library containing a 25-nucleotide random region is represented by 4^{25} ($\sim 10^{15}$) individual sequences available for partitioning.

Normally, the starting round contains **10^{14} - 10^{15} individual sequences.**

A, G, C, U(T)

$$4^1 = 4$$

$$4^2 = 16$$

$$4^3 = 64$$

$$4^4 = 256$$

$$4^5 = 1024$$

.....

.....

.....

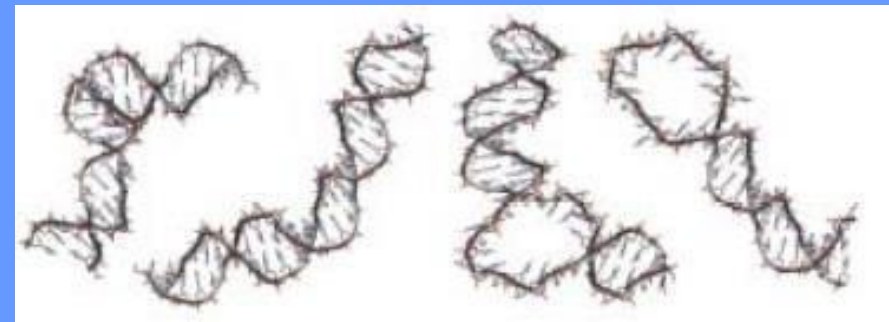
$$4^{25} = 1125899906842624$$



Pool of randomized DNA or RNA



10^{15} different sequences!!!!



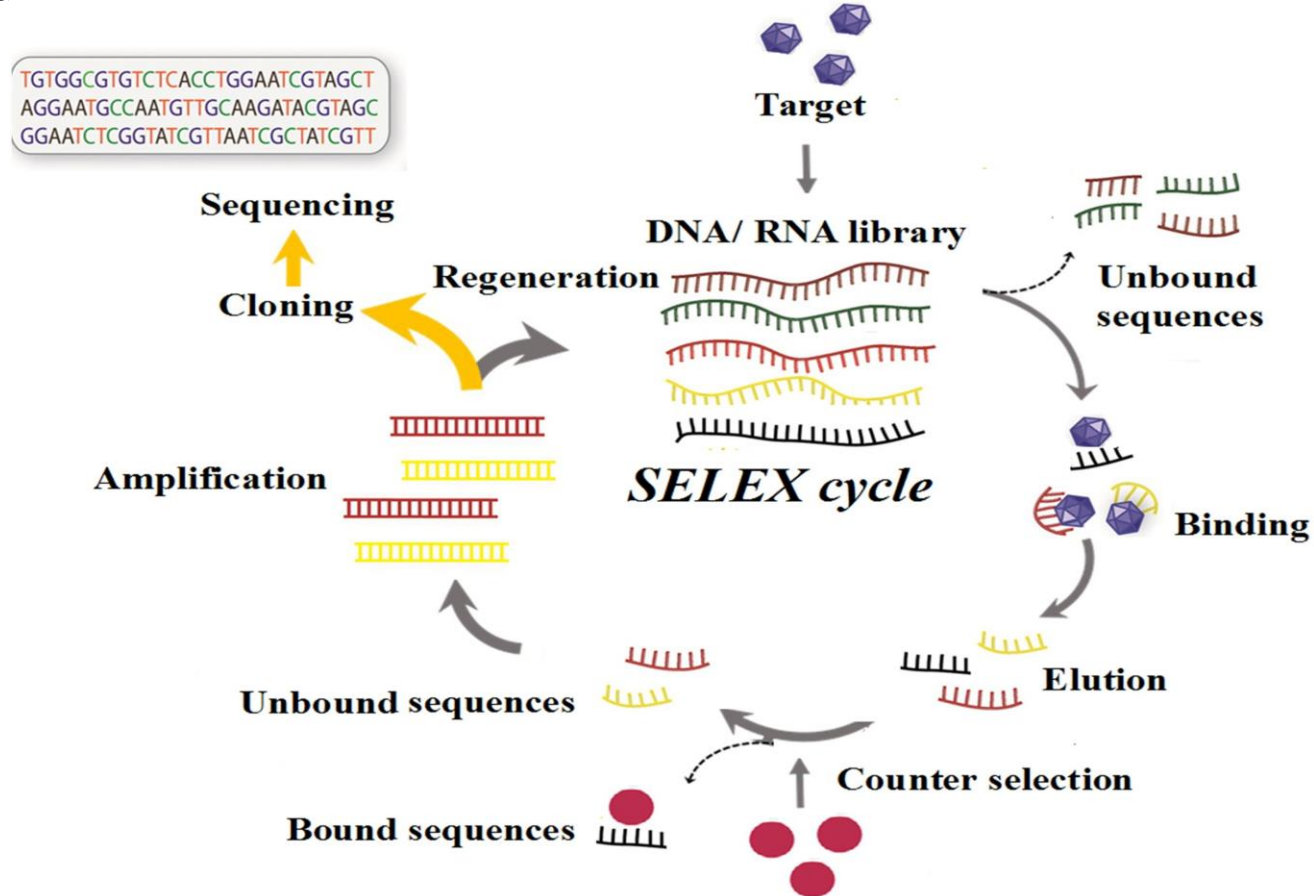


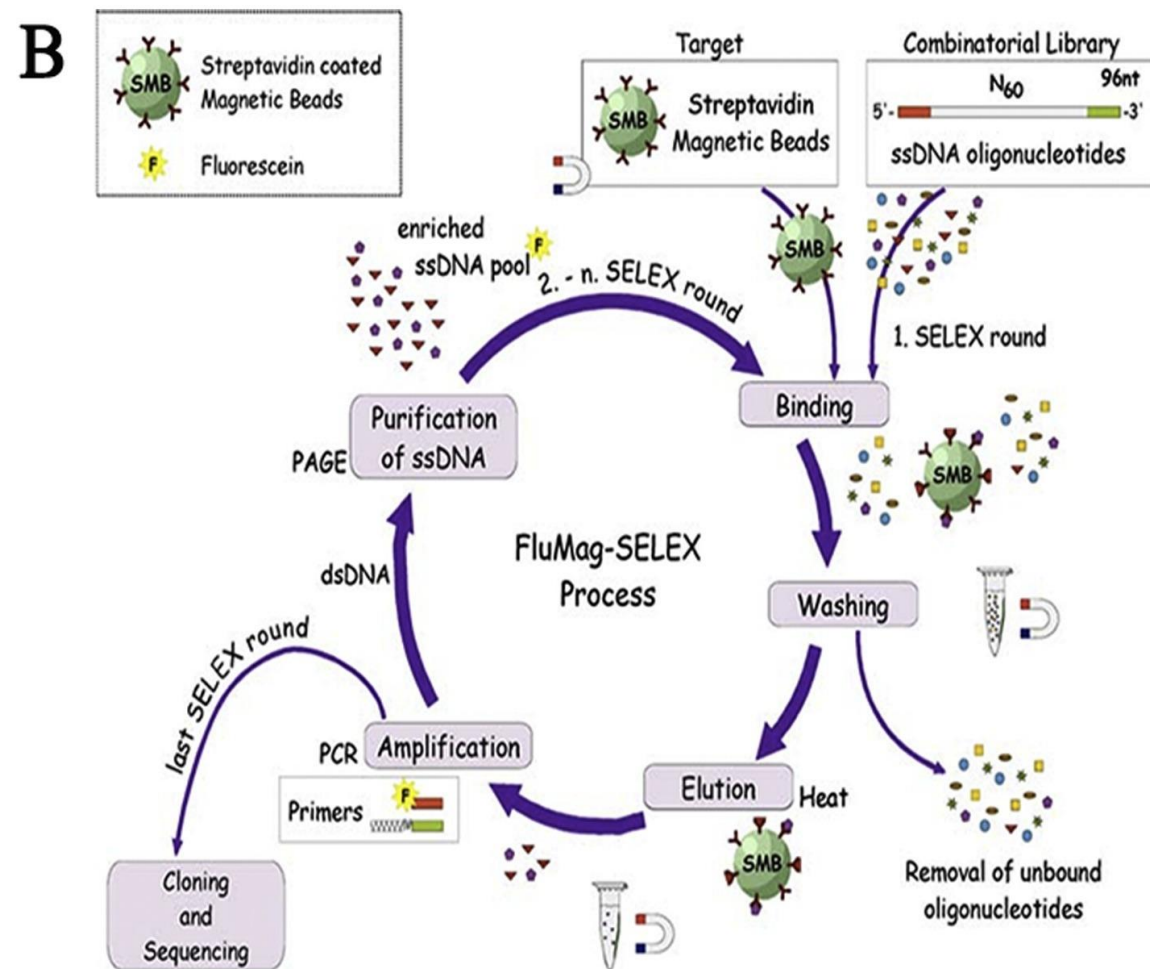
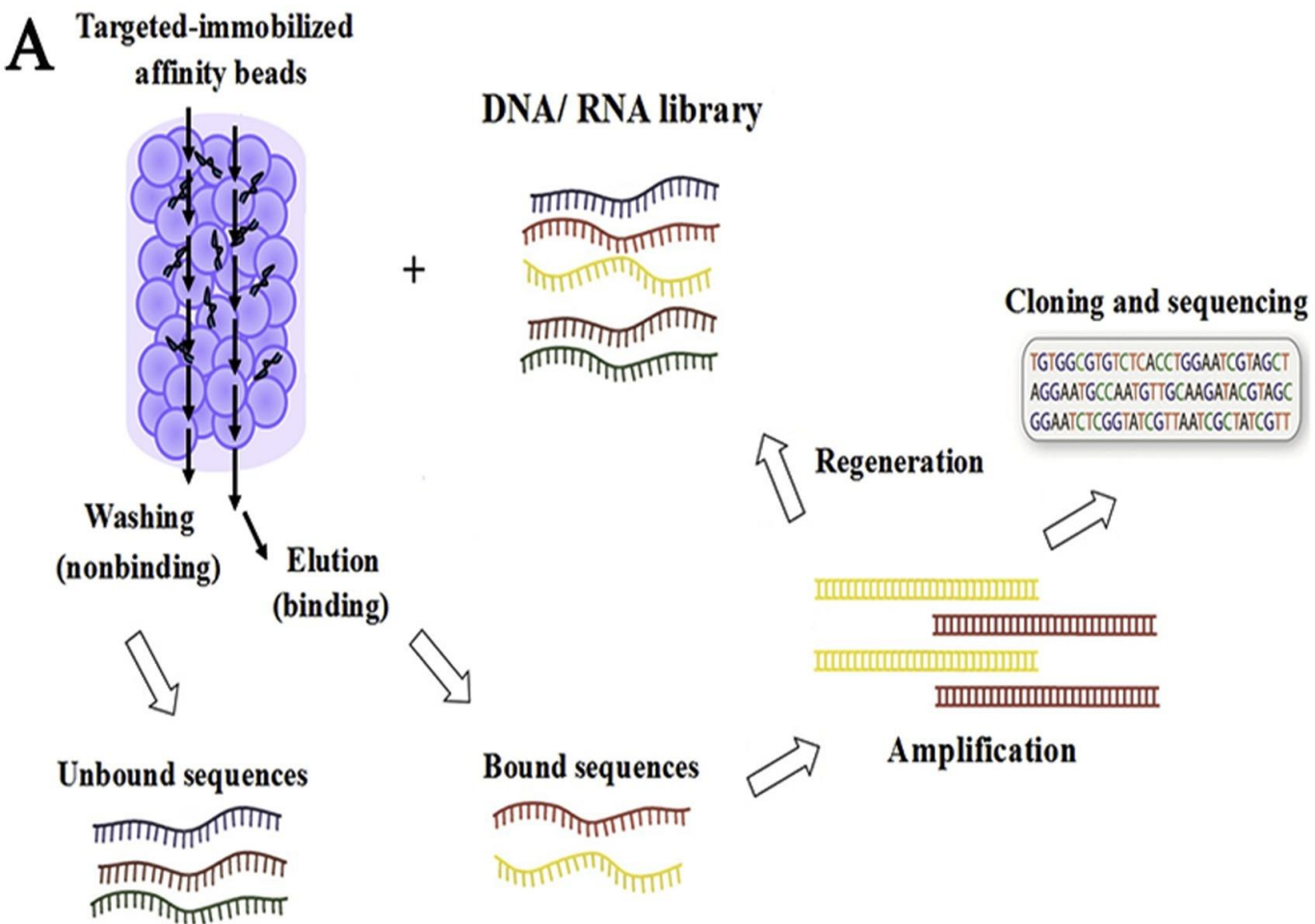
Review

Aptamers used for biosensors and targeted therapy

Yi Ning, Jue Hu, Fangguo Lu*

Department of Microbiology, The Medicine School of Hunan University of Chinese Medicine, Chansha, Hunan, 410208, PR China





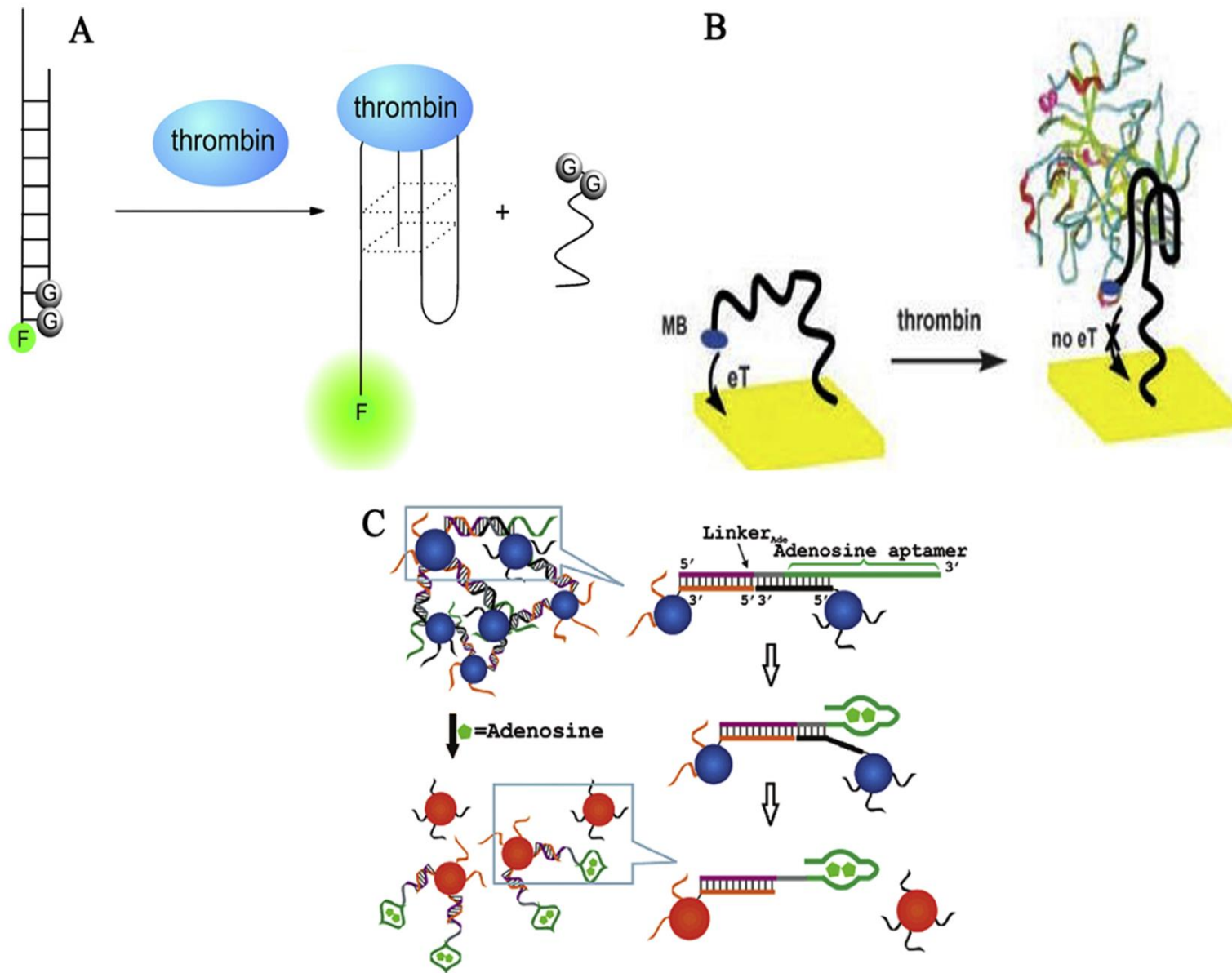
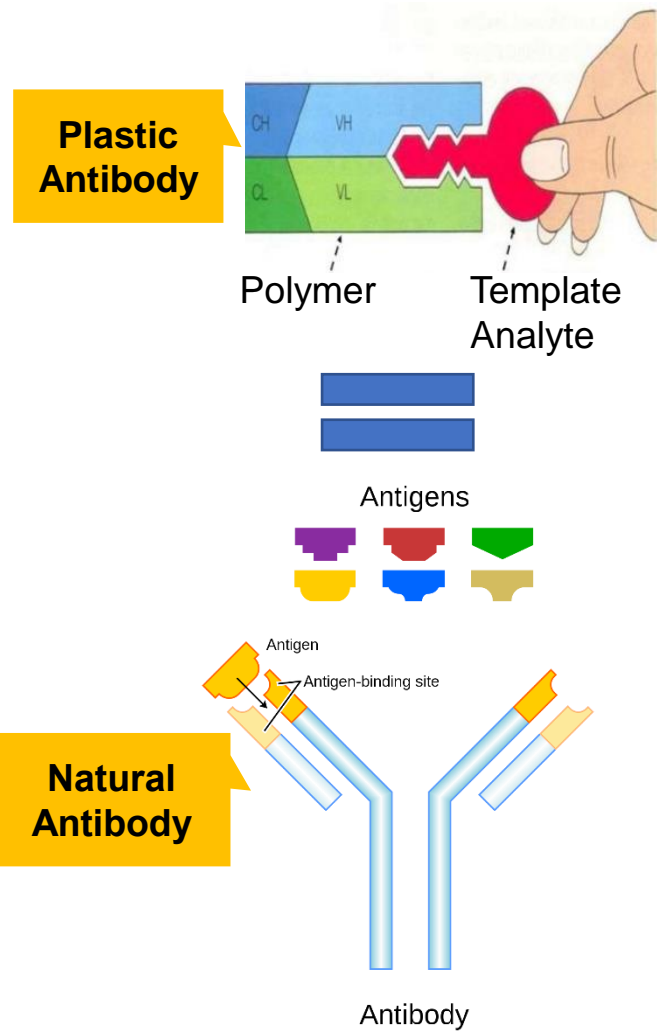
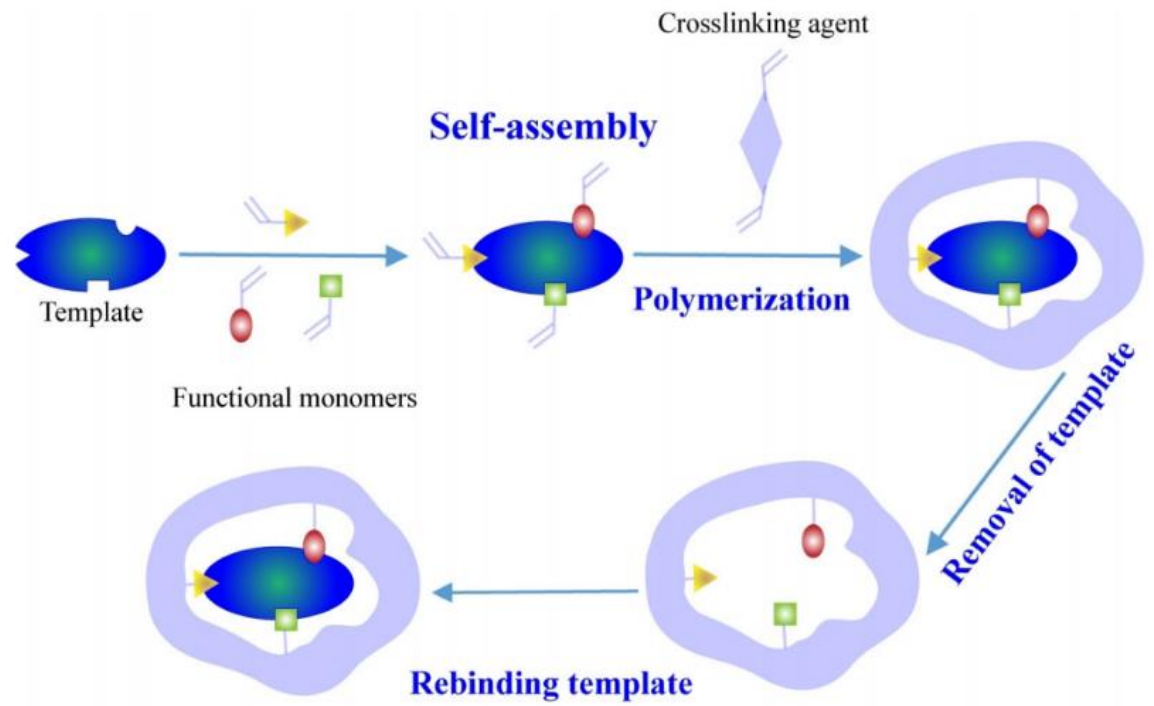


Fig. 5. Various signals generated by aptasensor based on structure-switching designs. (A) A schematic representation of the fluorescent aptasensor for thrombin assay. Thrombin-induced structure change of the aptamer from quenching-state into G-quartet structure could lead to fluorescence enhancement. [Fig. 5A](#) adapted from ref. [100]; (B) A schematic representation of the electrochemical aptasensor for thrombin assay. Before adding the thrombin, MB covalently labeled onto aptamer could transfer electron with the electrode surface due to the flexible conformation of the aptamer. Upon adding the thrombin a G-quadruplex structure was formed and the MB moiety was far away from the electrode surface, resulting in the electrochemical signal-off. [Fig. 5B](#) adapted from ref. [105]; (C) A schematic representation of the colorimetric aptasensor for adenosine assay. Gold nanoparticles are functionalized with aptamer. Addition of the adenosine results in nanoparticles linking together and aggregating, thus causing the change in color. [Fig. 5C](#) adapted from ref. [107]. Copyright (2007) American Chemical Society.



Molecularly imprinted polymers (MIPs) are synthetic receptors for a targeted molecule. As such, they are analogues of the natural antibody–antigen systems

DOI: 10.1021/acs.chemrev.8b00171 Chem. Rev. 2019, 119, 94–119



Scheme 1. Schematic representation of the synthesis of molecularly imprinted polymers (MIPs).

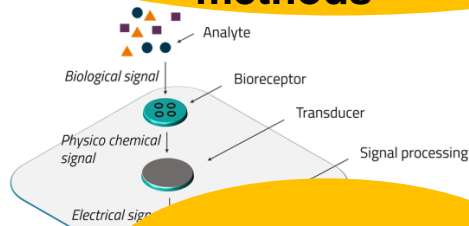
Abdellatif Ait Lahcen[a] and Aziz Amine*[a], 2018

MIP-State of the art

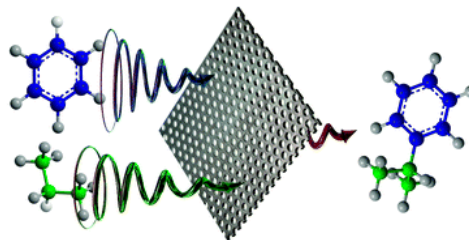
MIPs Applications

MIPs are excellent materials with high selectivity and are widely used for:

Sample preparation in bio analytical methods

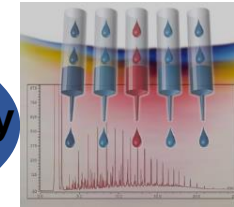


Sensors applications



Catalysis

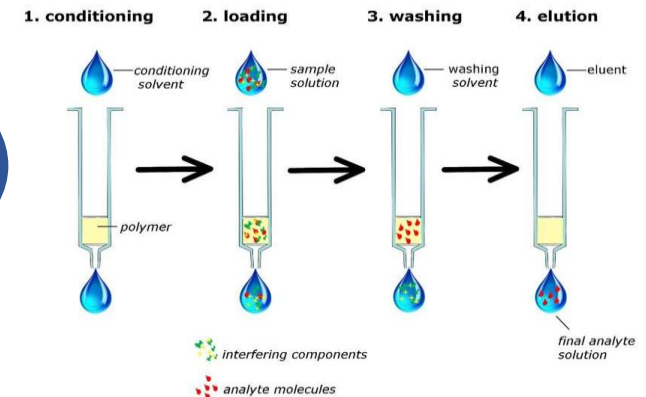
Chromatography



Drug delivery



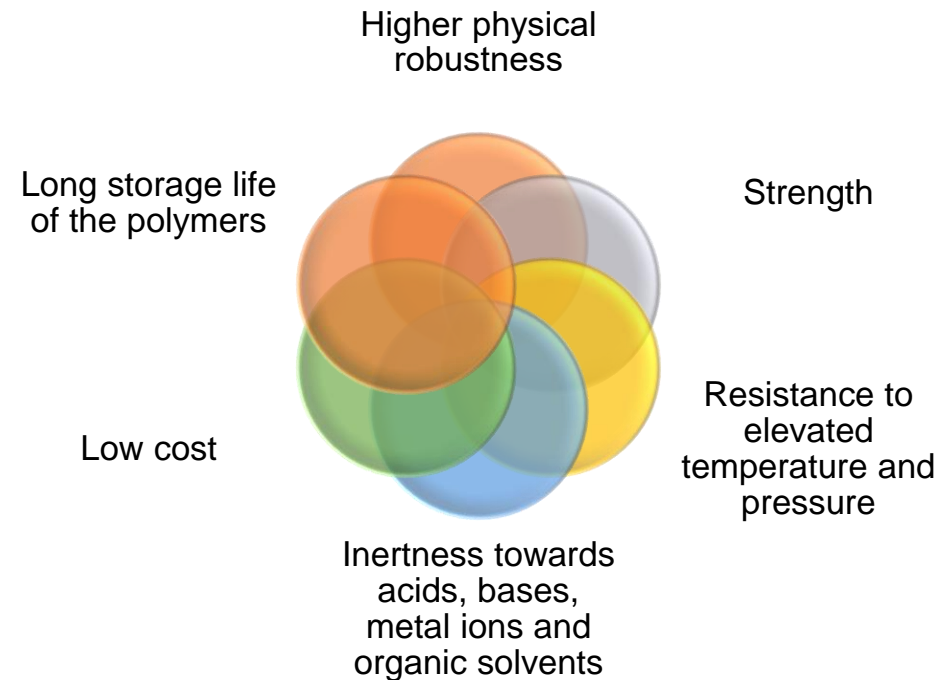
Solid phase extraction



Advantages of MIPs

- ❖ High **selectivity** and **affinity** for the **target molecule** used in the imprinting procedure.

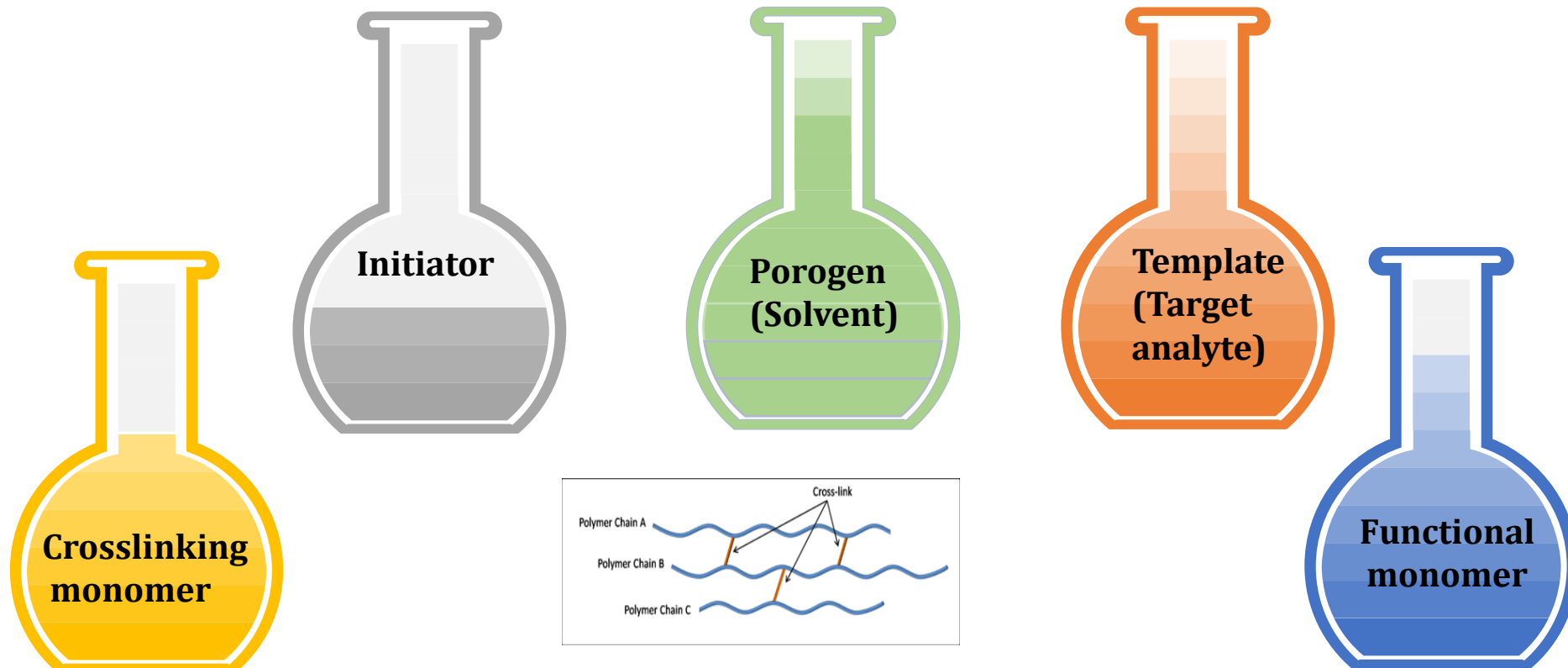
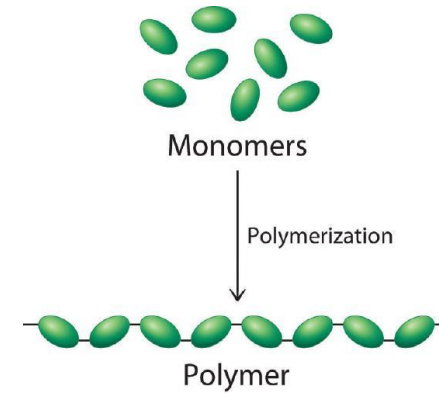
Compared to biological systems such as proteins and nucleic acids MIP has:



02 MIP-State of the art

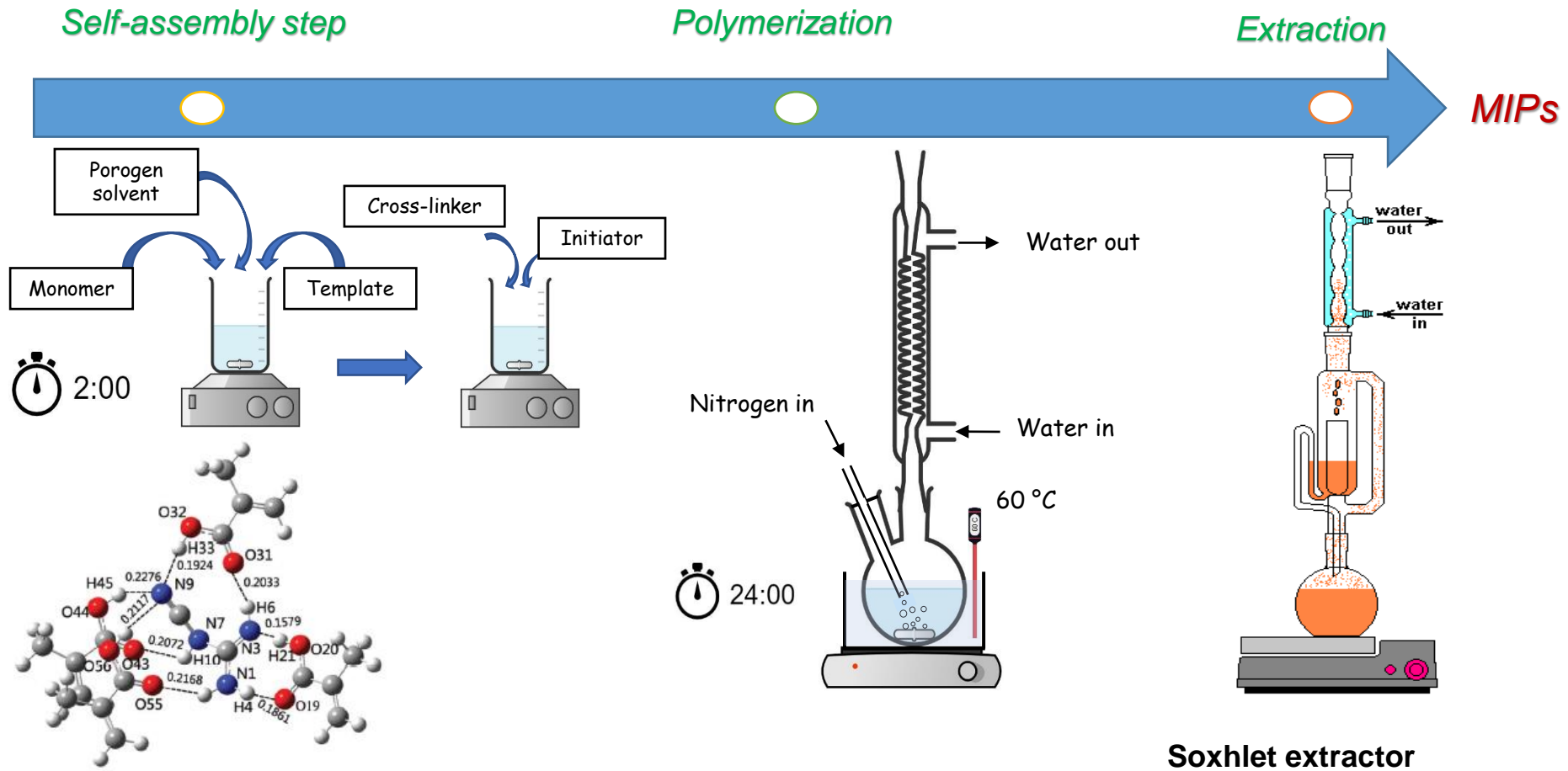
MIPs Synthesis

Components of MIP Mixture



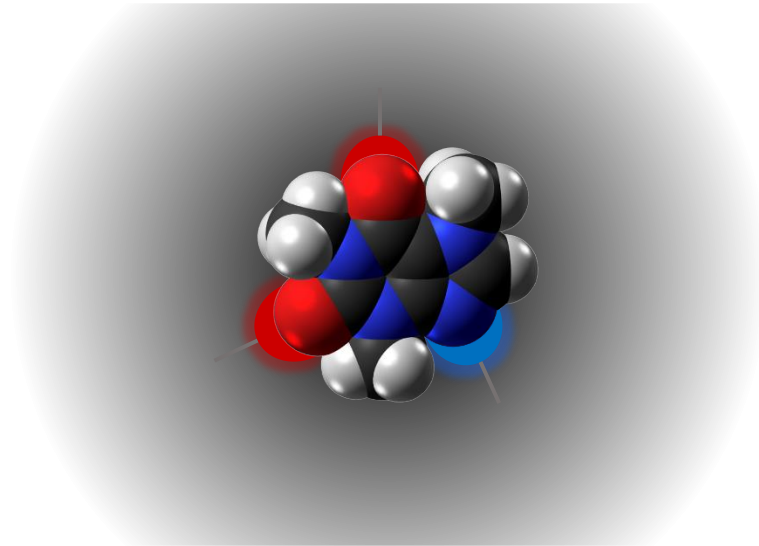
MIPs Synthesis

General procedure



MIP synthesis

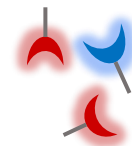
*Sulfamethoxazole
MIPs Synthesis*



Selective rebinding



**Template
(Sulfamethoxazole)**



Monomer (Methacrylamide MMA)

MIP-Synthesis

MIPs Synthesis

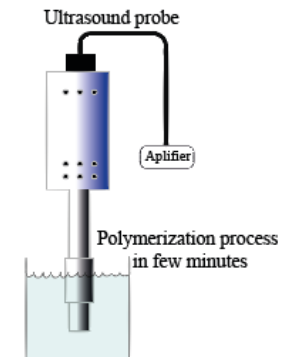
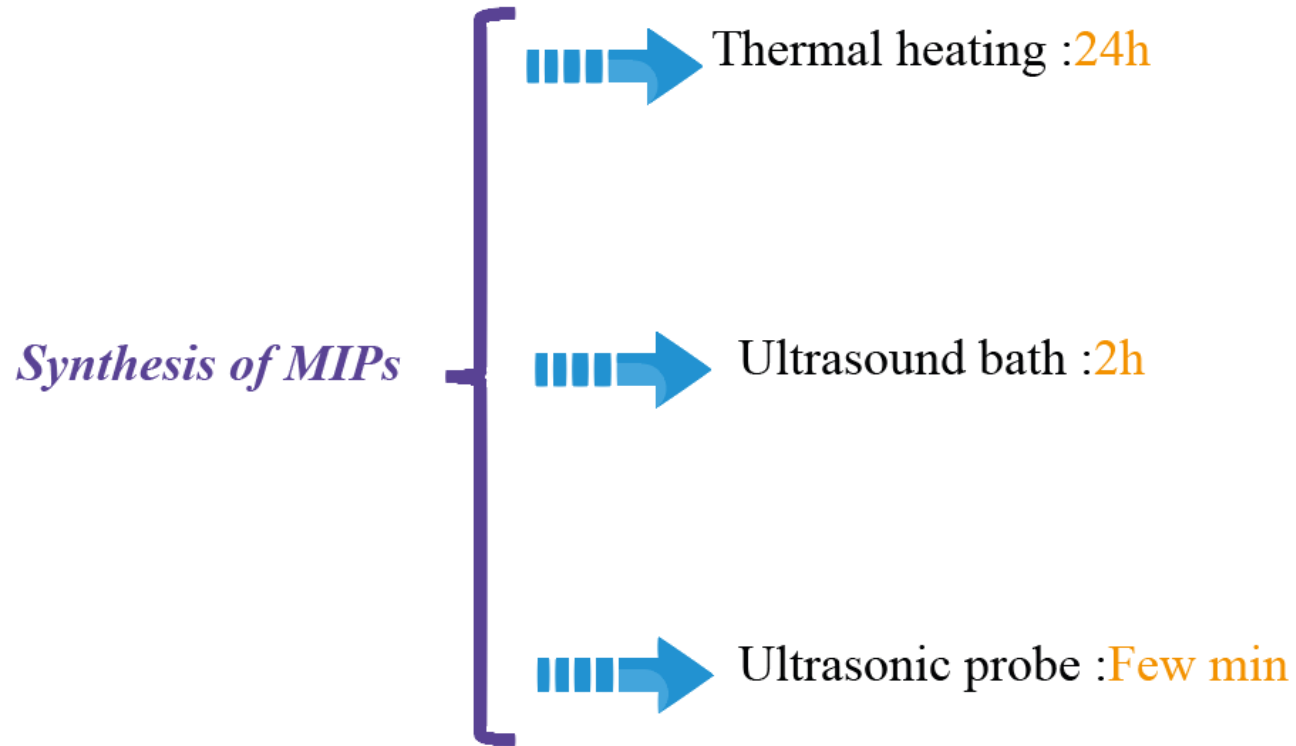


Figure : Synthesis of magnetic molecularly imprinted polymer

03 MIP-Synthesis

Theoretical optimizations prior to MIP s synthesis

Selection of the functional monomer

Prepolymer	E _{Monomer} (Hartree)	E _{Complex}	ΔE (kcal/mol)
Sulfamethoxazole:SMX	-1169.32	-	
SMX-Acrylamide	-245.92	-1415.29	-31.37
SMX- 4-vinyl pyridine	-323.88	-1493.25	-31.37
SMX-Methacrylic acid	-304.788	-1474.13	-13.80
SMX-Methacrylamide	-285.03	-1454.41	-37.65

Selection of the solvent

Complexes monomer-template-solvent	E _{complex} (Hartree)
SMX- Methacrylamide-ETOH	<u>-1608.60</u>
SMX- Methacrylamide-DMSO	<u>-2004.76</u>
SMX- Methacrylamide-DMF	<u>-1701.53</u>
SMX- Methacrylamide-ACETONE	<u>-1646.392</u>
SMX- Methacrylamide-ACETONITRILE	<u>-1586.45</u>
SMX- Methacrylamide-TOLUENE	<u>-1724.49</u>
SMX- Methacrylamide-WATER	<u>-1530.38</u>
SMX- Methacrylamide-METHANOL	<u>-1569.47</u>

Methacrylamide -SMX have highest interaction energy in DMSO solvent due to the formation of a more stable complex.

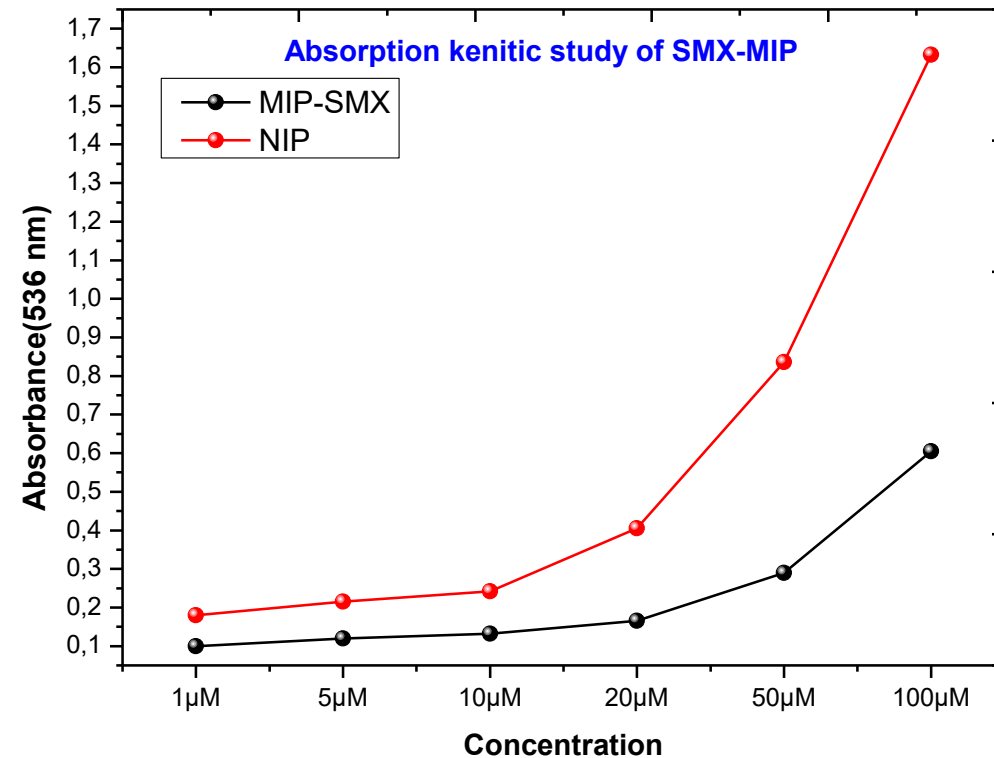
MIPs synthesis optimizations

Optimization of time and amplitude of synthesis was done to select the best parameters for MIP-Ultrasound probe synthesis

	Parameters	Comment	Polymer quality
MMA -MIP 22-07-2020	10 MIN /20A	Polymer was formed	++
MMA -NIP 22-07-2020	10 MIN /20A	Polymer was formed	++
MMA -MIP 23-07-2020	7. 5MIN /30A	Polymer was formed	+++
MAA-NIP 23-07-2020	7. 5MIN /30A	Polymer was formed	+++
MMA-MIP 23-07-2020	5 MIN /20A	Polymer was formed	++++
MMA-NIP 23-07-2020	5 MIN /20A	Polymer was formed	++++

5 min as time of synthesis and 20 as pulse amplitude was selected

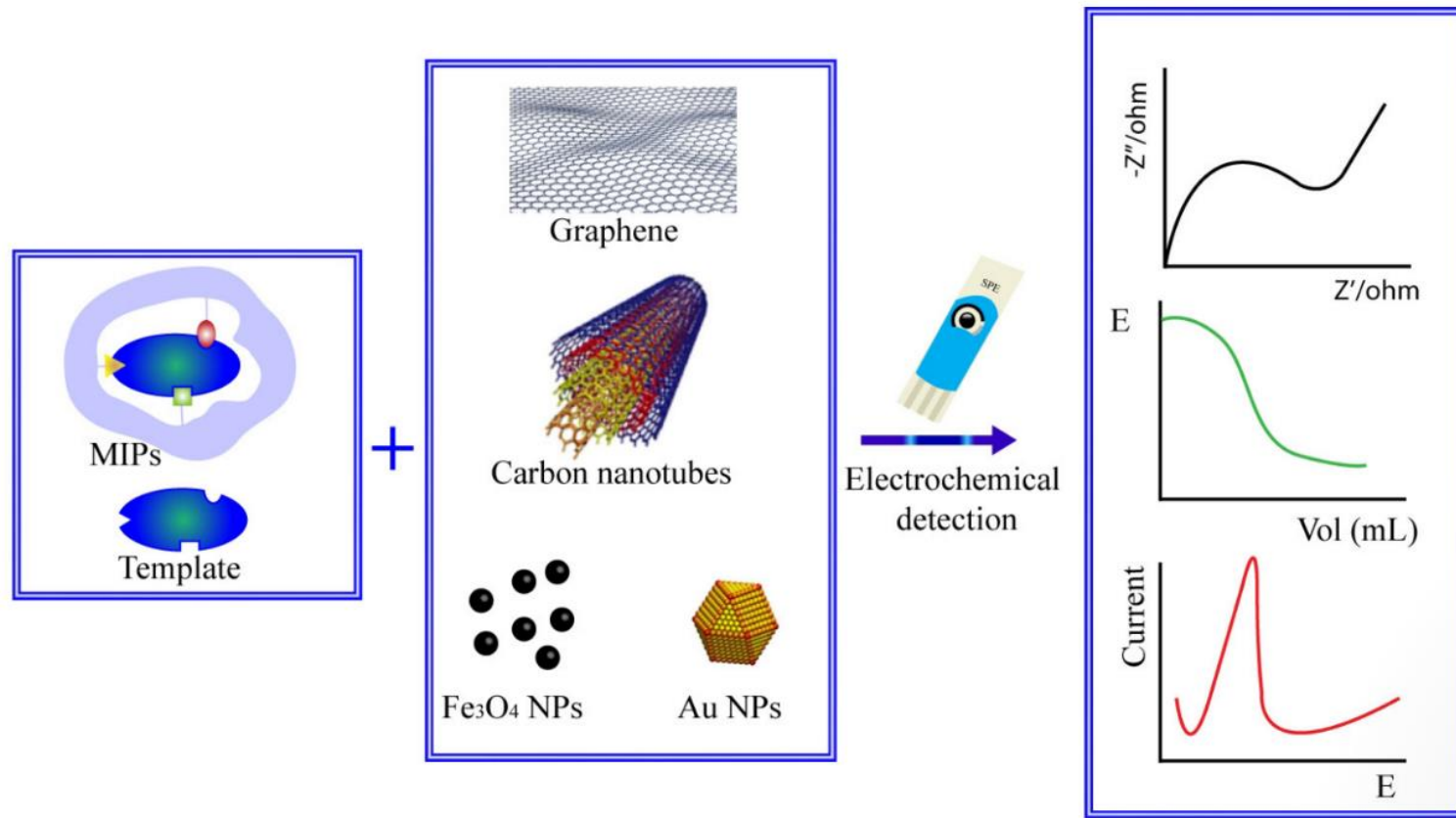
Graph of the un-retained template



MIP has higher capacity to capture the template compared to non imprinted polymer

02 MIP-State of the art

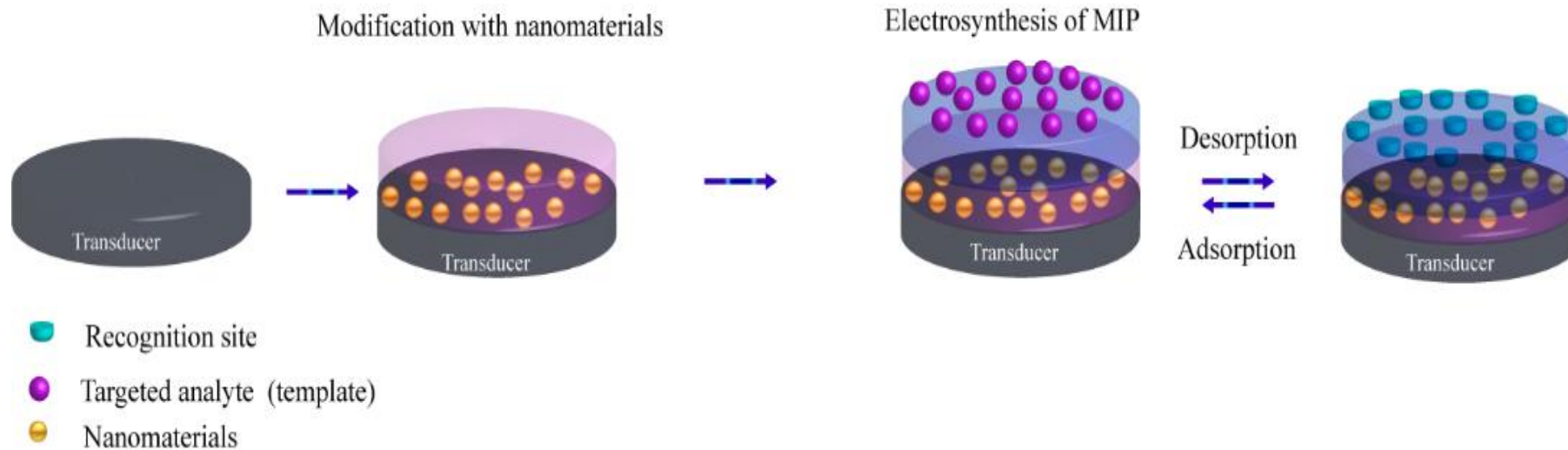
MIP based electrochemical sensors and nanomaterials



Scheme of MIP based electrochemical sensors and nanomaterials.

02 MIP-State of the art

MIP based electrochemical sensors and nanomaterials
Electrosynthesis of MIPs



~~Initiator~~

~~Crosslinking monomer~~

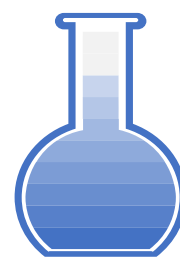
Template
(Target analyte)



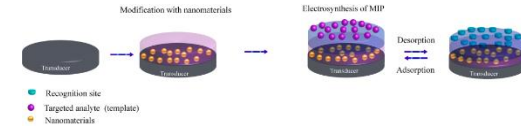
Porogen
(Solvent)
Buffer



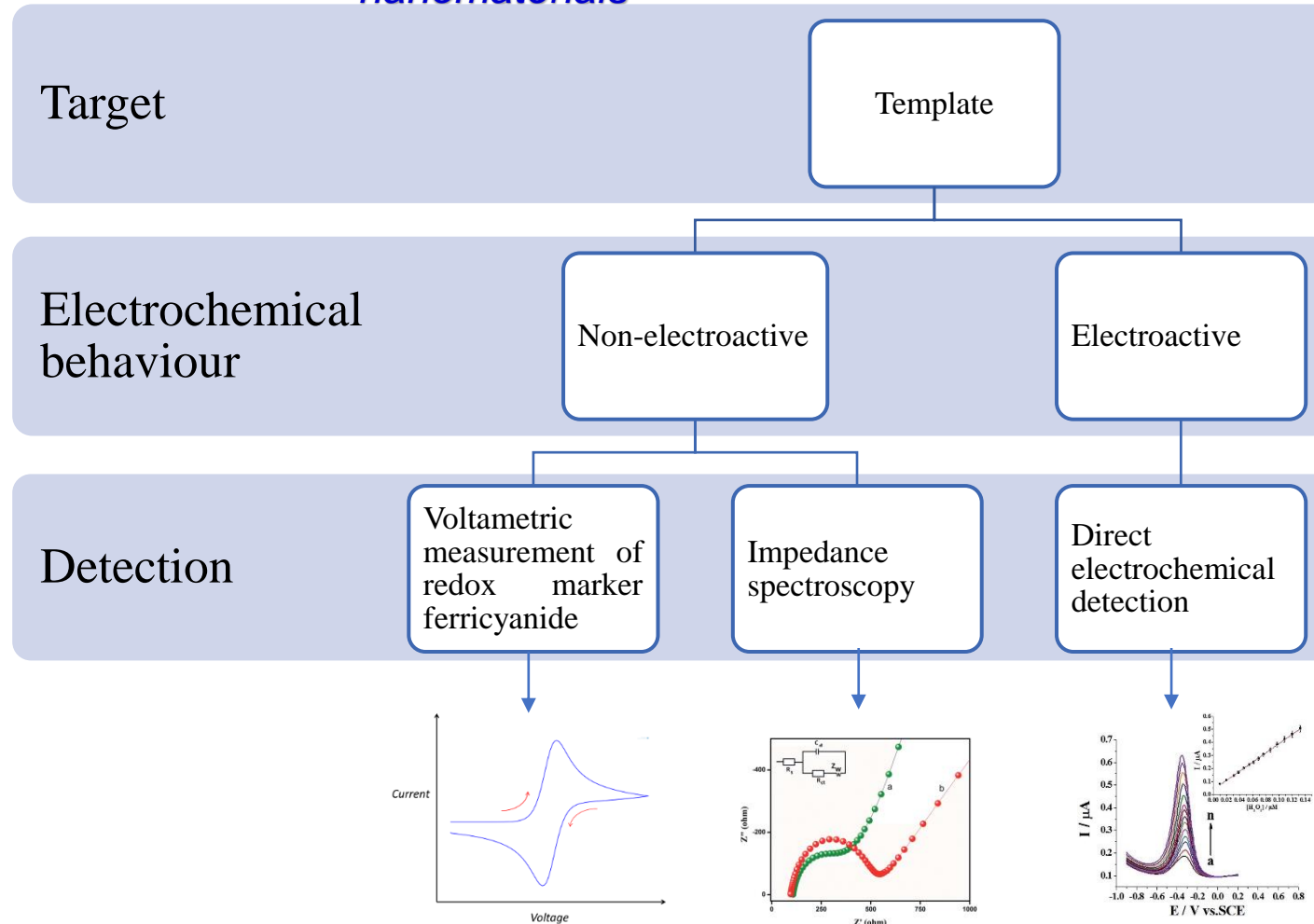
Functional monomer



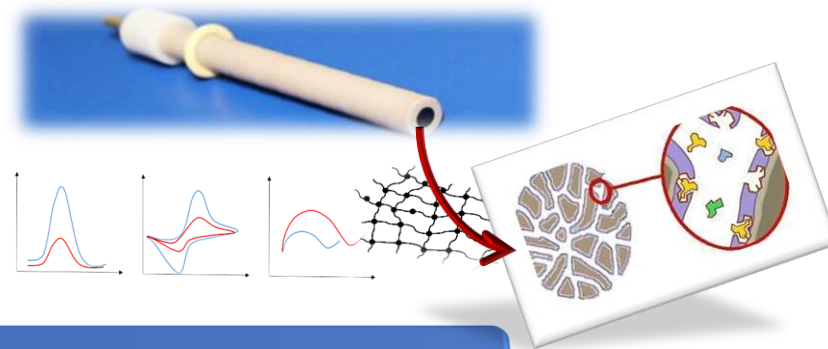
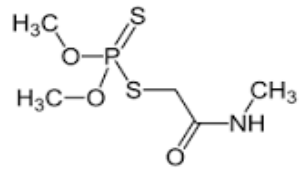
MIP-State of the art



MIP based electrochemical sensors and nanomaterials



MIP-MEPS based sensing strategy for the selective assay of dimethoate. Application to wheat flour samples



DIMETHOATE MONITORING IN WHEAT FLOUR

SAMPLE
PREPARATION

ANALYTE
DETECTION

MICROEXTRACTION
BY PACKED SORBENT
(MEPS)

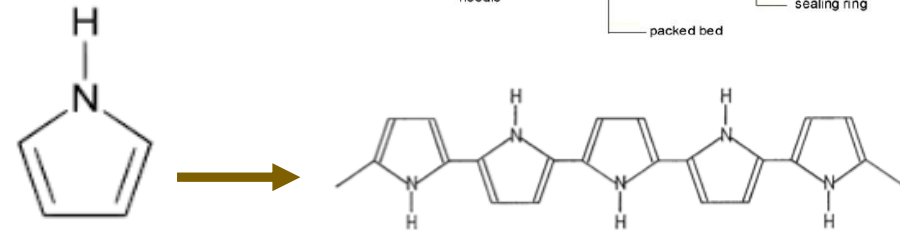
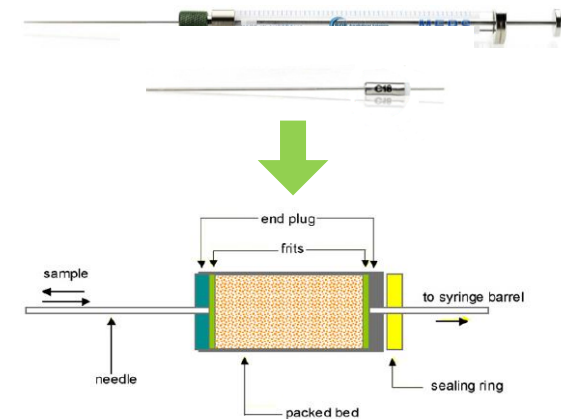
MIP-GLASSY CARBON
ELECTRODE



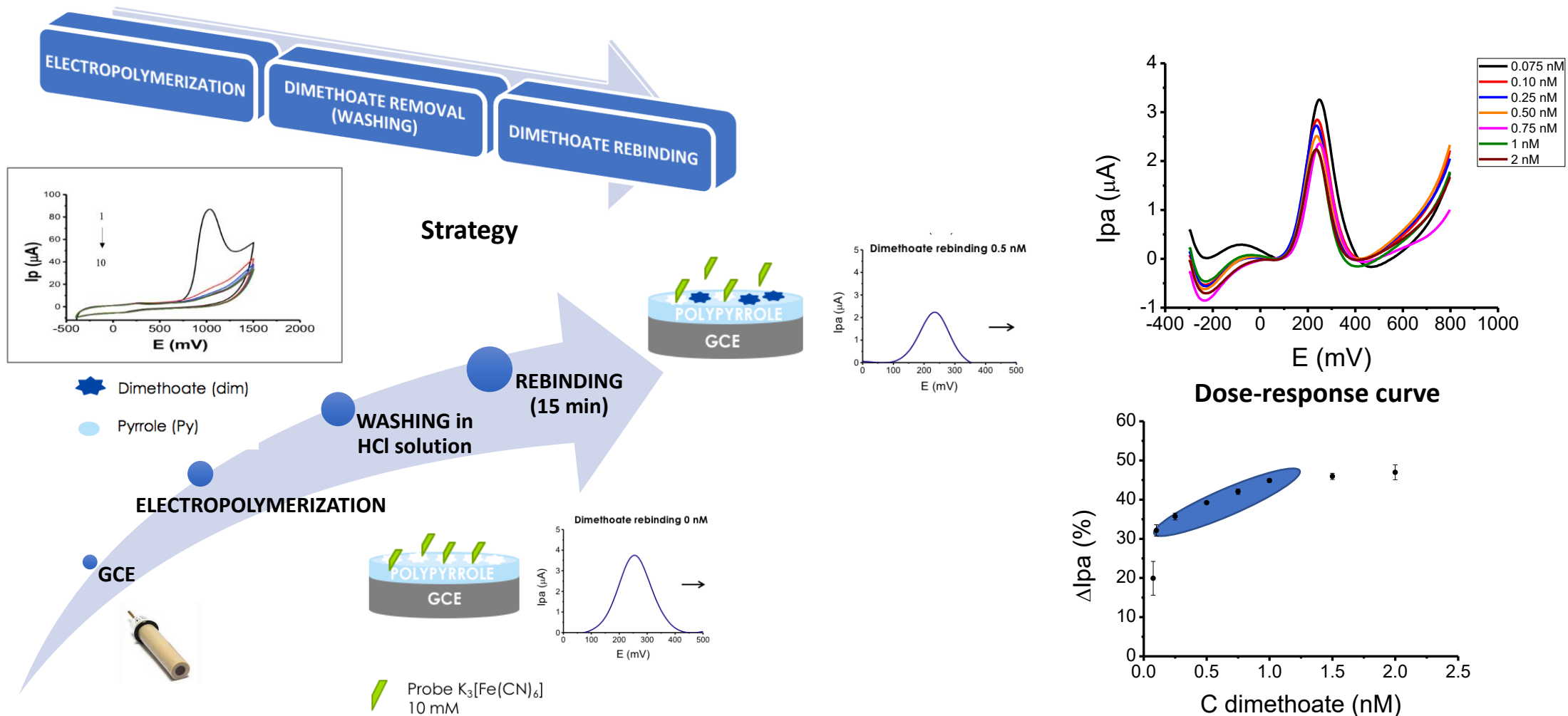
MIP-MEPS based sensing strategy for the selective assay of dimethoate. Application to wheat flour samples

D. Capoferri^a, M. Del Carlo^{a,1}, N. Ntshongontshi^b, E.I. Iwuoha^b, M. Sergi^a, F. Di Ottavio^a, D. Compagnone^{a,*,1}

^a Faculty of Biosciences and Technologies for Food, Agriculture and Environment, University of Teramo, via R. Balzarotti 1, 64100 Teramo, Italy
^b Sensor Lab, Department of Chemistry, University of the Western Cape, Bellville 7530, South Africa



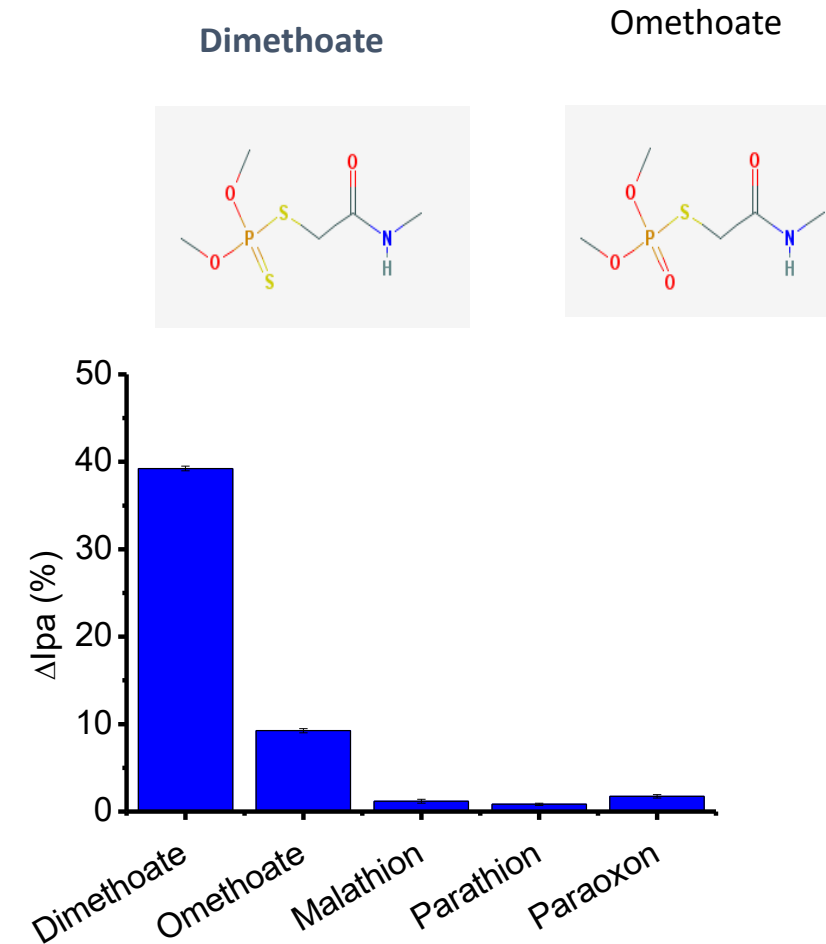
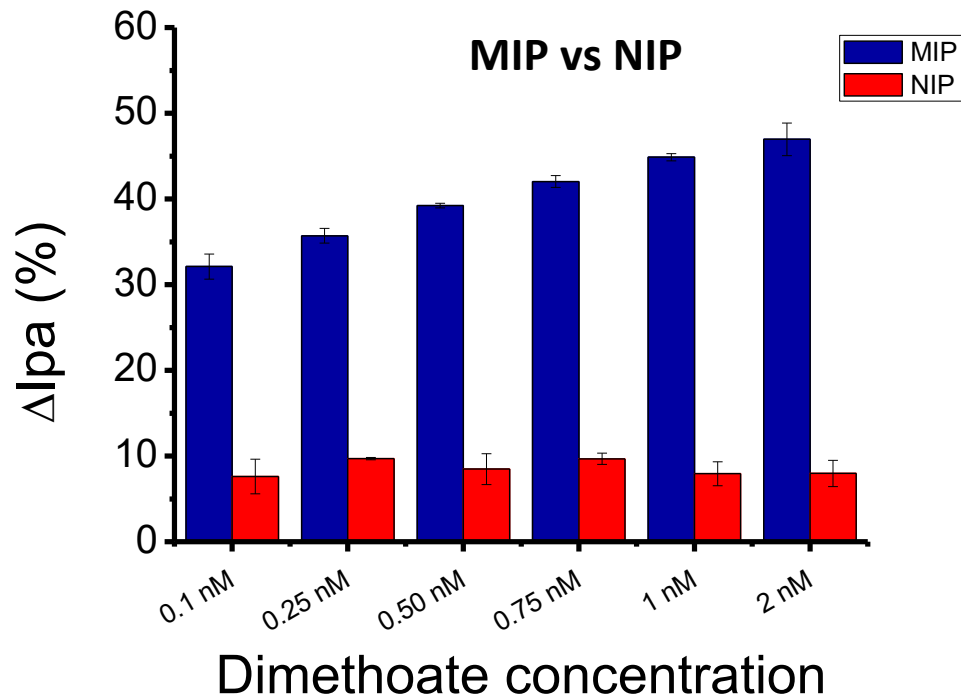
MIP-MEPS based sensing strategy for the selective assay of dimethoate. Application to wheat flour samples



MIP-MEPS based sensing strategy for the selective assay of dimethoate. Application to wheat flour samples

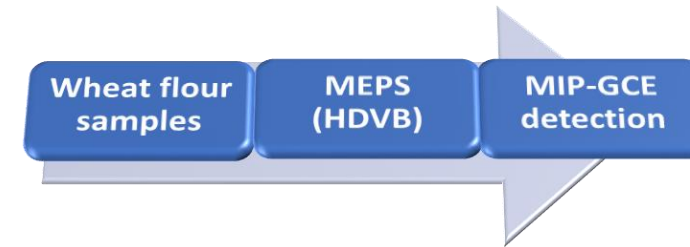
ΔI_{pa} (%)	Repeatability (RSD %)	Reproducibility (RSD %)
0.5 nM dimethoate (n=3)	0.68	2.72
1 nM dimethoate (n=3)	0.95	5.51

ΔI_{pa} (%) for malathion, parathion and paraoxon after the rebinding step was negligible; **omethoate** gave a response of **23%**.



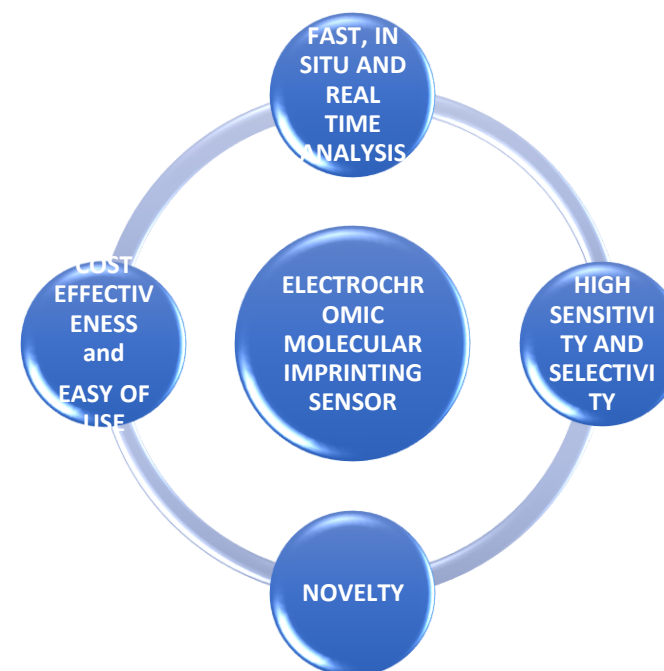
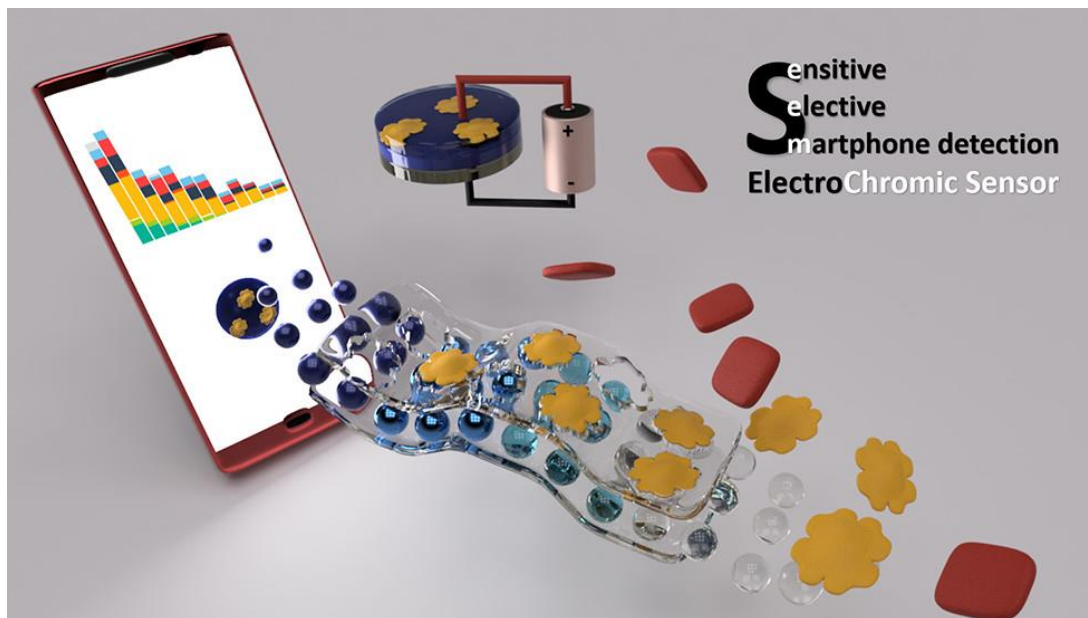
MIP-MEPS based sensing strategy for the selective assay of dimethoate. Application to wheat flour samples

Wheat flour samples: MIP vs. UHPLC-MS/MS



Samples	MIP-GCE RELATIVE ERROR (%) of dimethoate concentration ($\mu\text{g kg}^{-1}$)	MIP-GCE SD of dimethoate concentration ($\mu\text{g kg}^{-1}$)
Wheat flour spiked with dimethoate 0.5 MRL	+13.5	0.52
Wheat flour spiked with dimethoate 0.5 MRL + mix	+4.6	2.37
Wheat flour spiked with dimethoate MRL	-21.1	1.24
Wheat flour spiked with dimethoate MRL + mix	-21.2	1.36
Wheat flour spiked with dimethoate 1.5 MRL	+16.7	0.74
Wheat flour spiked with dimethoate 1.5 MRL + mix	-0.4	1.69
Wheat flour spiked with dimethoate MRL + omethoate (1:1)	+3.5	2.70
Wheat flour spiked with dimethoate MRL + omethoate (1:10)	-15.5	0.86

Electrochromic Molecular Imprinting Sensor for Visual and Smartphone-Based Detections



analytical
chemistry

Cite This: Anal. Chem. XXXX, XXX, XXX-XXX

Article

pubs.acs.org/ac

Electrochromic Molecular Imprinting Sensor for Visual and Smartphone-Based Detections

Denise Capoferri,^{†,‡,§} Ruslan Álvarez-Diduk,^{†,§} Michele Del Carlo,[‡] Dario Compagnone,[‡] and Arben Merkoçi^{†,*,†,||}

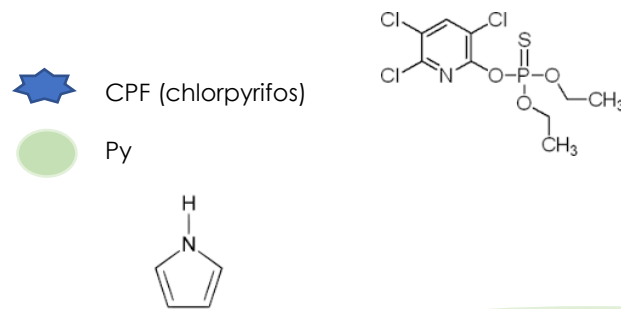
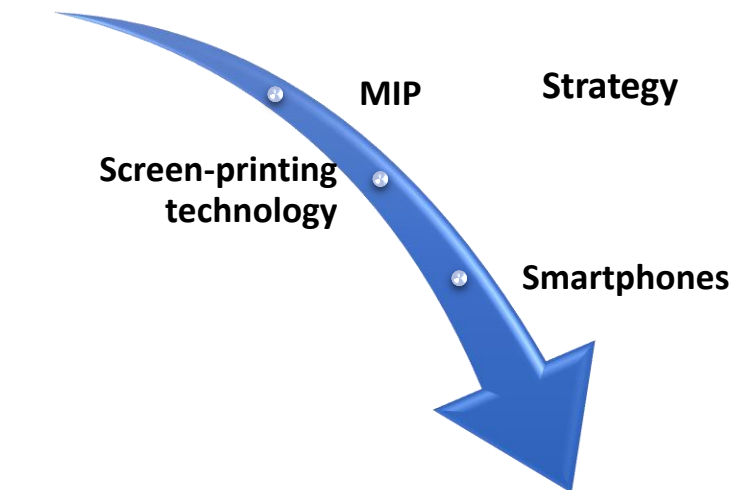
[†]Nanobioelectronics and Biosensor Group, Catalan Institute of Nanoscience and Nanotechnology (ICN2), CSIC, The Barcelona Institute of Science and Technology, Campus UAB, Bellaterra, 08193, Barcelona, Spain

[‡]Faculty of Biosciences and Technologies for Food, Agriculture and Environment, University of Teramo, via R. Balzarini 1, 64100 Teramo, Italy

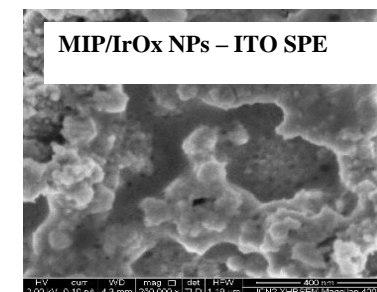
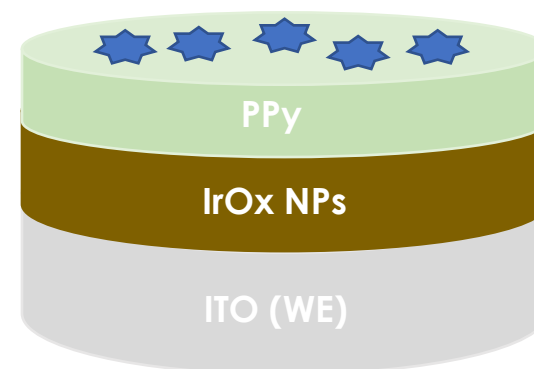
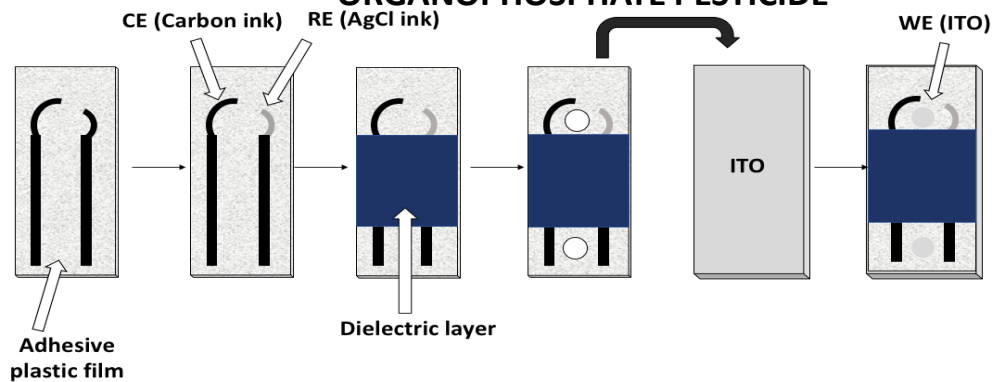
[§]Catalan Institution for Research and Advanced Studies (ICREA), Pg. Lluís Companys 23, 08010 Barcelona, Spain

Electrochromic Molecular Imprinting Sensor for Visual and Smartphone-Based Detections

Electrochromism

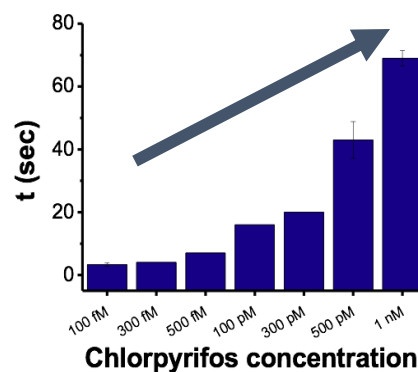
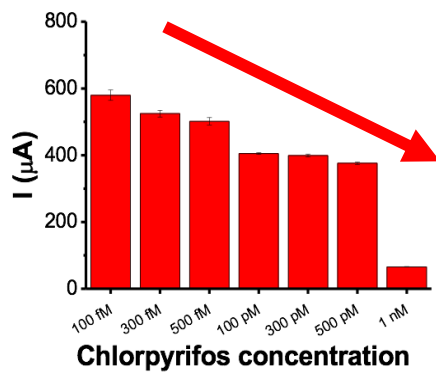
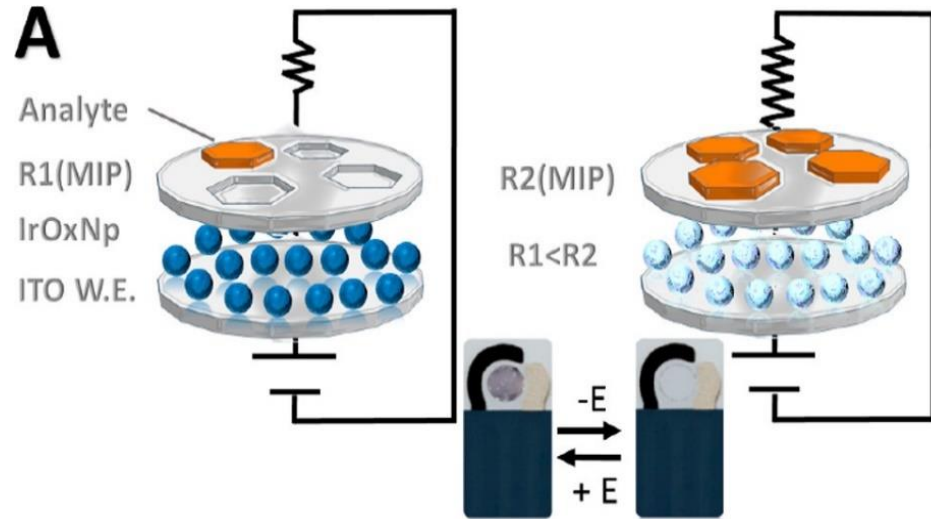


**ELECTROCHROMIC MOLECULAR
IMPRINTING SENSOR for an
ORGANOPHOSPHATE PESTICIDE**



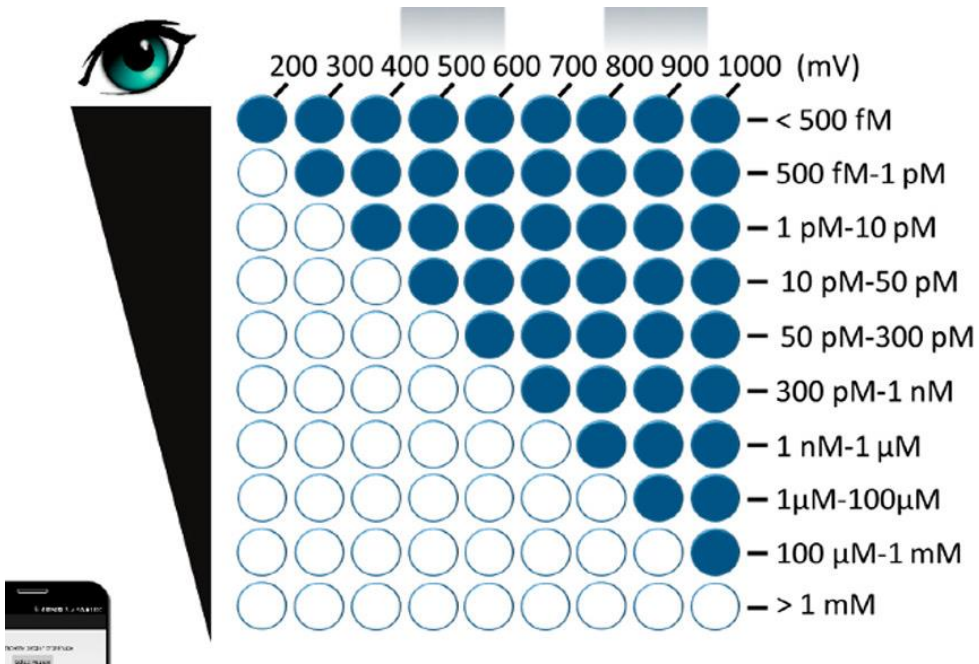
Electrochromic Molecular Imprinting Sensor for Visual and Smartphone-Based Detections

WORKING PRINCIPLE

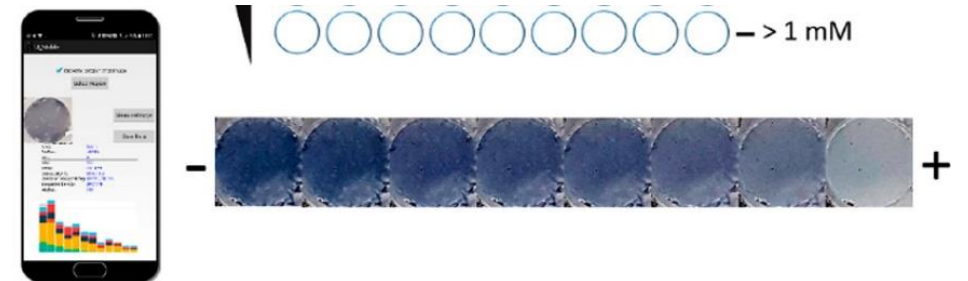
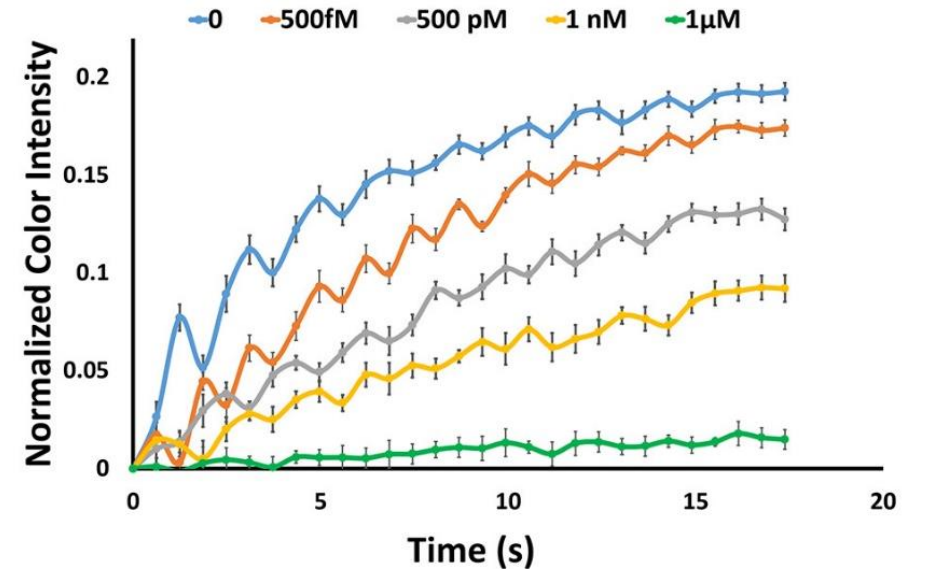


Electrochromic Molecular Imprinting Sensor for Visual and Smartphone-Based Detections

VISUAL APPROACH

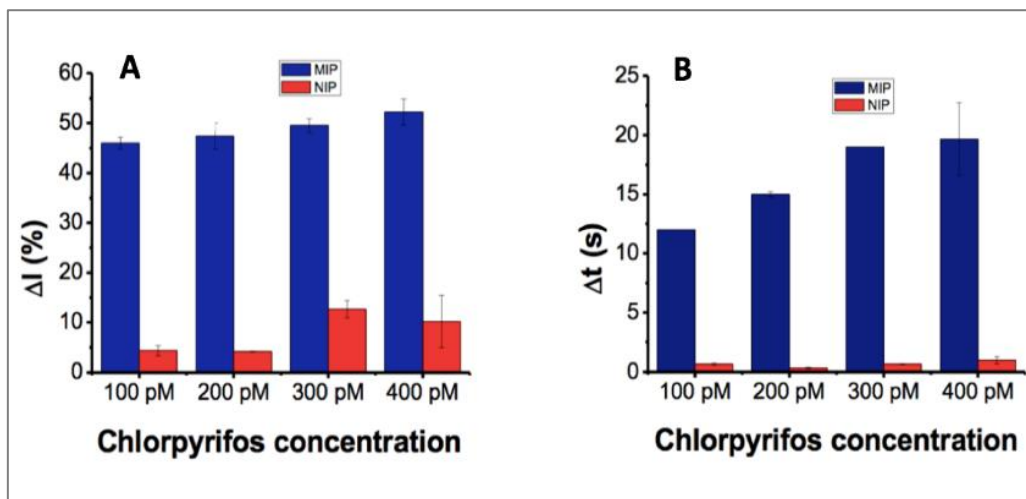


SMARTPHONE APPROACH



Electrochromic Molecular Imprinting Sensor for Visual and Smartphone-Based Detections

MIP vs NIP



Recovery values of chlorpyrifos in spiked drinking water samples (n = 3) using the current response

Added (Spiked)	Found	Recovery (%)	RSD (%)
500 fM	517.19 fM	103.44 ± 16.14	15.60
500 pM	471.45 pM	94.29 ± 17.92	19.00
1 nM	0.99 nM	99.50 ± 19.90	20.00
1 μM	0.98 μM	97.55 ± 25.87	26.52
1 mM	1.07 mM	106.57 ± 15.30	14.36

SELECTIVITY (500 mV-1000 mV)

